IMPACTS OF SYNOPTIC ATMOSPHERIC CIRCULATIONS AND TOPOGRAPHIC CONDITIONS ON SUSTAINED STRONG SURFACE WINDS OVER SOUTHERN NUNAVUT

Daniel Nadeau

M.Sc.

Department of Atmospheric and Oceanic Sciences

McGill University
Montréal,Quebec
09-19-2007

A thesis submitted to McGill University in partial fulfilment of the requirements of the degree of Master of Science

© Daniel Nadeau 2007

DEDICATION

To Daniel Ouedraogo

ACKNOWLEDGEMENTS

I am very grateful to my supervisor Dr. Ronald Stewart. His enthusiasm and support throughout this research was sincerely appreciated. He offered me the unique opportunity to do field work in the Arctic and that has become a highlight of my life. I would like to express thanks to Dr. Nikolai Nawri, for his guidance, scientific rigor and patience. I appreciated him as a scientific advisor, a squash partner, a hiking friend and a roommate. I am grateful to Jay Anderson, for his excellent suggestions at the ArcticNet meeting 2006. I would like to thank Dr. Eyad Atallah, a knowledgeable and relax guide into the sometimes obscure world of synoptic meteorology. I thank Michael Havas, the best computer guy I have ever met. I am also grateful to Shawn Milrad, for his precious help with GEMPAK and interpretation of synoptic maps. I would like to thank Dr. William Henson, who helped me define my events and taught me how to use NARR data. I would also like to thank Julie Thériault for her precious help with my thesis. Finally, I would like to thank my wife Elisabeth to whom I owe so much. She was my source of inspiration. I would like to thank my parents Marquis and Violette, my sister Chantal as well as my brother Pierre-Luc for their love and support. This research was sponsored by the Natural Sciences and Engineering Research Council of Canada.

ABSTRACT

Strong surface winds are an inherent aspect of the eastern Canadian Arctic climate yet few studies have focused on these features. As a result, arctic winds are often poorly predicted by current weather forecasting models. To better predict the arctic weather, we need to understand the role of the Arctic's unique geographical and meteorological features such as mountains, sea-ice and very stable atmospheric stratification. In this study, we hypothesize that these features have an impact on high wind events in the eastern Canadian Arctic. To test this, we examine the long-term data records of six meteorological stations across southern Nunavut. We also develop a severity index to characterize high wind events, based on duration, maximum gusts and mean wind speed observed. By studying the five most severe high wind events and the motion of storm systems generating strong winds, we identified how the Arctic's geographical and meteorological features enhanced strong surface winds. High wind events are usually associated with intense cyclones located over Hudson Bay or Labrador Sea, particularly in wintertime. Under this large scale setting, blocking and channeling due to the stable boundary-layer stratification typically occur at Clyde River and Iqaluit, enhancing the surface wind speed. Over flatter terrain, high wind events typically occur when the station is situated in a region of strong synoptic pressure gradient between an anticyclone and a cyclone.

ABRÉGÉ

Malgré leur rôle prépondérant au sein du climat arctique canadien méridional, peu d'études se sont intéressées aux vents violents de surface. Conséquemment, les prévisions météorologiques à leur sujet sont souvent imprécises. Afin d'améliorer les modèles de prévisions météorologiques dans l'Arctique, nous devons mieux doser la contribution des particularités géographiques et météorologiques inhérente à cette région, notamment la glace de mer, le relief accidenté et l'importante stabilité atmosphérique. Dans cette étude, nous supposons que ces particularités contribuent à la formation d'événements de vents violents dans l'Arctique canadien méridional. Afin de tester cette hypothèse, nous étudions les données météorologiques de six stations réparties dans le sud du Nunavut. Pour ce faire, nous développons un indice de sévérité basé sur trois paramètres des événements de vents violents: la durée, les rafales maximales observées et la vitesse moyenne du vent. Suite à notre étude, nous observons que les événements de vents violents sont typiquement associés à la présence d'intenses dépréssions situées au-dessus de la baie d'Hudson ou de la mer du Labrador, particulièrement en hiver. Sous l'influence de ces systèmes, des phénomènes de blocage et d'effet de canal sont typiquement observés à Clyde River et Iqaluit, modifiant ainsi la vitesse et la direction des vents de surface. Quant aux stations en terrain plat, les événements de vents violents sont davantage provoqués par de forts gradients de pression synoptiques, lorsque la station est située entre un cyclone et un anticyclone.

TABLE OF CONTENTS

DED	ICATI	ON
ACK	NOWI	LEDGEMENTS
ABS	TRAC	Γ iv
ABR	ÉGÉ	
LIST	OF T	ABLES
LIST	OF F	IGURES
1	Introd	uction
	1.1 1.2	Research Objectives
2	Wind	Basic Variables and Stations Used in this Study
	2.1 2.2 2.3	Definition of High Wind Events
3	Overv	iew of High Wind Events across Southern Nunavut
	3.1 3.2 3.3 3.4	Introduction20Maximum Values of High Wind Events Parameters20High Wind Events at Each Location21Severity Distribution22
	3.5	Trends in High Wind Events

4	Seasor	nal Occurrence of High Wind Events
	4.1 4.2 4.3	Introduction27Methods27Results28
5	Prevai	ling Wind Directions during High Wind Events
	5.1	Introduction
	5.2	Methods
	5.4	Results 38 5.3.1 Baker Lake 38 5.3.2 Cambridge Bay 39 5.3.3 Clyde River 40 5.3.4 Coral Harbour 41 5.3.5 Hall Beach 42 5.3.6 Iqaluit 43 5.3.7 Distribution of Wind Regimes 44 Discussion of Wind Regime Results 44 5.4.1 Baker Lake 44 5.4.2 Cambridge Bay 45 5.4.3 Clyde River 45 5.4.4 Coral Harbour 45 5.4.5 Hall Beach 45 5.4.6 Iqaluit 46
		5.4.7 Overall Discussion
6	Meteo	rological Conditions Leading to High Wind Events
	6.1	Introduction496.1.1 Synoptic Climatology506.1.2 The Circumpolar Vortex506.1.3 Atmospheric stability52
	6.2	Methods526.2.1North American Regional Reanalysis Data526.2.2Approach53
	6.3	Baker Lake

		6.3.2 Average Surface Conditions Leading to High Wind Events. 5
	6.4	Cambridge Bay
		6.4.1 The Five Most Severe High Wind Events 5
		6.4.2 Average Surface Conditions Leading to High Wind Events . 5
	6.5	Clyde River
		6.5.1 The Five Most Severe High Wind Events 5
		6.5.2 Average Surface Conditions Leading to High Wind Events . 6
	6.6	Coral Harbour
		6.6.1 The Five Most Severe High Wind Events 6
		6.6.2 Average Surface Conditions Leading to High Wind Events . 6
	6.7	Hall Beach
		6.7.1 The Five Most Severe High Wind Events 6
		6.7.2 Average Surface Conditions Leading to High Wind Events . 6
	6.8	Iqaluit
		6.8.1 The Five Most Severe High Wind Events 6
		6.8.2 Average Surface Conditions Leading to High Wind Events . 6
	6.9	Conclusions
7	Tran	slation of Storm Systems Generating High Wind Events
	7.1	Introduction
		7.1.1 Review of Storm Tracks Affecting Southern Nunavut 7
	7.2	Storm Tracks Associated with High Wind Events
		7.2.1 Methods
		7.2.2 Baker Lake
		7.2.3 Cambridge Bay
		7.2.4 Clyde River
		7.2.5 Coral Harbour
7		7.2.6 Hall Beach
		7.2.7 Iqaluit
	7.3	Cyclone Frequency Maps during High Wind Events 8
		7.3.1 Overall
		7.3.2 Baker Lake
		7.3.3 Cambridge Bay
		7.3.4 Clyde River
		7.3.5 Coral Harbour
		7.3.6 Hall Beach
		7.3.7 Iqaluit
	7.4	Spatial Connection of High Wind Events

		1.4.1 Methods	10
		7.4.2 Results	98
	7.5	Overall Discussion)[
8	Conclu	ding Remarks)7
	8.1	Thesis Summary)7
Refe	erence	11	26

LIST OF TABLES

<u>Table</u>	<u>p</u>	age
2-1	List of stations and periods of hourly observations used in this study .	12
3–1	Maximum values of maximum hourly wind speed, mean wind speed and duration of HWEs ever recorded at the stations of interest	20
3-2	HWEs distribution among stations	22
5-1	Distribution of wind regimes	48
6-1	The five most severe NNW HWEs at Baker Lake	55
6-2	The five most severe NW HWEs at Cambridge Bay	57
6–3	The five most severe NW HWEs at Clyde River	60
6-4	The five most severe NNW HWEs at Coral Harbour	63
6-5	The five most severe WNW HWEs at Hall Beach	65
6-6	The five most severe NW HWEs at Iqaluit	67
8-1	Frequency distribution of hourly winds during HWEs at Baker Lake .	111
8-2	Frequency distribution of hourly winds during HWEs at Cambridge Bay	112
8-3	Frequency distribution of hourly winds during HWEs at Clyde River .	113
8-4	Frequency distribution of hourly winds during HWEs at Coral Harbour	114
8-5	Frequency distribution of hourly winds during HWEs at Hall Beach .	115
8-6	Frequency distribution of hourly winds during HWEs at Iqaluit	116

LIST OF FIGURES

Figure		page
1–1	Map of Nunavut showing its 28 communities	1
1-2	Thesis organization	8
2-1	Location of the stations of interest used in this study	13
2-2	Site of Baker Lake meteorological station	14
2-3	Site of Cambridge Bay meteorological station	15
2-4	Site of Coral Harbour meteorological station	16
2-5	Site of Hall Beach meteorological station	17
2-6	Site of Clyde River meteorological station	19
2-7	Site of Iqaluit meteorological station	19
3-1	Severity distribution among HWEs	23
3-2	Decadal trends in the number of HWEs	24
3-3	Decadal trends in the mean HWE severity	25
3-4	Trends in the mean severity for values above the 95th percentile $$. $$.	25
3-5	Trends in the maximum decadal HWE severity	26
4-1	Overall seasonal occurrence of HWEs for all stations	28
4-2	Seasonal occurrence of HWEs at each station	29
5-1	Cold-air damming in the Appalachian mountains	34
5-2	Qualitative representation of pressure-driven channeling	35
5–3	Qualitative representation of downward turbulent flux of momentum .	36

5-4	Wind directions during HWEs at Baker Lake	38
5-5	Wind directions during HWEs at Cambridge Bay	39
5–6	Wind directions during HWEs at Clyde River	40
5-7	Wind directions during HWEs at Coral Harbour	41
5–8	Wind directions during HWEs at Hall Beach	42
5–9	Wind directions during HWEs at Iqaluit	43
5-10	Mean pressure pattern over the Canadian Arctic for January \dots	47
6–1	Fields of 500 hPa geopotential height for four selected months \dots	51
6-2	Composite surface map of synoptic conditions during the peak intensity of the five most severe NNW HWEs at Baker Lake	56
6–3	Composite surface map of synoptic conditions during the peak intensity of the five most severe NW HWEs at Cambridge Bay	58
6–4	Composite surface map of synoptic conditions during the peak intensity of the five most severe NW HWEs at Clyde River	61
6–5	Composite surface map of synoptic conditions during the peak intensity of the five most severe NNW HWEs at Coral Harbour	64
6–6	Composite surface map of synoptic conditions during the peak intensity of the five most severe WNW HWEs at Hall Beach	66
6–7	Composite surface map of synoptic conditions during the peak intensity of the five most severe NW HWEs at Iqaluit	69
6-8	Mean atmospheric profile during the peak intensity of the five most severe NW HWEs at Iqaluit	70
7-1	Storm tracks affecting the Canadian Arctic	74
7–2	Methodology for the identification of storm tracks associated with HWEs for each station	76
7–3	Storm tracks for HWEs at Baker Lake	77

7-4	Storm tracks for HWEs at Cambridge Bay	79
7–5	Storm tracks for HWEs at Clyde River	81
7–6	Storm tracks for HWEs at Coral Harbour	83
7-7	Storm tracks for HWEs at Hall Beach	84
7–8	Storm tracks for HWEs at Iqaluit	86
7–9	Cyclone frequencies for all HWEs and all stations	88
7–10	Average storm speed for all HWEs and all stations	89
7–11	Cyclone frequencies during HWEs at Baker Lake	91
7–12	Cyclone frequencies during HWEs at Cambridge Bay	92
7–13	Cyclone frequencies during HWEs at Clyde River	93
7–14	Cyclone frequencies during HWEs at Coral Harbour	94
7–15	Cyclone frequencies during HWEs at Hall Beach	95
7–16	Cyclone frequencies during HWEs at Iqaluit	96
7–17	Delays between occurrences of local maxima in wind speed time series	97
7–18	Average cross-correlation spectrum for wind speed time series at Cambridge Bay and Baker Lake	98
7–19	Average cross-correlation spectrum for wind speed time series at Baker Lake and Coral Harbour	100
7–20	Average cross-correlation spectrum for wind speed time series at Coral Harbour and Hall Beach	101
7–21	Average cross-correlation spectrum for wind speed time series at Hall Beach and Clyde River	103
7–22	Average cross-correlation spectrum for wind speed time series at Iqaluit and Clyde River	104
8–1	Individual surface maps of synoptic conditions during the peak intensity of the five most severe NNW HWEs at Baker Lake	117

8–2	Individual surface maps of synoptic conditions during the peak intensity of the five most severe NW HWEs at Cambridge Bay	118
8–3	Individual surface maps of synoptic conditions during the peak intensity of the five most severe NW HWEs at Clyde River	119
8–4	Individual surface maps of synoptic conditions during the peak intensity of the five most severe NNW HWEs at Coral Harbour	120
8–5	Individual surface maps of synoptic conditions during the peak intensity of the five most severe WNW HWEs at Hall Beach	121
8–6	Individual surface maps of synoptic conditions during the peak intensity of the five most severe NW HWEs at Iqaluit	122
8–7	Fields of mean 500 hPa geopotential height for the five most severe NNW HWEs at Baker Lake	123
8–8	Fields of mean 500 hPa geopotential height for the five most severe NW HWEs at Cambridge Bay	123
8–9	Fields of mean 500 hPa geopotential height for the five most severe NW HWEs at Clyde River	124
8–10	Fields of mean 500 hPa geopotential height for the five most severe NNW HWEs at Coral Harbour	124
8–11	Fields of mean 500 hPa geopotential height for the five most severe WNW HWEs at Hall Beach	124
8-12	Fields of mean 500 hPa geopotential height for the five most severe NW HWEs at Iqaluit	125
8–13	Composite surface map of synoptic conditions during the peak intensity of the five most severe N HWEs at Cambridge Bay	125

CHAPTER 1 Introduction

Nunavut, the largest territory of Canada with 2 million km², extends north and west of Hudson Bay and Hudson Strait, from the treeline to the North Pole (see Figure 1–1). The 30,000 inhabitants [1] of this hostile area of the eastern Canadian Arctic face one of the most extreme climates on Earth.



Figure 1–1: Map of Nunavut showing its 28 communities [2].

Among all the weather hazards experienced in Nunavut, strong surface wind is one of the most severe. In summer, strong surface winds can cause strong waves, high tides and flooding. For the 28 communities of Nunavut, all located close to a large water body, this can have severe impacts.

In winter, strong winds combine with other climate components, like snow and cold air temperature, to cause major hazards. Combined with snow, strong winds cause low visibility that can force airports to shut down. Communities, which heavily rely on air traffic (cargo and travel) thus become isolated. As an example, from February 8 to 18, 1979, at Iqaluit, sustained strong winds with gusts above 25 m/s led to extremely low visibility and kept residents indoors for 10 consecutive days [3]. In communities like Pangnirtung, some houses are fastened to the ground by cables to prevent wind damage. Combined with cold air temperatures, strong surface winds can also lead to severe wind chill factors. For instance, at Hall Beach, on January 13, 1975, surface winds of 17 m/s combined with air temperature at -46°C led to a wind chill of -86°C [4].

Inuit, who heavily rely on fishing and hunting, often expose themselves to strong winds and its associated hazards when they travel. Such impacts can be in any season. The accuracy of weather forecasts is thus very important for them so they can safely plan their trips. However, according to forecasters, Arctic winds are generally poorly predicted by current weather forecasting models.

To better predict the strong surface winds in the Arctic, we need to understand what are the factors contributing to their generation. According to Arctic meteorology manuals [5, 6, 7], there are five important parameters that determine wind speed in the Arctic:

- 1) the synoptic pressure gradients;
- 2) the static stability of the lower troposphere;
- 3) the configuration of terrain;
- 4) the geography;
- 5) the surface roughness.

If we evaluate these factors for Nunavut, we find that:

- 1) the eastern Nunavut is a zone of intense cyclonic activity [8];
- 2) the atmosphere is normally stably stratified year-round [9];
- 3) mountainous terrain is found in eastern Nunavut (Baffin Island and Ellesmere Island);
- 4) Nunavut is characterized by several large water bodies, islands and continental land;
- 5) due to the presence of small or non-existent vegetation, the surface roughness in the Arctic is small.

To adequately assess the importance of each of these parameters on the formation of strong surface winds in Nunavut, we need to first examine previous studies conducted on this subject.

Regarding the Canadian Arctic in general, some studies have focused on adverse weather. For instance, one study focused on the trends in the occurrence of freezing precipitation, blowing snow, fog and low ceilings [10]. Another study examined the occurrence of extreme precipitation events in the cold season within the Canadian Archipelago [11]. A recently submitted study examined a few autumn storms passing

over Baffin Island, with an emphasis on storm structure as well as the associated precipitation and winds [12]. Although strong winds were considered in these studies, they were not addressed in detail.

Regarding the western Canadian Arctic and Alaska, some research on surface winds has been recently conducted. For instance, blowing snow studies [13, 14] have used linearized numerical simulations to model severe wind events over a tundra landscape with modest topography in the western Canadian Arctic. A case study of high wind speed events generated by two deep cyclones in Barrow, Alaska was recently performed [15]. This study focused on the development processes of the two storms and on the contribution of ice cover on cyclonic activity in the western Arctic.

Regarding Nunavut, very little research has focused on surface winds. A recently submitted study [16] connected Inuit knowledge with operational hourly surface observations at Clyde River to study temporal trends of wind speed and direction. A climatological study of low-level jets over Frobisher Bay [9] has shown that winds are strongly affected by the local topography at Iqaluit. It was also found that the strongest winds are almost always oriented with the valley axis and that a low level jet is often observed a few hundred meters above the surface.

Each of these past studies of surface winds in Nunavut has only focused at one particular location. Numerous gaps consequently exist in our understanding of how strong surface winds vary across Nunavut and how the unique features of the Arctic contribute to their formation.

1.1 Research Objectives

Given the importance of Arctic winds and the lack of progress in addressing it, this thesis will focus on this issue. More specifically, it will focus on southern Nunavut since it is the region with the best data coverage in the eastern Canadian Arctic. To make progress, the thesis will furthermore focus on only two aspects of winds so that its objectives are:

- 1) to analyze climatological conditions associated with strong surface winds in southern Nunavut;
- 2) to better understand the roles of synoptic and topographic forcing mechanisms on the generation of strong surface winds in southern Nunavut.

Regarding climatological conditions, we aim to identify the prevailing wind directions during strong wind events and to examine when they preferentially occur over the year. In the climatological study of low-level jets at Iqaluit, it was shown that strong surface winds preferentially occur in winter [9], but whether or not this is representative of a general tendency in Nunavut remains to be examined.

Regarding synoptic forcing, we know that, provided the wind is in gradient balance, i.e. the flow is balanced, cyclones can have larger pressure gradients than anticyclones [17]. For this reason, a special emphasis is on cyclonic storm systems and their associated synoptic pressure gradients. In this context, we will address the following questions:

- Are there common cyclone paths leading to strong wind events at a particular location?
- What are the geographical and meteorological factors determining the location and formation of these cyclones?

• Can a cyclone propagating in the Arctic cause strong surface winds at more than one location?

Regarding topographic forcing, we aim to identify the regional characteristics of strong winds in southern Nunavut, by making connections between their occurrence and the local environment. In many cases, the surrounding topography forms local pressure gradients within the large-scale flow [6]. These pressure gradients can in turn strongly influence the wind speed and direction close to the surface. Very few studies [9, 18] have focused on such orographically-induced flows in Nunavut. Given the importance of topography on Baffin Island, a major aim of this research is to document cases of wind direction and speed being determined by the terrain configuration. In this context, we will address the following questions:

- What are the locations in southern Nunavut where surface topography contributes to the formation of strong winds?
- How does local topography influence strong winds?
- What is the role of atmospheric stability in this interaction?

Due to sparse data over the Arctic, the main focus of this study will be on synoptic disturbances leading to strong surface winds, although, as just discussed, we will also assess the contribution of the smaller-scale impacts of local topography. Correspondingly, we will focus on time-scales of at least a few hours.

However, the focus of this study is not only on maximum wind speeds. In discussions with scientific researchers in Iqaluit [19], it was pointed out that events which are most disruptive generally need to persist as well. As a tool to address this, we will study High Wind Events (HWEs), defined as hourly surface wind speed in

excess of 10 m/s for at least 3 h. More details on this definition will be provided in Chapter 2.

1.2 Thesis Structure

In this thesis, sections are written as somewhat independent units, each with an individual background introduction and description of specific methodology. In terms of structure, it is organized as shown in Figure 1–2.

General concepts and terminology will be introduced in Chapter 2, including the precise definition of a HWE.

In the first part of the thesis (Chapters 3 to 5), a climatology of HWEs will be developed. In Chapter 3, we will provide an overview of the HWEs results. The seasonal occurrence of HWEs will be analyzed in Chapter 4. In Chapter 5, the wind direction distribution of HWEs will be studied. Based on the existence of modes in this wind direction distribution, wind regimes will also be defined.

In the second and most substantive part of the thesis (Chapters 6 and 7), we will investigate how synoptic and topographic forcing contribute to the formation of HWEs. In Chapter 6, we will study the average synoptic and local conditions leading to the most severe HWEs. Chapter 7, we will study the motion of storm systems generating HWEs. More specifically, we will determine the storm tracks leading to HWEs, study cyclone activity associated to HWEs and investigate the spatial connection of HWEs.

The final section, Chapter 8, will summarize the major findings of this study.

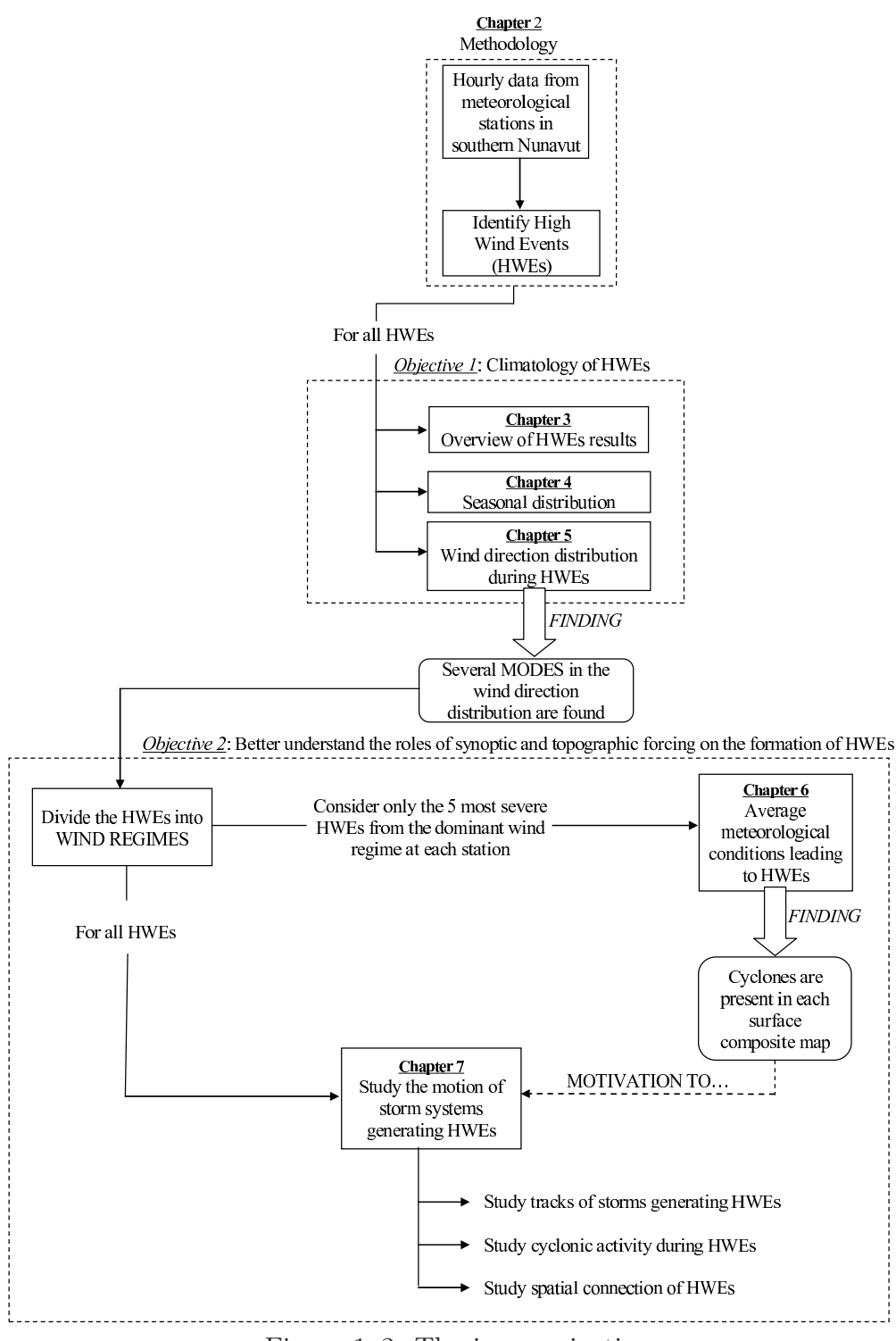


Figure 1–2: Thesis organization.

This chapter presents the general methodology used in this study. High Wind Events (HWEs), which are the basis for all the work carried out in this thesis, are defined and classified. The meteorological stations used in the study are also described. Chapters 4 to 7 will each have their own methods section, in which the specific methodology will be described.

2.1 Definition of High Wind Events

This thesis is concerned with strong winds in the Arctic. However, one has to consider what this means. Here, after consultation with scientists of the Nunavut Research Institute (NRI) [19], a specific definition is developed.

We define HWEs as hourly surface winds continuously in excess of 10 m/s for at least 3 h. This lower value of 10 m/s was used as a cutoff for the occurrence of low-level jets in a climatological study at Iqaluit [9]. This threshold has also been used in some previous studies to determine the occurrence of blowing snow in polar regions [20]. Below 10 m/s, there is relatively little blowing snow. The lower value of 3 h was chosen used to focus on sustained high wind speeds events. In addition, a maximum of 10% of missing hourly data is allowed between the beginning and the end of a HWE.

2.2 Classification of High Wind Events

To identify the most extreme cases, the HWEs are ranked according to a severity index S, defined by Equation 2.1. The severity is based on three factors associated with the HWE: the maximum hourly wind speed u_{max} , the mean wind speed \bar{u} and the duration τ .

$$S = a \frac{u_{max,event}}{u_{max,station}} + b \frac{\bar{u}_{event}}{max(\bar{u}_{station})} + c \frac{\tau_{event}}{max(\tau_{station})}$$
(2.1)

The equation represents a sum of three ratios; in each case, the characteristics of the current HWE are compared to the most extreme value found at the station of interest. a, b and c are weighting factors that determine the importance given to a certain parameter.

The maximum value of severity that can be achieved is equal to the sum of the three coefficients, chosen here to be 100. Thus, a 'perfect' HWE would feature the maximum hourly wind speed, the maximum mean wind speed and the longest duration ever recorded at a station. It is important to understand that the purpose of the severity index is not to compare HWEs from one station to the other, but rather to identify the most severe ones at each location of interest.

After consultation with scientists of the NRI [19], it was pointed out that the worst impact on a local community was normally influenced by the duration of severe wind events. Indeed, sustained winds can trap hunters on the land for several days or limit the delivery of goods for the community assuming air traffic is interrupted. The second most important factor was the maximum gust. Some structures can collapse after a certain threshold is reached in wind speed. The archive of 1-min Automated

Weather Observation System (AWOS) data started recently at Iqaluit, but at other communities only hourly observations are available. Since an hourly observation is a two-minute mean taken in the 10 first minutes following the hour [16], severe wind gusts could have occurred during periods in which the station was not recording. Thus, due to data limitations, we used the maximum hourly wind speed recorded during the event as an indicator of the maximum gust occurring during the HWE. The third parameter in importance is the mean wind speed. This parameter was given the least importance because it was not directly affecting the local population, but it was kept as an indicator of the intensity of the disturbance generating the HWE.

To reflect the relative importance of each parameter, it was decided, in consultation with NRI scientists, to use a=35, b=15 and c=50. Thus, Equation 2.1 becomes:

$$S = 35 \frac{u_{max,event}}{u_{max,station}} + 15 \frac{\bar{u}_{event}}{max(\bar{u}_{station})} + 50 \frac{\tau_{event}}{max(\tau_{station})}$$
(2.2)

2.3 Stations of Interest

By studying several stations in different geographical settings, we are able to measure the regional characteristics affecting the behavior of strong surface winds. This study is based on hourly observations from six Environment Canada meteorological stations (see Table 2–1 and Figure 2–1). Except in a few cases, these stations are assumed to make wind measurements even in extreme weather conditions. The data have furthermore been quality controlled by Environment Canada.

The six stations all offer long-term surface observations as well as sounding data starting at least in 1979, except for Clyde River. At this station, rawinsonde launches stopped in the 1970's. However, Clyde River was still selected because of its unique location on Baffin Island: a coastal site flanked by a mountain range parallel to the coast.

Table 2–1: List of stations and periods of hourly observations used in this study

Station	Latitude	Longitude	Elevation	Period
	(°N)	(°W)	(m)	
Baker Lake	64.3	96.1	18.0	Oct 1962 - Mar 2007
Cambridge Bay	69.1	105.1	27.4	Apr 1955 - Mar 2007
Clyde River	70.5	68.5	26.5	Apr 1977 - Mar 2007
Coral Harbour	64.2	83.4	64.0	Apr 1955 - Mar 2007
Hall Beach	68.8	81.2	8.2	Jan 1956 - Mar 2007
Iqaluit	63.8	68.6	33.5	Jan 1953 - Mar 2007

Prior to January 1971, all operational stations (Baker Lake, Cambridge Bay, Coral Harbour, Hall Beach and Iqaluit) were recording wind direction based on a 16-point scale (22.5° resolution). Since this date, wind directions are recorded based on a 36-point scale (10° resolution). This change in wind direction resolution does not affect the results of our study significantly, thus it is neglected.

The stations, each located at the community's airport, are distributed approximately evenly across southern Nunavut (see Figure 2–1).

Topography varies considerably across southern Nunavut. Within the continental sector of Nunavut and across the Canadian Arctic Archipelago, topography rarely exceeds 500 m. Thus, in terms of weather, the impacts of terrain are rather local than regional [4]. However, in the eastern Canadian Arctic one finds the highest

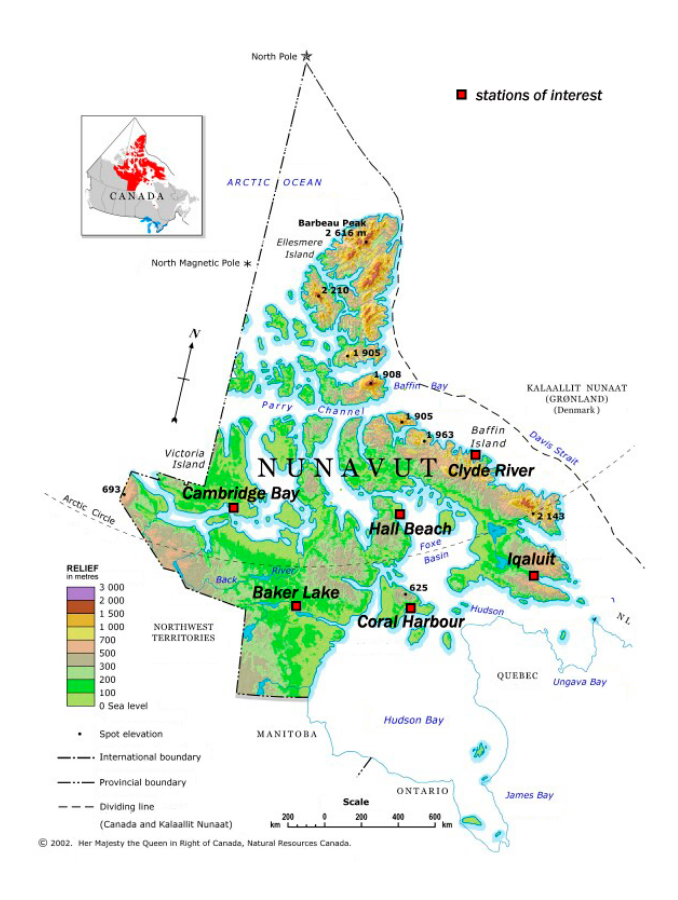


Figure 2–1: Location of the stations of interest used in this study. Adapted from [2]. peaks of North America east of the Rocky Mountains [21]. On Baffin Island, the highest summit, Mount Odin, reaches 2100 m [21]. The important contrast between topographic features in southeastern versus southwestern Nunavut could play a role in determining wind direction and wind speed. For this reason, the geographical environment of each station is detailed below.

2.3.1 Southwestern Nunavut

Baker Lake. Figure 2–2 illustrates the vicinity of the Baker Lake meteorological station. The community of Baker Lake is located at the northwest shore of Baker Lake, a 70 km x 35 km lake [21]. Hudson Bay is situated 300 km to the east-southeast. Terrain near Baker Lake is flat, except for low hills (150 m) to the north-northeast approximately 30 km away. The elevation in the NW-SE direction is low (never above 200 m). This corridor of low terrain is consistent with the blowing snow alley experienced in winter [22]. Indeed, higher elevations are found to the west and northeast of Baker Lake. To the west, terrain reaches 300 m approximately 400 km away, whereas to the northeast, elevation rises to 600 m approximately 300 km away. The hydrological network in this area is very complex, with many lakes and small rivers. The vegetation is characterized by small sparse trees [21].

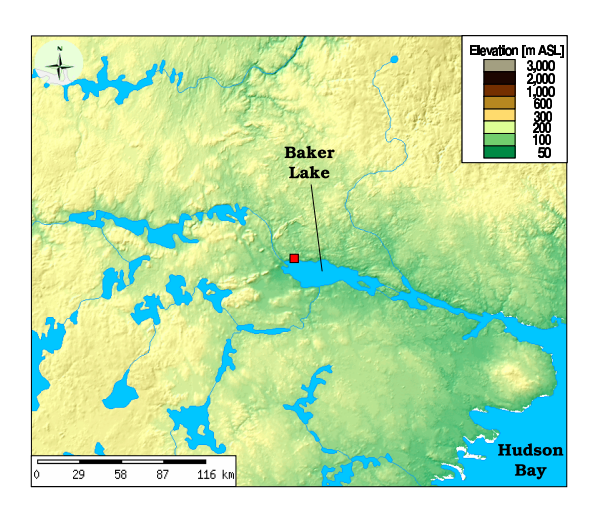


Figure 2–2: Site of Baker Lake meteorological station (red square). Adapted from [2].

Cambridge Bay. Figure 2–3 illustrates the vicinity of the Cambridge Bay meteorological station. Cambridge Bay is located on the southeastern coast of Victoria Island. This island is separated from the main continent by a series of narrow gulfs and straits. The closest of these passages is Dease Strait, which lies to the south and west of the station. The terrain in the area is very flat and the elevation is low, except for an isolated line of hills (highest peak at 210 m) found approximately 15 km to the northeast. There are a few large lakes in the vicinity, and the land is filled with lakes and small rivers [21].

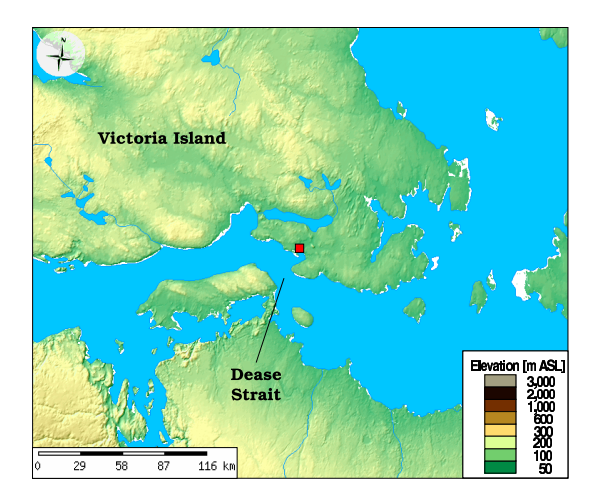


Figure 2–3: Site of Cambridge Bay meteorological station (red square). Adapted from [2].

2.3.2 South-Central Nunavut

Coral Harbour. Figure 2–4 illustrates the vicinity of the Coral Harbour meteorological station, which is located on the south side of Southampton Island. Most of the island has low terrain, except for a mountainous section facing Foxe Basin on the northeast coast. The terrain shows gradual slopes southward toward Coral

Harbour. The highest peaks are located approximately 40 km away from the station [21], situated 64 m above mean sea level. The station is a few kilometers away from South Bay. Southampton Island is surrounded by major water bodies to the south (Hudson Bay, 200 km) and to the northeast (Foxe Basin, 90 km).

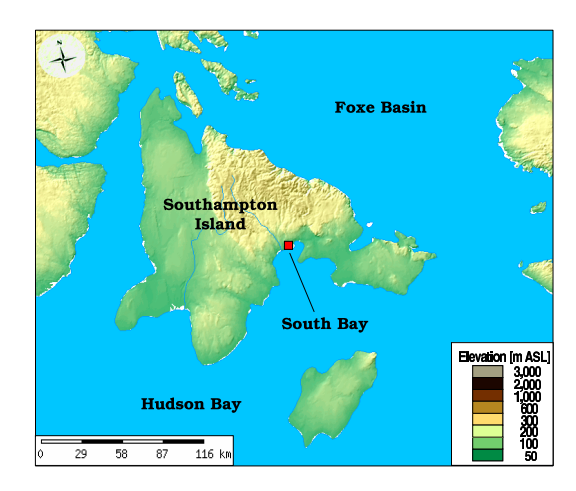


Figure 2–4: Site of Coral Harbour meteorological station (red square). Adapted from [2].

Hall Beach. Figure 2–5 illustrates the vicinity of the Hall Beach meteorological station. Hall Beach is located on Melville Peninsula, which is attached to the continent by its southwestern section. Most of the peninsula is characterized by elevated terrain of approximately 300 m, except its flat northeastern part (60 km wide, 150 km long). Along the west shore of the peninsula (150 km away from Hall Beach), terrain rises to 500 m (see Figure 2–1). Hall Beach is located of the northeast flat side, along the waters of Foxe Basin.

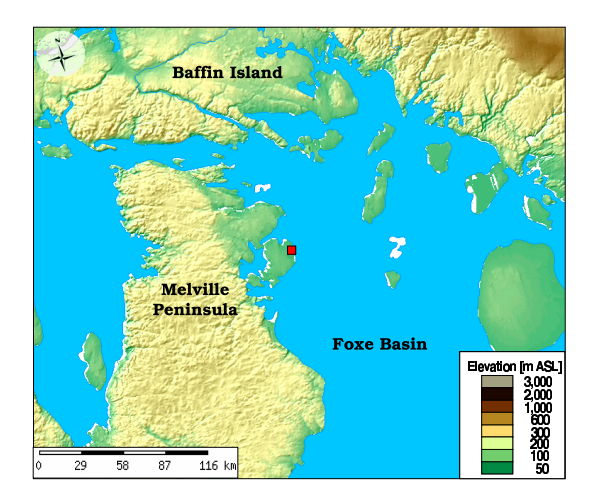


Figure 2–5: Site of Hall Beach meteorological station (red square). Adapted from [2].

2.3.3 Southeastern Nunavut: Baffin Island

Baffin Island, the fifth largest island in the world [5], is approximately 1600 km x 800 km. The west shore is mostly characterized by low terrain (see Figure 2–1). In the east, the island has significant terrain: mountains, icecaps, glaciers. Some peaks reach 2000 m [21]. However, these features are not homogeneous: they are traversed by many inlets, fjords and narrow passages [21]. The island is treeless, and the absence of significant features on the ground leads to low surface roughness [9].

Clyde River. Figure 2–6 illustrates the vicinity of the Clyde River meteorological station, which is located on the east coast of Baffin Island. The station is a few kilometers away from Baffin Bay. Its location at the mouth of Patricia Bay is coincident with the end of a 100-km east-west oriented fjord named Clyde Inlet. This section of Baffin Island has numerous fjords with different orientations. Clyde River's immediate vicinity features is low-lying terrain, except for isolated hills to the southeast. The main topographic feature in the area is the 1000 m NW-SE oriented mountain range on the eastern side of Baffin Island, approximately 70 km to the west.

Iqaluit. Figure 2–7 illustrates the vicinity of the Iqaluit meteorological station. Iqaluit is located on the northwestern end of Frobisher Bay, on the southeastern part of Baffin Island. It is part of a fjord-valley combination with a NW-SE orientation (see Figure 2–1). To the northwest of the station is the Sylvia Grinell river valley. To the west-southwest, the ridges of Meta Incognita Peninsula reaches elevations of 600 m, whereas some peaks reach 750 m. To the north-northeast of the station, on Hall

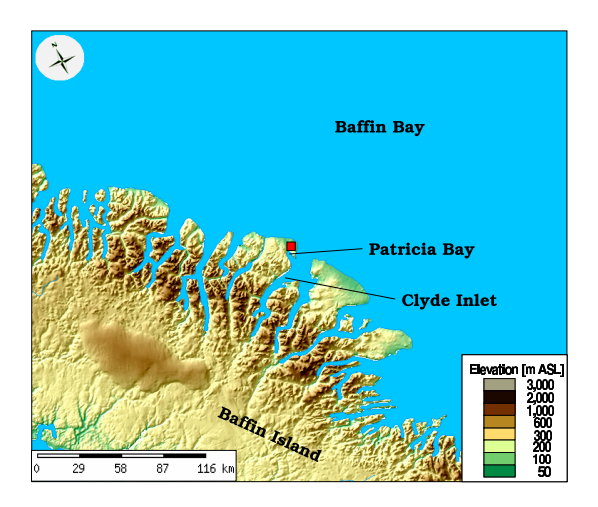


Figure 2–6: Site of Clyde River meteorological station (red square). Adapted from [2].

Peninsula, the terrain is on average higher: 100 km away from Iqaluit, elevations of 1000 m are found.

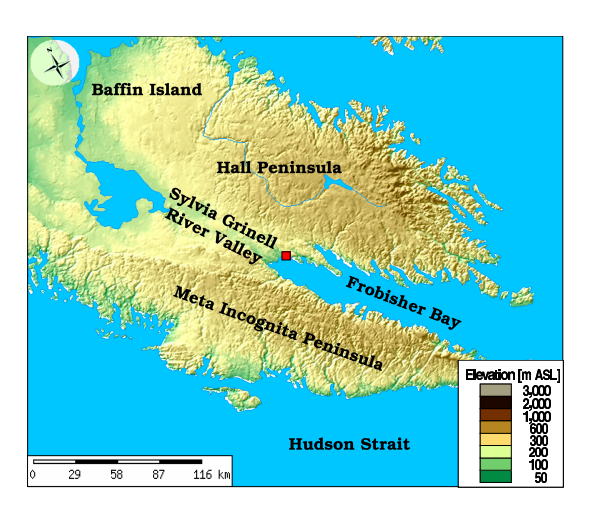


Figure 2–7: Site of Iqaluit meteorological station (red square). Adapted from [2].

${\bf CHAPTER~3}$ Overview of High Wind Events across Southern Nunavut

3.1 Introduction

Using hourly observations from the six Environment Canada meteorological stations, High Wind Events (HWEs) are identified. The objective of this chapter is to provide an overview of these events. The maximum values of HWEs parameters are first listed in Section 3.2. Second, the HWEs distribution among stations is described in Section 3.3. Third, the HWEs severity distribution is detailed in Section 3.4. Finally, trends in the occurrence and severity of HWEs are calculated in Section 3.5.

3.2 Maximum Values of High Wind Events Parameters

In Equation 2.2, the maximum values of u_{max} , \bar{u} and τ at the stations of interest are needed. These maximum values are listed in Table 3–1.

Table 3–1: Maximum values of maximum hourly wind speed u_{max} , mean wind speed \bar{u} and duration τ of HWEs ever recorded at the stations of interest.

Station	Maximum u_{max}	Maximum \bar{u}	Maximum τ
	(m/s)	(m/s)	(h)
Baker Lake	34.4	19.0	147
Cambridge Bay	28.1	19.3	103
Clyde River	31.4	18.9	94
Coral Harbour	40.3	22.0	118
Hall Beach	29.4	22.1	86
Iqaluit	35.8	28.8	155

Overall, maximum values of these variables occurred at only two stations. The maximum hourly wind speed recorded during a HWE was 40.3 m/s. It occurred at Coral Harbour, in a HWE lasting 37 h, with a mean wind speed of 22.0 m/s. The largest mean wind speed within a HWE was recorded at Iqaluit. That specific HWE lasted 4 h and had an average speed of 28.8 m/s. The longest duration within a HWE was also recorded at Iqaluit. In this case, wind speed was in excess of 10 m/s for 155 consecutive hours. Also, note the important contrast with the maximum τ at Hall Beach (86 h): it is almost twice as long at Iqaluit.

An inconsistency was found in the HWE data recorded at Clyde River. It appears unusual that 56% of the maximum hourly wind speed recorded for HWEs were identical, i.e. 25.8 m/s. This value corresponds exactly to 50 knots. The existence of this recurring threshold suggests a saturation problem with the wind sensor signal above 25.8 m/s. Since in this study we consider events as a whole and are not interested in the evolution of meteorological parameters within the event, this inconsistency is not significant.

3.3 High Wind Events at Each Location

The distribution of HWEs among stations is presented in Table 3–2. Baker Lake is the station with the largest annual number of HWEs (79). This is consistent with its status of the 'blizzard capital of Canada' [21]. Indeed, on average, Baker Lake receives more blizzards per year than any meteorological stations in the Canadian Arctic. Since these winter storm systems are typically associated with strong surface winds, it is not surprising that the largest number of HWEs per year occurred at Baker Lake.

Table 3–2: HWEs distribution among stations.

	Total	Years	Years Annual Most severe HWE				S va	lues	
Station	number	of	number	Start date	u_{max}	\bar{u}	au	S_{max}	S_{min}
	of HWEs	data	of HWEs	(mm-dd-yy)	(m/s)	(m/s)	(h)		
Baker Lake	3,534	44.5	79	11-11-69	24.2	16.8	147	87.9	27.6
Cambridge Bay	3,559	52.0	68	10-02-74	28.1	18.9	85	90.9	33.8
Clyde River	1,091	30.0	36	01-04-80	25.8	15.4	86	86.8	31.7
Coral Harbour	2,854	52.0	55	11-22-90	25.8	16.1	118	83.4	25.4
Hall Beach	2,737	51.3	53	09-27-75	24.7	17.0	78	86.3	32.1
Iqaluit	3,044	54.3	56	02-10-79	23.1	15.9	155	80.8	25.5
Total	16.819			•	•	-			

On the other hand, the station with the smallest annual number of HWEs is Clyde River (36). This station is likely to be protected by the important NW-SE mountain barrier located to its west, as described in Section 2.3.3.

3.4 Severity Distribution

The severity distribution of HWEs is presented in Figure 3–1. To allow for comparisons between the individual stations, the severity distribution is calculated on an annual basis.

In all cases, very few HWEs have S > 60. This means that very few HWEs have values of u_{max} , \bar{u} , and τ close the maxima found in Table 3–1 all occurring at the same time. At all stations, the distribution are positively skewed, indicating as expected that most of the HWEs have a low severity.

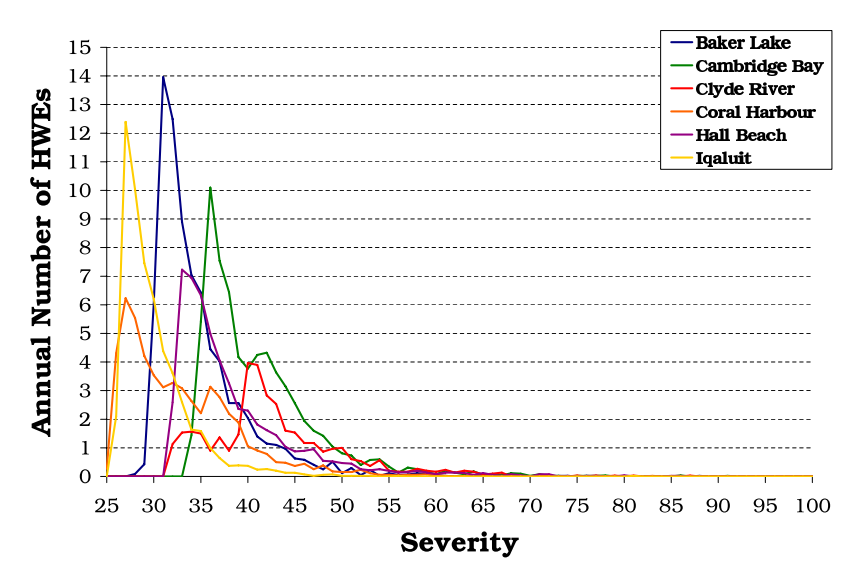


Figure 3–1: Severity distribution among HWEs.

Regarding the HWE results at each location, as shown in Table 3–2, the most severe HWE occurred at Cambridge Bay (with S=90.9). The least severe HWE, with S=25.4, occurred at Coral Harbour. The Coral Harbour severity distribution contains a major peak at S=27, but there are also two minor peaks at S=32 and S=36. Similarly, Clyde River shows a significant spread in its distribution. Clyde River has the smallest annual number of HWEs, but the largest mean severity ($\bar{S}=42.8$). Thus, although HWEs do not occur very often at this location, they are more likely to be more severe when they do. Iqaluit only has one narrow peak in its distribution, as for Baker Lake. On the other hand, some stations have more than one peak in their distribution; Cambridge Bay and Hall Beach have two, Coral Harbour and Clyde River have three.

3.5 Trends in High Wind Events

Here, an examination was developed for all stations as to whether, on decadalscales, there was any indication of change in the occurrence and severity of HWEs. In all cases, only decades in which stations had complete data coverage were studied.

First, decadal trends in the number of HWEs per station are presented in Figure 3–2.

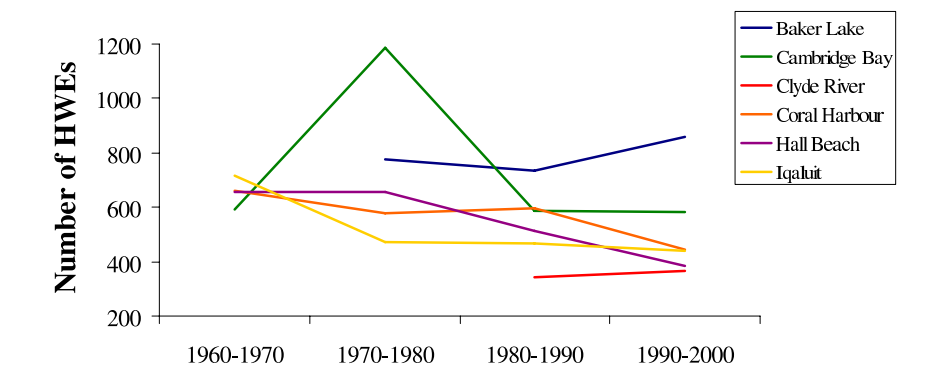


Figure 3–2: Decadal trends in the number of HWEs.

As seen in Figure 3–2, no overall obvious trend in the number of HWES is found. At four stations (Cambridge Bay, Coral Harbour, Hall Beach and Iqaluit), the number of HWEs per decade slightly decreases with time. At Baker Lake and Clyde River, the number slightly increases with time. However, these variations are not consistent from one station to the other.

Second, we need to investigate how the severity of HWEs has varied over the past decades. To address this, trends in the mean decadal HWE severity are presented in Figure 3–3.

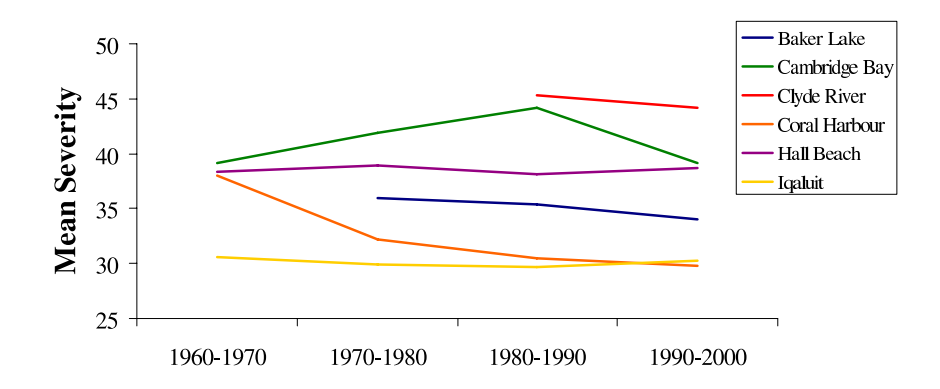


Figure 3–3: Decadal trends in the mean HWE severity.

As seen in Figure 3–3, the mean HWE severity tends to stay approximately the same over the decades.

Third, trends in the mean severity for values above the 95^{th} percentile were computed (see Figure 3–4).

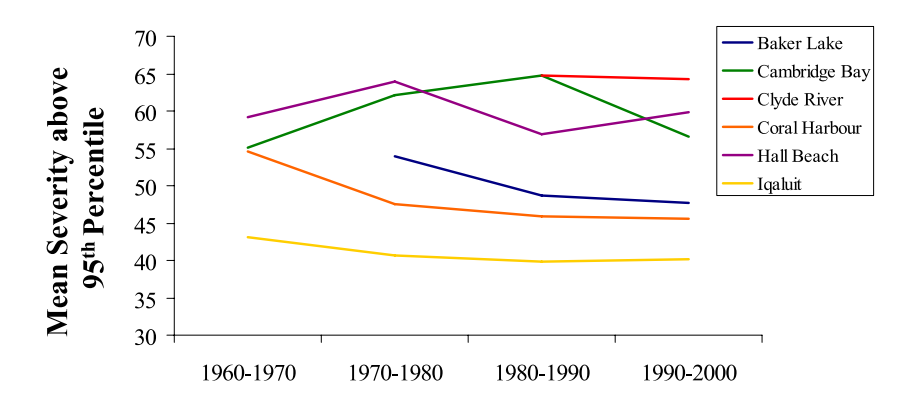


Figure 3–4: Trends in the mean severity for values above the 95th percentile.

As seen in Figure 3–4, no overall trend in the mean severity of the top 5 decadal percentile is observed. At most stations (i.e. Clyde River, Coral Harbour, Hall Beach and Iqaluit), this parameter has been slightly decreasing over the past decades whereas at the two other stations, it has been slightly increasing.

Finally, trends in the maximum HWE severity per station are presented in Figure 3–5.

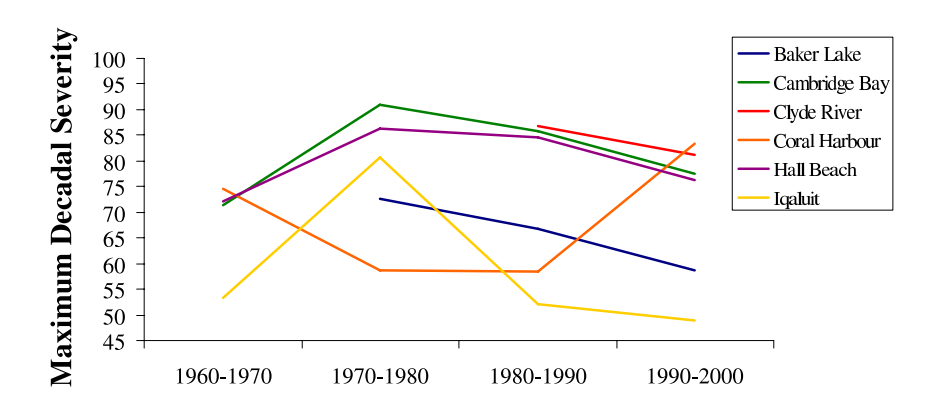


Figure 3–5: Trends in the maximum decadal HWE severity.

As shown in Figure 3–5, at Baker Lake and Clyde River, there is a slight decreasing tendency. At Cambridge Bay and Hall Beach, the maximum severity per decade slightly increase. However, no trends are observed for Coral Harbour and Iqaluit. There is thus no consistent trend in the values of the maximum severity observed per decade.

To summarize, no significant decadal trend in the number, mean severity and maximum severity of HWEs was observed.

CHAPTER 4 Seasonal Occurrence of High Wind Events

4.1 Introduction

One of the objectives of this study is to develop a climatology of High Wind Events (HWEs). In this specific chapter, we investigate how the occurrence of HWEs varies by season.

To a large extent, strong wind events depend on the existence of large-scale pressure gradients, which vary from one season to the other, depending on cyclonic activity and intensity. In a recent study of seasonal variations in cyclonic intensity, it was found that the cold season (October to April) experienced a greater cyclonic intensity than the months of the warm season (May to September) [23]. In this case, intensity refers to local deviations from the monthly mean surface pressure. Additionally, it was found that in winter an increased number of storm systems reaching the Arctic originates from the mid-latitudes, and that on average, these storm systems are deeper than the ones originating in the Arctic [23].

This chapter will study the seasonal distribution of HWEs and try to relate it to the seasonal variations in cyclonic intensity observed in the Canadian Arctic.

4.2 Methods

Following [9, 10], we divide seasons into 3-month groups: winter (January to March), spring (April to June), summer (July to September) and autumn (October to

December). For the periods of data used in this study (see Table 2–1), the frequency of seasonal occurrence of HWEs is then determined.

4.3 Results

Figure 4–1 shows the overall seasonal distribution for the total number of HWEs recorded at the six different stations.

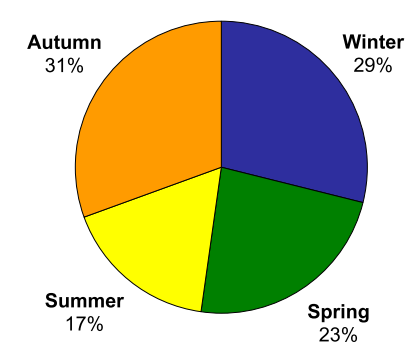


Figure 4–1: Overall seasonal occurrence of HWEs for all stations.

Overall, in southern Nunavut, autumn is associated with the largest number of HWEs. In autumn, the cyclones are typically more energetic due to greater air mass contrasts and since open water is at its maximum [21]. Autumn is closely followed by winter (only 2% less HWEs observed), spring and to a less extent summer.

The seasonal distribution of HWEs at each individual station is shown in Figure 4–2.

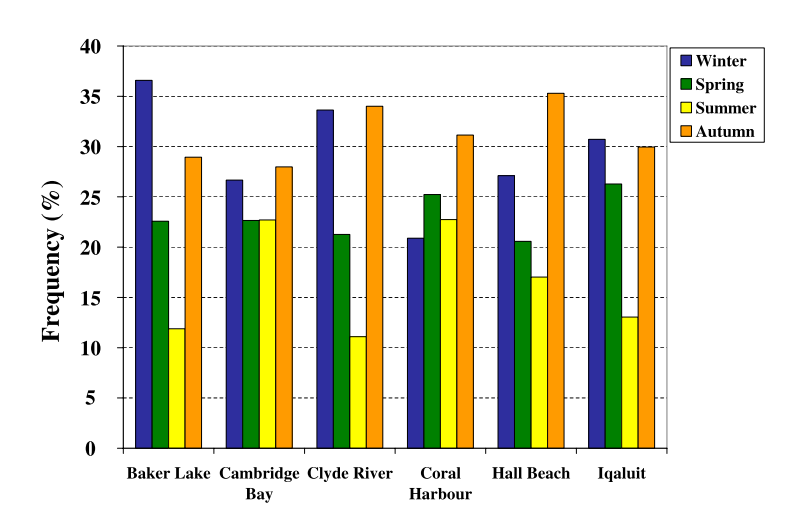


Figure 4–2: Seasonal occurrence of HWEs at each station.

Similarities of geographical setting could explain the resemblances between seasonal distributions at different stations. For instance, Coral Harbour and Hall Beach, which are located only 500 km apart, are both located close to at least one major water body: Foxe Basin and Hudson Bay for Coral Harbour, Foxe Basin for Hall Beach. For both stations, the autumn is, by at least 5%, the most active season in terms of severe wind events.

At Cambridge Bay, Clyde River and Iqaluit, the distribution of HWEs is well-balanced between winter and autumn. At Iqaluit, the seasonal distribution is in accordance with the climatological study of low-level jets at Iqaluit [9], which shows that high winds at the surface on an hourly basis are most frequently observed during autumn and winter.

Clyde River and Iqaluit also show a similar seasonal occurrence of HWEs: the percentage of HWEs in winter and in autumn is almost equal, and spring has more HWEs than summer. The similarity between these two stations could also be explained by the proximity to the same storm tracks. Indeed, it is known that in autumn, storms from the Atlantic enter Davis Strait via Labrador Sea [4]. In Section 7.4, we will further consider the impacts of the same storm systems at different locations.

At all stations except Coral Harbour, the two seasons with the most severe wind events are autumn and winter. For instance, at Baker Lake, 37% of severe wind events occur in winter. At this location, the occurrence of HWEs in summer is only a third of the wintertime cases.

As just mentioned, Coral Harbour is the only location where winter is the season with the smallest percentage of HWEs. Since there is not a lot of variation for the occurrence of HWEs between spring, summer and autumn at Coral Harbour, the fact that winter is the season with the smallest occurrence of HWEs could also be not statistically significant. Mean winter climatological fields of geopotential height at 500 hPa were inspected [8] in the vicinity of Coral Harbour to measure if upperair support could explain this. The lack of significant spatial variations in the 500 hPa gpm field over the stations used in this study suggests that sub-synoptic-scale processes could explain why winter is the season with the smallest occurrence of HWEs at Coral Harbour. Perhaps the mountains to the north of the station could protect Coral Harbour from the prevailing northwesterly winds in winter [21].

Overall, the cold season (autumn and winter [23]) is the one in which most of the HWEs (60%, see Figure 4–1) are observed in southern Nunavut. This is consistent with the greatest large-scale pressure gradients typically being observed at that period [23].

CHAPTER 5 Prevailing Wind Directions during High Wind Events

5.1 Introduction

As a component of the climatology of High Wind Events (HWEs), in this specific chapter we investigate the wind direction distribution during HWEs. This will indicate if there is a relationship between the station's environment and the favored wind directions during HWEs.

Characteristics of the topography in the vicinity of a meteorological station can strongly affect wind direction and speed at low levels. There are three important parameters that influence the behavior of a flow approaching a topographic feature [7]:

- 1) the static stability of boundary-layer stratification;
- 2) the terrain characteristics (height, slope ...);
- 3) the magnitude of the approaching wind.

In the Arctic, the atmosphere remains relatively stably stratified throughout the year [9]. As a result, orographic lifting is often not sufficient to overcome this negative buoyancy and the low-level air is thus constrained to flow around topographic features [20]. Moreover, due to the ensuing limited vertical turbulent flux of momentum, this situation often disconnects the winds close to the surface from those above.

In this study, two orographic-induced flows will be discussed: barrier jets in Section 5.1.1 and channeled winds in Section 5.1.2. The prevailing wind directions

will then be studied for cases when severe winds affected the stations of interest. The effects of the station's environment (topography, hydrography, proximity to storm tracks) on wind direction will be studied. Based on the predominance of certain wind directions for strong surface winds, the High Wind Events (HWEs) will then be divided into different categories, referred to here as wind regimes.

5.1.1 Barrier jets

When cold and stably-stratified air is persistently impinging on a high mountain range, due to its resistance to lifting, the airmass can be blocked and accumulate against the barrier [7]. This situation is called cold air damming. Due to large differences in potential temperatures between the cold air at low level and the warmer air aloft, a local pressure gradient builds perpendicular to the mountain range [24]. The air at low levels is then forced to flow parallel to the coastal topography, with the barrier to its right in the Northern Hemisphere [24]. This low-level jet is called a barrier jet.

Cold-air damming is known to occur along the eastern flank of the Appalachian Mountains (as an example, see Figure 5–1), but also along the east coast of Baffin Island [25]. Of all the stations considered in this study, cold air damming can only occur at Clyde River since it is the only station located on the eastern flank of a major mountain range.

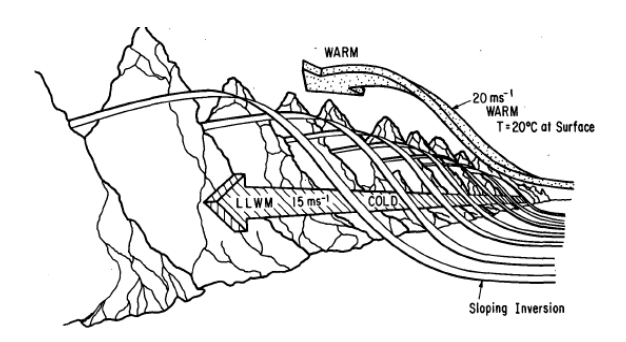


Figure 5–1: Example of cold-air damming in the Appalachian mountains (1200 UTC 22 March 1985). The barrier jet is represented by the low-level wind maximum (LLWM). Adapted from [26].

5.1.2 Channeling

Channeling results due to the interaction between overlying winds and valley winds. Different mechanisms describe this interaction:

- 1) pressure-driven channeling;
- 2) downward turbulent flux of momentum;
- 3) thermal forcing.

Pressure-driven channeling occurs when large-scale pressure gradients have a component along the valley axis, i.e., if the overlying flow has a component perpendicular to the valley. Assuming a x-axis parallel to the valley axis and an angle α between the x-axis and the overlying flow, the along-valley component of the geostrophic pressure gradient ∇p is described by the following relationship [27]:

$$\frac{\partial p}{\partial x} = |\nabla p| \sin \alpha \tag{5.1}$$

From Equation 5.1, we see that when the overlying flow is perpendicular to the valley axis (i.e. $\alpha = 90$ or 270°), pressure-driven channeling is maximized. Pressure-driven channeling produces along-valley winds (see Figure 5–2). Then, within the valley, the winds blow from high pressure to low pressure [7].

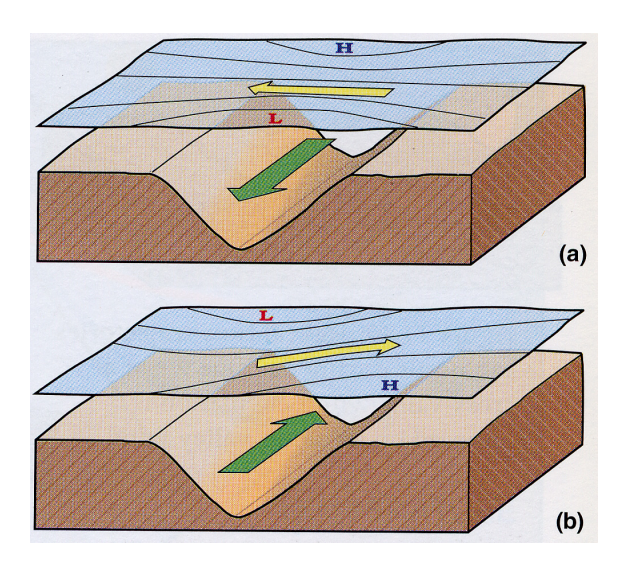


Figure 5–2: Different positions of a cyclone and an anticyclone in a situation of pressure-driven channeling. In a), pressure-driven channeling is maximized, whereas it is less optimal in b). Overlying winds are in yellow, valley winds are in green. Adapted from [7].

Downward turbulent flux of momentum takes place when the wind above ridgetop level has a component along the valley axis at lower levels (see Figure 5–3). It is intensified when the stratification is unstable or neutral, and in shallow valleys with a flat surface [7], as the vertical momentum exchange between valley winds and overlying winds is enhanced.

In a recent climatology of low-level jets at Iqaluit, it was found that thermal effects are not a significant factor in the formation of strong winds [9]. In this study, thermally-driven wind circulations are therefore neglected. Thus, the emphasis is

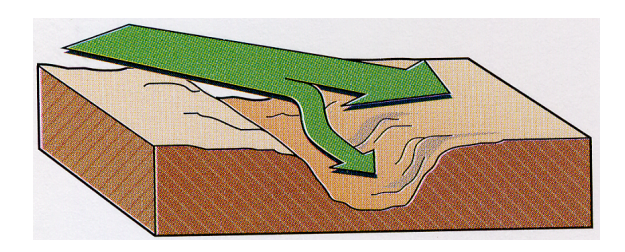


Figure 5–3: Qualitative representation of downward turbulent flux of momentum. Adapted from [7].

placed on two of the contributing factors: pressure-driven channeling and downward turbulent flux of momentum.

Considering only large-scale pressure gradients and assuming a straight valley with a steady geostrophic wind above ridge-top level, two ideal scenarios can occur. As mentioned previously, pressure-driven channeling is the most efficient contributing factor in a situation in which the geostrophic wind above ridge-top level is perpendicular to the valley axis, maximizing the horizontal along-valley pressure gradient. However, the downward turbulent flux of momentum would be maximized when the geostrophic wind is aligned with the valley axis. Indeed, downward momentum transfer associated with cross-valley winds would lead to strong turbulence inside the valley and dissipation of energy [9]. Qualitatively, there is thus an inverse relationship between pressure-driven channeling and downward turbulent flux of momentum: when one is optimized, the other is minimized. In general, both pressure-driven channeling and downward turbulent flux of momentum contribute to valley winds.

When the winds above ridge-top level are weak to intermediate, pressure-driven channeling is the dominant forcing factor for the valley winds. In cases of strong

winds above mountain-top level, downward turbulent flux of momentum is a significant forcing mechanism for the boundary-layer flow when the atmosphere is weakly stable [27, 18], since the vertical exchange of momentum is enhanced.

Of all the stations considered in this study, only Iqaluit is situated in a topographic setting favoring the occurrence of channeling, since it is located in a largescale fjord-river valley configuration.

5.2 Methods

For the calculation of wind roses, we used Environment Canada hourly observations of winds (speed and direction) only during HWEs. The resulting wind rose shows the frequency distribution of wind directions during HWEs. They are divided in 16 sectors and 4 wind classes: 10.0 - 12.5 m/s; 12.5 - 15.0 m/s; 15.0 - 17.5 m/s; 17.5 m/s and more.

We inspect the wind direction distribution at the 10°-resolution, identify local maxima and define a 50° sector for each of them. Each of these local extrema is called a wind regime. In some cases, we defined wind regimes based on the local configuration of terrain, to allow important wind directions to be studied as well. These include downslope winds in Iqaluit and Clyde River.

Then, we identified the most frequently occurring wind direction (i.e the mode of the wind direction distribution) for each HWE and associated it with the appropriate wind regime. It is important to note that this method is not effective when important shifts in wind direction are seen during the HWE. Indeed, considering the mode of the wind direction distribution excludes all the other wind directions that could have been observed. HWEs in which no modes in the wind distribution are observed are not considered in this study. They only represent 3% of the total number of HWEs.

5.3 Results

5.3.1 Baker Lake

Hourly observations of surface winds during HWEs at Baker Lake are presented in Figure 5–4.

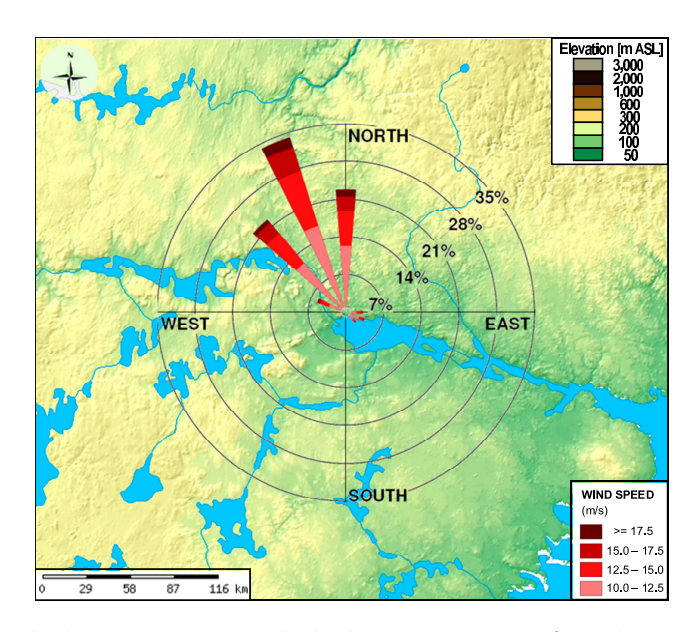


Figure 5–4: Wind directions recorded during HWEs for the period 10/1962 to 03/2007 at Baker Lake (located at center of the wind rose). Background map adapted from [2].

It should be noted that 79% of winds comes from either the NW, NNW or N. Winds from the northwest quadrant are regularly associated with blowing snow events [21]. Of the surface winds occurring during HWEs, 84% are below 15 m/s (see Table 8–1). The northerly winds represent 45% of winds above 17.5 m/s. The wind regime appears unimodal, but an inspection of the local maxima in the wind

direction distribution reveals 3 wind regimes: NNW (66% of the HWEs), WNW (17% if the HWEs) and ESE (8.5% of HWEs) (see Table 5–1). The east-southeasterlies typically occur when storm systems approach Baker Lake from the west [21].

5.3.2 Cambridge Bay

Hourly observations of surface winds during HWEs at Cambridge Bay are presented in Figure 5–5.

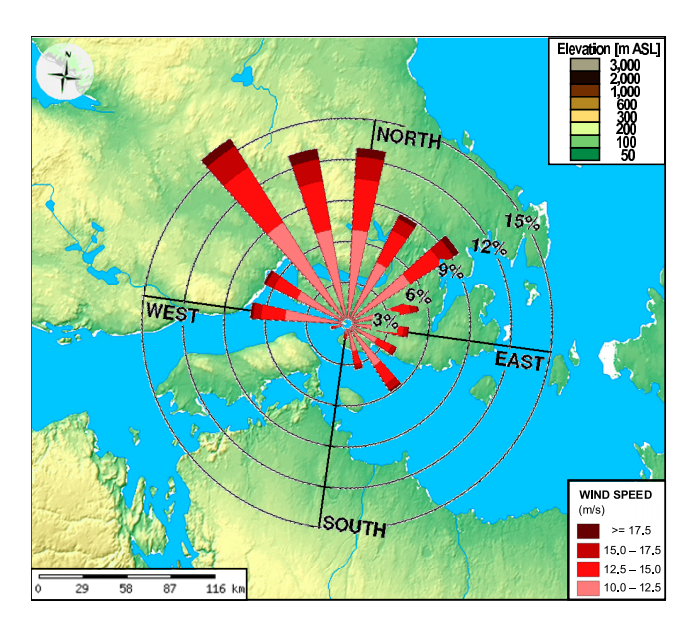


Figure 5–5: Wind directions recorded during HWEs for the period 04/1955 to 03/2007 at Cambridge Bay (located at center of the wind rose). Background map adapted from [2].

Cambridge Bay is the station illustrating the largest diversity in prevailing wind directions during HWEs, a vast majority of them have a northerly component. Of the hourly data observed during HWEs, 14% exceed 15 m/s (see Table 8–2).

Five local maxima were identified based on the wind rose: NW (27% of the HWEs), N (22% of the HWEs), W (14% of the HWEs), NE (14% of the HWEs) and SE (12% of the HWEs) (see Table 5–1).

5.3.3 Clyde River

Hourly observations of surface winds during HWEs at Clyde River are presented in Figure 5–6. At Clyde River, winds almost exclusively originate from the NW

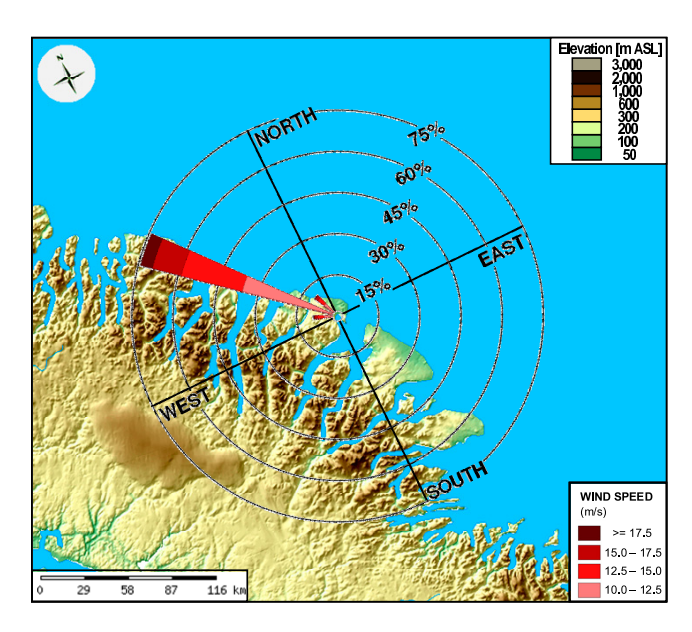


Figure 5–6: Wind directions recorded during HWEs for the period 04/1977 to 03/2007 at Clyde River (located at center of the wind rose). Background map adapted from [2].

quadrant. Although too small to be seen on Figure 5–6, the proportion of SE winds is extremely low. It is important to note that 10% of the downslope winds (from the SW) are greater than 17.5 m/s, whereas for the northwesterlies, this value is almost two times less (5.9%) (see Table 8–3). However, 81% of hourly wind speeds exceeding 17.5 m/s originated from the NW. Wind regimes at Clyde River appear unimodal,

but downslope winds (from the SW) are also considered. Thus, there are two wind regimes at Clyde River, as shown in Table 5–1): NW (88% of all the HWEs) and SW (5.2% of all the HWEs).

5.3.4 Coral Harbour

Hourly observations of surface winds during HWEs at Coral Harbour are presented in Figure 5–7.

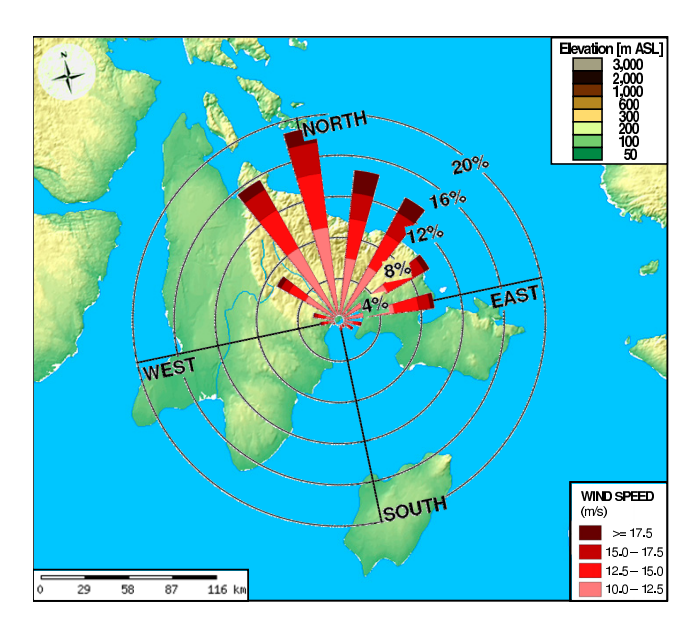


Figure 5–7: Wind directions recorded during HWEs for the period 04/1955 to 03/2007 at Coral Harbour (located at center of the wind rose). Background map adapted from [2].

It is important to note that 82% of the winds have a northerly component. Coral Harbour has 23% of surface winds above 15 m/s (see Table 8–4). This represents the largest percentage of strong winds over all the stations. This is also the station that has recorded the largest hourly wind speed (40 m/s, see Table 3–1). Winds from the NNE showed the highest speeds: 15% of the winds were above 17.5 m/s. No

well-defined narrow ranges of prevailing wind directions are found at Coral Harbour. Three wind regimes were identified: NNW, NE and E (see Table 5–1). The two main dominant ones come from the NNW (38% of the HWEs), and the NE (30% of the HWEs). E blow predominantly in 18% of the cases.

5.3.5 Hall Beach

Hourly observations of surface winds during HWEs at Hall Beach are presented in Figure 5–8.

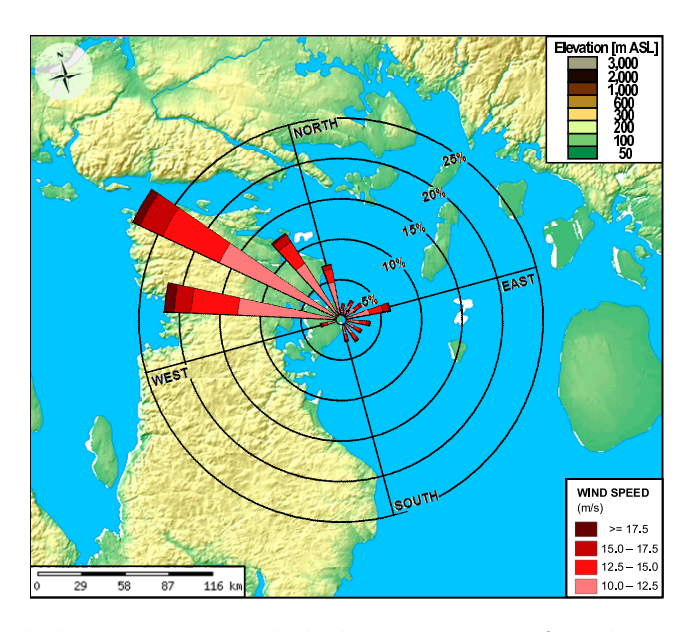


Figure 5–8: Wind directions recorded during HWEs for the period 01/1956 to 03/2007 at Hall Beach (located at center of the wind rose). Background map adapted from [2].

At Hall Beach, the majority of surface winds during HWEs come from the NW. At this meteorological station, 34% of the winds greater than 17.5 m/s were from the WNW (see Table 8–5). This is the wind direction associated with the highest percentage of strong winds. On the other hand, 92% of the winds from the N were

smaller than 15 m/s. We can conclude that this is not a wind direction typically associated with strong surface winds. Overall, only 3.3% of the surface winds during HWEs were greater than 17.5 m/s. There are two dominant modes at Hall Beach: WNW (37% of the HWEs) and NNW (32% of the HWEs). A third wind regime was also defined, ESE, which represents only 9.6% of the cases of severe winds (see Table 5–1).

5.3.6 Iqaluit

Hourly observations of surface wind directions during HWEs at Iqaluit are presented in Figure 5–9.

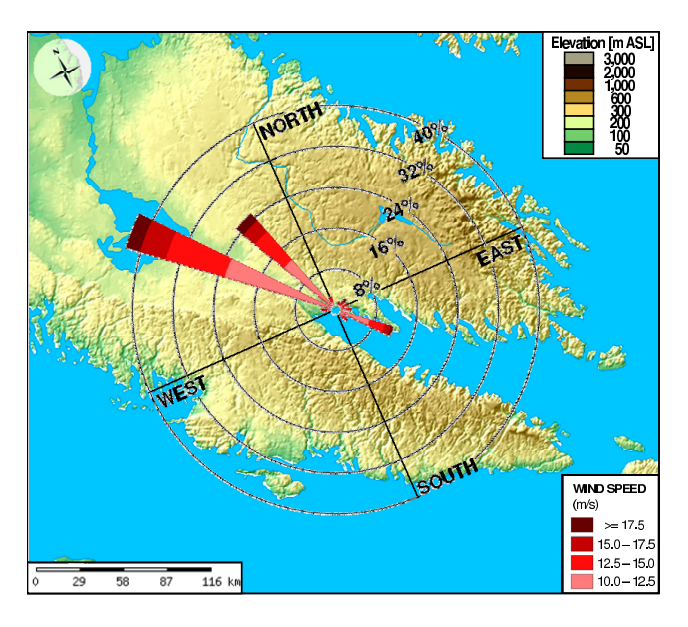


Figure 5–9: Wind directions recorded during HWEs for the period 01/1953 to 03/2007 at Iqaluit (located at center of the wind rose). Background map adapted from [2].

Winds are closely aligned with the valley 89% of the time, mostly from the northwest. Although very small on Figure 5–9, the cross-barrier flows (NE, SW) represent 11% of strong surface winds (see Table 8–6). Note that 24% of the ENE

winds were greater than 17.5 m/s, whereas only 6.5% of NW winds were greater than 17.5 m/s.

Although the bimodal distribution is obvious here, the ENE downslope winds are considered. Thus, three wind regimes are also considered at Iqaluit. In order of importance: NW, SE and ENE (see Table 5–1). Indeed, 66.8% of the HWEs at Iqaluit are dominated by NW winds. The other wind regime aligned with the fjord-river valley combination at Iqaluit, SE, showed a lower percentage: 18%. Finally, ENE were found in majority in 7.4% of the severe wind events.

5.3.7 Distribution of Wind Regimes

As a summary, the distribution of wind regimes for each station is illustrated in Table 5–1.

5.4 Discussion of Wind Regime Results

5.4.1 Baker Lake

Baker Lake is located on flat terrain, but the orographic features show slightly elevated terrain to the southwest and northeast and a flat corridor in the opposite directions. This low level alley is well-aligned with the prevailing NNW winds at Baker Lake (see Figure 5–4). Two factors could explain the northerly prevailing wind direction at Baker Lake: the proximity of Hudson Bay, a zone where cyclones tend to stall, and its location in the blowing snow corridor in wintertime (see Chapter 4).

5.4.2 Cambridge Bay

Flat terrain and the near absence of vegetation make Cambridge Bay vulnerable to strong winds from several directions [22]. Indeed, at Cambridge Bay, five wind regimes above with a frequency of occurrence greater than 10% are found, as shown in Table 5–1.

5.4.3 Clyde River

The prevailing winds during HWEs at Clyde River are strongly aligned with the mountain barrier, which is in the NW-SE orientation (see Figure 5–6). The unimodal distribution is composed of NW winds, and a very low percentage of SE winds. This suggests that cold air damming could occur during strong wind events and form barrier jets.

5.4.4 Coral Harbour

Due to the presence of terrain to the north of Coral Harbour, the prevailing northerly winds cause subsiding flow. This subsiding flow, combined with the significant land masses to the northwest, results in a climate that is mostly continental [28], except for a few months in summer. This is unique considering the proximity of the community to large water bodies (Hudson Bay, Foxe Basin). Indeed, based on the station's location, we would suspect a maritime climate.

5.4.5 Hall Beach

The distribution of wind regimes does not seem to be affected by the local topography at Hall Beach (see Figure 5–8). The vicinity of the station is very flat and there are no prominent mountainous features in the area. This is the station

with the smallest proportion of wind speeds above 15 m/s (13%). On the other hand, Coral Harbour, found only 500 km to the south, shows the highest frequency of winds above 15 m/s. Although the stations are close to each other, the strong winds could be the result of very different storm tracks.

5.4.6 Iqaluit

From Figure 5–9, it can be seen that terrain affects wind direction for strong wind events at Iqaluit. The mean bimodal (NW-SE) distribution, aligned with the local topography axis, is an indication that channeling is occurring. The fact that ENE winds are more often associated with high wind speeds than along-valley winds might be an indication of a threshold in wind speed at upper levels. When the winds aloft are strong, and especially in cases of weak static stability, they can force the winds at lower levels to adjust to geostrophic balance.

5.4.7 Overall Discussion

At all stations, the most important wind regime originates from the NW quadrant. Climatologically, this could be explained by the presence of high pressure to the west of the stations and low pressure in the Baffin Bay region in winter [5] (see Figure 5–10).

At Iqaluit and Clyde River, there is a tendency for winds to align with the local topography axis. The wind roses of these two stations (see Figures 5–6 and 5–9) suggest that orographic-induced flows are observed during strong wind events. Additionally, a greater percentage of downslope winds are associated with high wind speeds than in the case of winds aligned with the topography. Thus, the relationship

between the winds above and below mountain-top level is likely to be key factor in the generation of strong surface winds at these two locations.

Stations located on flat terrain (Baker Lake, Cambridge Bay, Coral Harbour and Hall Beach) tend to have a greater spread in the distribution of prevailing wind directions. This suggests their absence of topography exposes them to several wind directions.

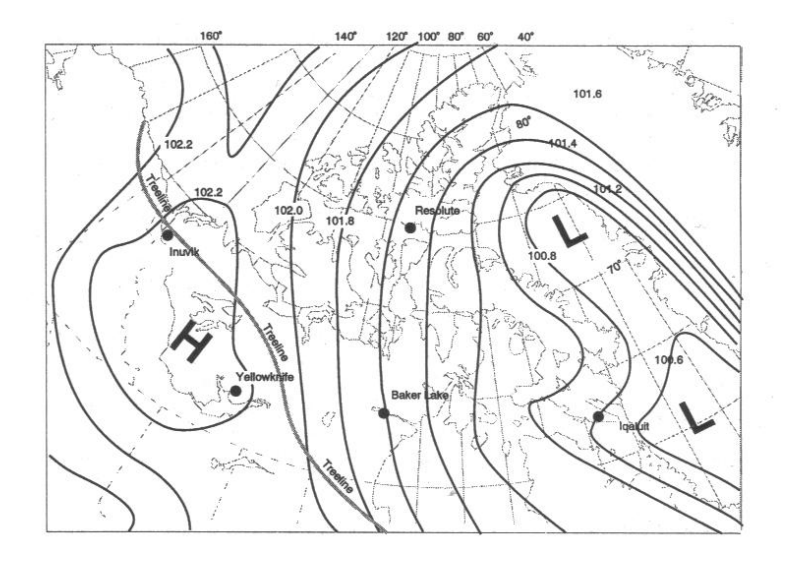


Figure 5–10: Mean pressure pattern over the Canadian Arctic for January. Adapted from [29].

Table 5–1: Frequency distribution of wind regimes during HWEs at each station. The wind regimes are presented in their order of importance. Frequency refers to the fraction of HWEs characterized by a particular wind regime. Dominant wind regimes are bolded.

Station	Wind regime	Frequency		
		(%)		
Baker Lake	NNW	66.1		
	WNW	16.7		
	others	8.74		
	ESE	8.46		
Cambridge Bay	NW	26.6		
	N	22.2		
	W	13.9		
	NE	13.6		
	SE	12.4		
	others	11.3		
	NW	88.3		
Clyde River	others	6.51		
	SW	5.22		
	NNW	37.5		
Coral Harbour	NE	30.0		
	E	17.5		
	others	15.0		
Hall Beach	WNW	37.3		
	NNW	32.3		
	others	20.8		
	ESE	9.61		
Iqaluit	NW	66.8		
	SE	18.1		
	others	7.75		
	ENE	7.39		

6.1 Introduction

In Chapters 3 to 5, we developed a climatology for all High Wind Events (HWEs). Because of their probable strong impact on communities, it is important to examine the most severe ones in more detail.

In this chapter, we will therefore investigate the large-scale conditions leading to the five most severe HWEs from the dominant wind regime at each station. Composite surface maps of the most severe HWEs will be produced and discussed to highlight similarities and differences between the different stations used in this study.

To accomplish this, model products from global reanalyses will be used. In recent years, with the improvement of data assimilation techniques and their increased resolution, global reanalyses are an important tool for the study of the Arctic atmosphere [30].

Before discussing our analysis in Sections 6.2 to 6.9, we will consider three aspects of the Arctic large-scale weather systems: synoptic climatology in Section 6.1.1, circumpolar vortex in Section 6.1.2 and atmospheric stability in Section 6.1.3.

6.1.1 Synoptic Climatology

Large-scale synoptic pressure gradients are a major factor leading to the formation of HWEs in southern Nunavut. Thus, it is important to study the spatial and temporal distribution of zones of synoptic activity.

In the Canadian Arctic, the cyclonic activity highly varies meridionally. The cyclone frequencies (cyclone passages per month) are higher in the eastern half of the Canadian Arctic than in the western half [8, 6, 4], particularly over Baffin Bay [31, 6]. In the western half, high pressure is found from the southeastern Arctic Ocean to the Prairies [21] (see Figure 5–10). This anticyclone-cyclone synoptic configuration results in a blowing snow alley due to strong northwesterly winds in the central Canadian Arctic archipelago [10].

Out of the total number of cyclones observed in the Arctic, 25% originate from lower latitudes [23]. These extra-tropical cyclones are typically occluded or in the final stages of their existence [32]. It should be noted however that in some sectors of the Arctic such as Baffin Bay, these storms can re-develop over open waters, even in winter [5].

6.1.2 The Circumpolar Vortex

In the Arctic, surface weather disturbances are strongly influenced by the position and strength of the polar vortex, which extends from the middle troposphere to the stratosphere [33]. The jet streams associated with the polar vortex can steer surface disturbances and force them to strengthen, to propagate or to weaken. The zones located directly below the circumpolar vortex are characterized by the presence of occluded, stalled and very cold cyclones [5].

During spring and summer, the north-south temperature gradient decreases and the circumpolar vortex reduces in both size and strength. However, as winter approaches, the circumpolar vortex progressively gains in size and strength, as seen on Figure 6–1.

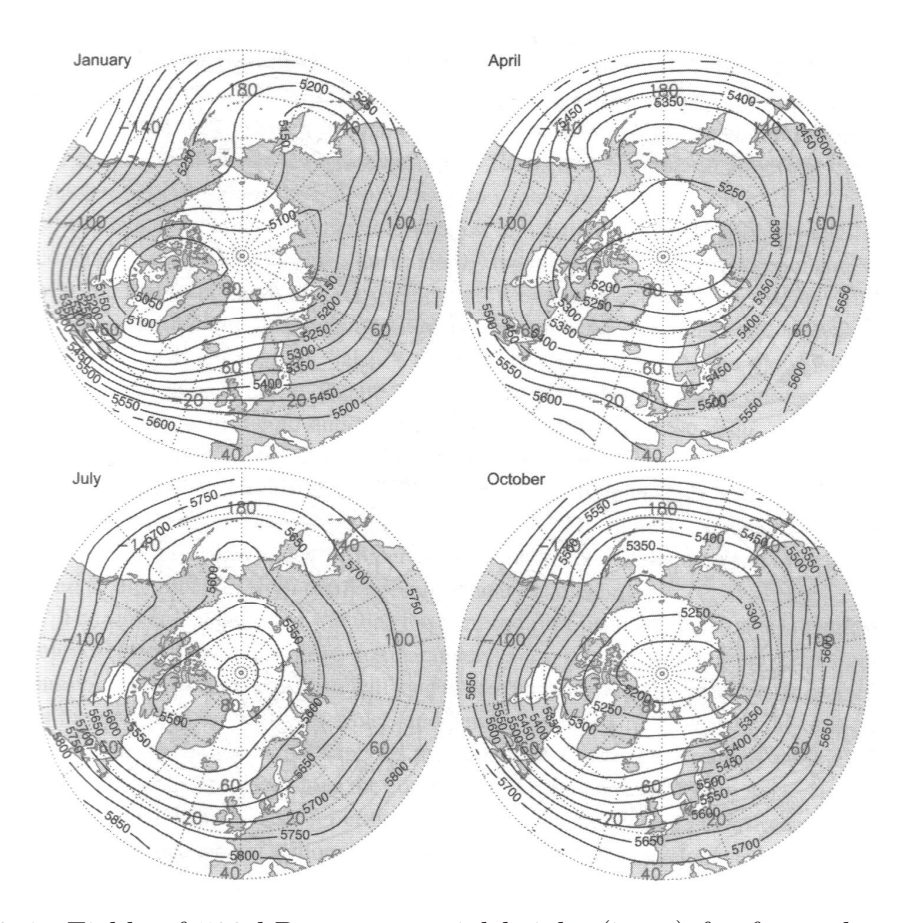


Figure 6–1: Fields of 500 hPa geopotential height (in m) for four selected months over the period 1970 to 1999, with NCEP/NCAR data. Adapted from [8].

6.1.3 Atmospheric stability

In the Arctic, due to intense radiation losses, temperature inversions (i.e. atmospheric layers in which temperature is increasing with height) are often observed close to the surface [6].

Inversions are most often observed in winter, since the snow cover increases the albedo (i.e. surface's reflectivity) which in turns prevents the surface from warming [8]. In the most extreme cases, 100 m above the surface, air temperatures can be 30°C warmer than at the surface [5]. However, on average in the Arctic winter, the difference in temperature from the bottom to the top of the inversion is 10-12°C [8].

When a temperature inversion is observed in the troposphere, it means that static stability is increased and therefore vertical mixing is reduced. The increase in static stability can disconnect the flow close to the surface from the flow aloft [20]. This can lead to strong variations in the vertical wind profile. On the other hand, in cases of neutral or weak static stability, the ensuing turbulent mixing smoothes the wind profile.

6.2 Methods

In this chapter, average meteorological conditions are determined using the North American Regional Reanalysis (NARR, see Section 6.2.1).

6.2.1 North American Regional Reanalysis Data

The NARR is a set of long-term meteorological data. It contains all the meteorological information available (temperature, wind, pressure, precipitation ...) from a variety of measurement techniques including rawinsondes, surface observations and

aircraft measurements. It offers a 32-km ($\approx 0.3^{\circ}$) spatial resolution with 29 pressure levels and a temporal resolution of 3 h, for the period from 1979 to present. Model forecasts act as a 'first guess' from one cycle to the next [34]. NARR was designed to characterize the North American terrestrial atmosphere, but it also covers parts of the Atlantic, Pacific and Arctic Oceans.

To our knowledge, this is one of the first time that NARR data are used to investigate the large-scale conditions associated with strong wind events over southern Nunavut.

NARR has been used to study wind fields over complex terrain in midlatitudes. For instance, a recent study has used NARR wind fields to validate model outputs of pollutant dispersion over complex terrain in the western United States [35]. Another study has used NARR winds in combination with moisture fluxes to study the formation of low-level jets over the Great Plains in the Central United States [36].

A few studies have used NARR meteorological for the Canadian Arctic, for instance in a study on cloud detection for the whole Canada [37] and in a snow hydrology study over subarctic Canada [38].

6.2.2 Approach

In Sections 6.3 to 6.8, the five most severe HWEs for the dominant wind regime at every station (see Table 5–1) are documented.

Composite maps of these events are then calculated. As part of the documentation, they are plotted at the time of maximum wind speed as determined the NARR 3-hourly temporal resolution, hereafter referred to as *peak intensity*. The NARR reanalysis data are used in combination with GEMPAK [39], a meteorological software

package, to perform field operations (like averaging) and displaying of parameters. Although severe HWEs were observed before 1979, due to the temporal coverage of NARR, only the HWEs occurring in the period from January 1979 to March 2007 are studied.

For each station, the five cases were analyzed individually (see Appendix B). They were each associated with large-scale atmospheric surface characteristics similar to those shown from Figures 6–2 to 6–7, even if in some cases the events occurred in different seasons.

To investigate the interaction between overlying winds and valley winds at Iqaluit, average atmospheric profiles were computed for the five most severe HWEs from the NW wind regime. The 12-hourly routine soundings launched from this Environment Canada meteorological station are considered in NARR reanalysis and ensure reliable data for this operation.

6.3 Baker Lake

The five most severe HWEs for the period 04/1979 to 04/2007 for the dominant wind regime at Baker Lake are presented in Section 6.3.1. Then, a surface composite map of these events is calculated and discussed in Section 6.3.2.

6.3.1 The Five Most Severe High Wind Events

The five most severe HWEs from the dominant NNW wind regime at Baker Lake are presented in Table 6–1. Recall that this dominant wind regime was determined in Section 5.3.1.

Table 6–1: The five most severe NNW HWEs at Baker Lake.

		Basic values		Weighted values				
HWE rank	Starting date	u_{max}	\bar{u}	au	u_{max}	\bar{u}	au	S
	(mm-dd-yy)	(m/s)	(m/s)	(h)				(out of 100)
1	12-27-85	27.8	18.5	70	28.3	14.6	23.8	66.7
2	11-29-80	23.6	17.7	79	24.0	14.0	26.9	64.9
3	01-04-99	21.7	15.2	72	22.1	12.0	24.4	58.5
4	02-02-99	20.0	14.0	74	20.3	11.1	25.2	56.6
5	01-14-82	25.8	15.0	54	26.3	11.8	18.4	56.5

All the events presented in Table 6–1 occurred in the cold season, defined in Section 4.2. We should also note that HWEs 3 and 4 occurred within 1 month of each other.

There is no major gap between the values of S for HWEs 1 to 5, as they vary between 56 and 66. The most severe HWEs has a mean wind speed close to the maximum value of 19.0 m/s ever recorded at Baker Lake (see Table 3–1). The maximum wind speed is to the severity S for HWEs 1 and 5, whereas for HWEs 2 to 4, the greatest contributing term to S is the duration of the HWE.

6.3.2 Average Surface Conditions Leading to High Wind Events

The surface composite map of the five most severe NNW HWEs at their peak intensity at Baker Lake is shown in Figure 6–2.

Typically during severe HWEs, the station is situated between a cyclone over Foxe Channel (northeastern Hudson Bay) and an anticyclone over the northern part of the Rocky Mountains, in a zone of intense synoptic pressure gradient. The surface wind direction in the vicinity of Baker Lake is consistent with the large-scale forcing, i.e. the 10-m winds are approximately geostrophic.

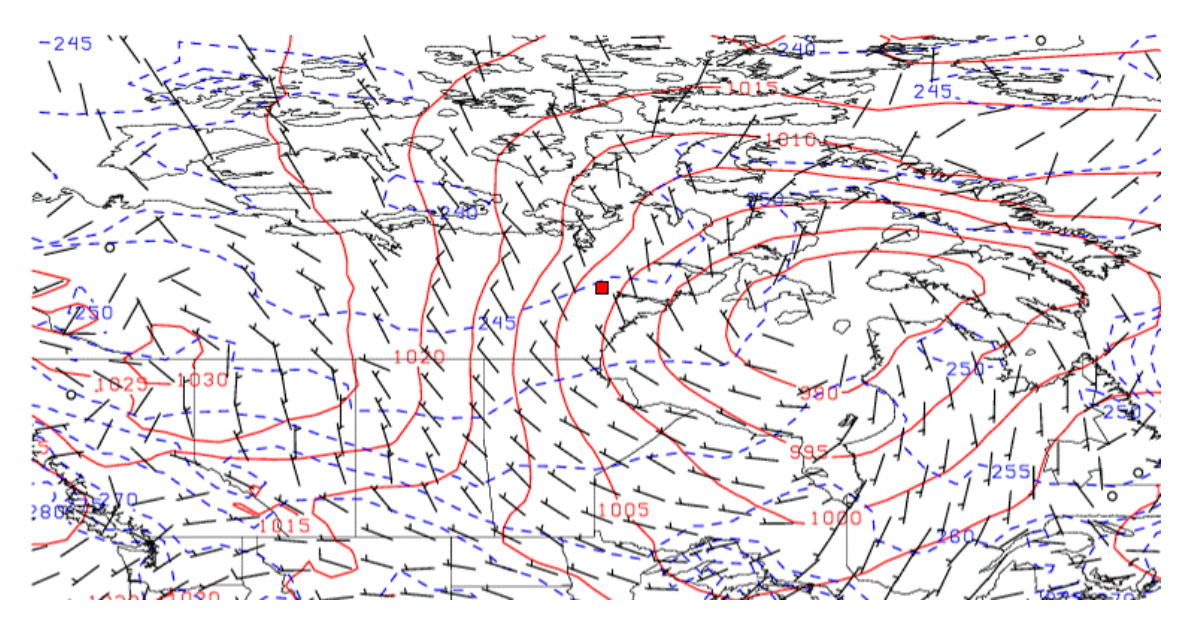


Figure 6–2: Composite surface map of synoptic conditions during the peak intensity (as defined in Section 6.2.2) of the five most severe NNW HWEs at Baker Lake (indicated by a red square). Isobars of mean sea level pressure (in hPa) are plotted in solid red lines. Isotherms (in K) are shown by the blue dotted lines. The vectors represent the 10-m wind field (in m/s).

The surface cyclone located over northeastern Hudson Bay is supported by a 500-hPa cut-off low pressure system situated over western Hudson Bay (see Figure 8–7 in Appendix C). The slight westward tilt of the cyclone with height indicates that the surface cyclone is intensifying, since it is located under a region of divergence at the upper levels. Diabatic forcing is not a key factor in maintaining the surface cyclone since the five HWEs considered in Figure 6–2 almost exclusively occurred in winter (see Table 6–1), and since Hudson Bay is frozen during this time of the year [21].

The surface map of the most severe HWE was also inspected, in which we observed an intense low pressure system (965 hPa versus 980 hPa for the composite)

located over southern Baffin Island. The associated strong pressure gradient explains the fact that the greatest contribution of S is from the maximum wind speed for HWE 1 (see Table 6–1).

6.4 Cambridge Bay

The five most severe HWEs for the period 04/1979 to 04/2007 for the dominant wind regime at Cambridge Bay are presented in Section 6.4.1. Then, a surface composite map of these events is calculated and discussed in Section 6.4.2.

6.4.1 The Five Most Severe High Wind Events

The five most severe HWEs from the dominant NW wind regime at Cambridge Bay are presented in Table 6–2. Recall that this dominant wind regime was determined in Section 5.3.2.

Table 6–2: The five most severe NW HWEs at Cambridge Bay.

		Basic values			Weighted values			
HWE rank	Starting date	u_{max}	\bar{u}	au	u_{max}	\bar{u}	τ	S
	(mm-dd-yy)	(m/s)	(m/s)	(h)				(out of 100)
1	11-03-87	19.4	15.0	103	24.2	11.7	50.0	85.9
2	01-06-80	24.7	17.4	65	30.8	13.5	31.6	75.9
3	04-08-86	24.7	16.3	64	30.8	12.7	31.0	74.5
4	09-23-00	20.6	16.1	67	25.7	12.5	32.5	70.7
5	03-22-79	25.8	13.0	48	32.1	10.1	23.4	65.6

As seen in Table 6–2, three of the most severe HWEs occurred in the cold season. Two of the most severe HWEs occurred in the warm season: HWE 3 in April and HWE 4 in September. These latter events occurred respectively slightly after the end of winter and slightly before the start of autumn.

The HWE with the longest duration (with $\tau=103$) also was the most severe. This event has the lowest value of maximum wind speed and the second lowest value of mean wind speed found in Table 6–2. Its high severity is mainly due to the contribution of duration to S. HWE 5 has the lowest mean wind speed and smallest duration, but the highest value of maximum wind speed. The added contribution of duration and mean wind speed is equal to the contribution of maximum wind speed to S.

6.4.2 Average Surface Conditions Leading to High Wind Events

The surface composite map of the five most severe NW HWEs at their peak intensity at Cambridge Bay is shown in Figure 6–3.

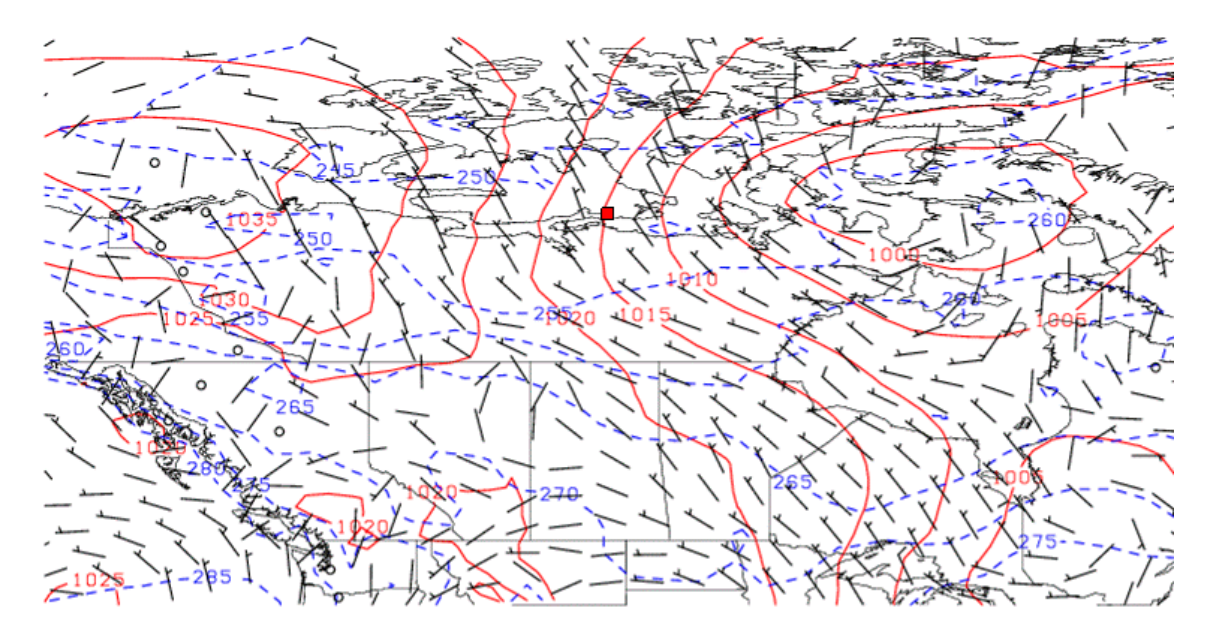


Figure 6–3: Composite surface map of synoptic conditions during the peak intensity (as defined in Section 6.2.2) of the five most severe NW HWEs at Cambridge Bay (indicated by a red square). Isobars of mean sea level pressure (in hPa) are plotted in solid red lines. Isotherms (in K) are shown by the blue dotted lines. The vectors represent the 10-m wind field (in m/s).

Typically during severe HWEs, the station is located between a low pressure system to the east (over northern Baffin Island) and a high pressure system over Beaufort Sea, in the western Canadian Arctic. This 'corridor of strong pressure gradient' [22] regularly affects Cambridge Bay. In winter, when the pressure gradient is strong enough, this corridor is associated with blowing snow [22].

A weak upper-level trough at 500 hPa (see Figure 8–8 in Appendix C) provides upper-level support for the surface cyclone. Its westward tilt with height indicates that the low pressure system is intensifying.

The most severe HWE at Cambridge Bay has a pattern extremely similar to the composite map shown in 6–3, except that the low pressure system to the east of the station is deeper (985 hPa versus 1000 hPa for the composite). It is thus the persistence of the anticyclone-cyclone couplet that is responsible for the high severity of the HWE 1.

6.5 Clyde River

The five most severe HWEs for the period 04/1979 to 04/2007 for the dominant wind regime at Clyde River are presented in Section 6.5.1. Then, a surface composite map of these events is calculated and discussed in Section 6.5.2.

6.5.1 The Five Most Severe High Wind Events

The five most severe HWEs from the dominant NW wind regime at Clyde River are presented in Table 6–3. Recall that this dominant wind regime was determined in Section 5.3.3.

Table 6–3: The five most severe NW HWEs at Clyde River.

		Basic values			Weighted values			
HWE rank	Starting date	u_{max}	\bar{u}	au	u_{max}	\bar{u}	au	S
	(mm-dd-yy)	(m/s)	(m/s)	(h)				(out of 100)
1	01-04-80	25.8	15.4	86	28.8	12.2	45.8	86.8
2	12-22-91	25.8	15.8	75	28.8	12.5	40.0	81.3
3	11-24-85	25.8	14.5	72	28.8	11.5	38.3	78.6
4	01-04-91	25.8	14.5	68	28.8	11.5	36.2	76.5
5	01-14-97	25.8	15.8	63	28.8	12.5	33.6	74.9

All the HWEs presented in Table 6–4 occurred in winter. Note that HWEs 2 and 4 occurred within one month of each other. The range of severity observed is small, as S varies from 74.9 to 86.8.

As noted in Chapter 3, the values of maximum wind speed appear limited at Clyde River thus the associated weighted values of u_{max} are all identical. The contribution of the mean wind speed to S is very similar for all HWEs listed in Table 6–3. As a result, the HWEs are ranked according to the contribution of duration to S.

6.5.2 Average Surface Conditions Leading to High Wind Events

The surface composite map of the five most severe NW HWEs at their peak intensity at Clyde River is shown in Figure 6–4. Variations in the position of the low pressure system were observed (from Hudson Strait to the eastern part of Labrador Sea) in the inspection of individual cases. The average position is a surface cyclone over located over central Labrador Sea. However, the main feature of this composite map is the presence of cold air damming at Clyde River, observed in all cases.

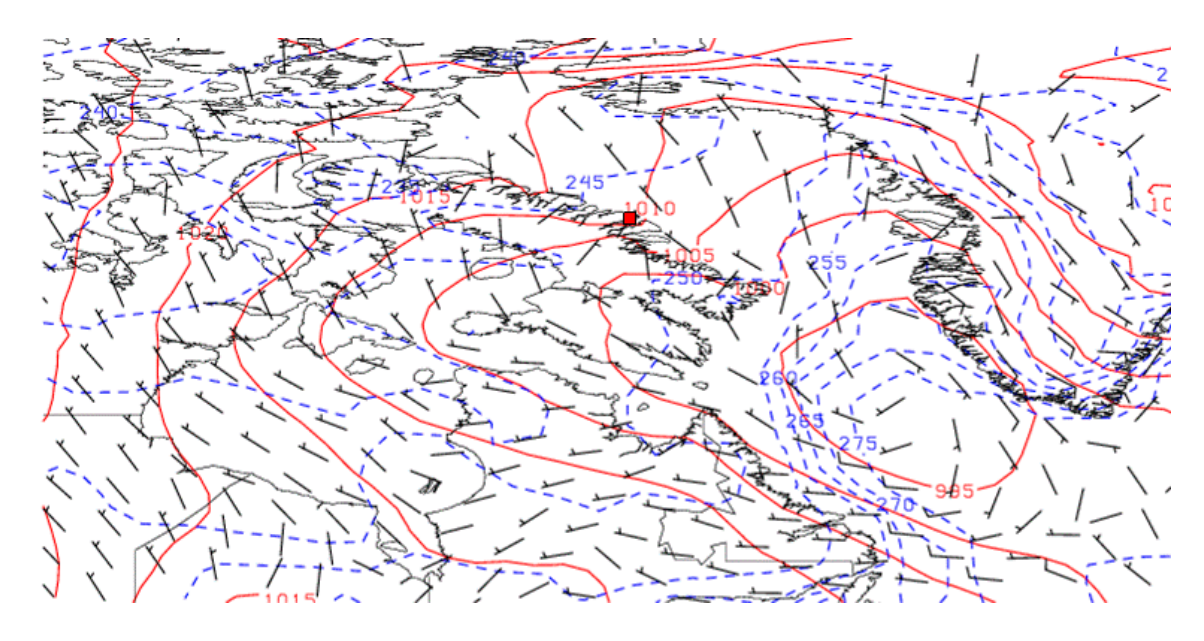


Figure 6–4: Composite surface map of synoptic conditions during the peak intensity (as defined in Section 6.2.2) of the five most severe NW HWEs at Clyde River (indicated by a red square). Isobars of mean sea level pressure (in hPa) are plotted in solid red lines. Isotherms (in K) are shown by the blue dotted lines. The vectors represent the 10-m wind field (in m/s).

The pressure trough on the east coast of Baffin Bay is due to upsloping air. This synoptic configuration is consistent with a previous climatology at Clyde River [21]. It was mentioned that for Clyde River, blizzard conditions can be associated with the existence of a pressure trough parallel to the north-eastern coast of Baffin Island, extending from Baffin Bay to Davis Strait. The presence of a thermal trough along the Baffin Island coast is indicative of cold air advection (note the northerly wind in Baffin Bay). In the vicinity of Clyde River, the 10-m wind vectors are pointing parallel to the coast, with the mountain range to their right. The low-level flow at Clyde River can therefore be classified as a barrier jet, driven by the along-barrier large-scale pressure gradient, and by the cross-barrier baroclinic zone.

Two zones of steep thermal gradient are associated with the surface cyclone situated in Labrador Sea. The steepest thermal gradient is perpendicular to the isolines, pointing from low to high. The least intense thermal gradient, which is oriented E-W, traverses the eastern sector of Labrador Sea.

In terms of upper-level support, the surface cyclone is vertically tilted, as a major cut-off low is found above the Ungava Peninsula of northern Quebec (see Figure 8–9 in Appendix C). Thus, the surface cyclone is intensifying.

The surface synoptic map for the most severe HWE at Clyde River was inspected and showed a deep cyclone (965 hPa) located over central Labrador. The two zones of thermal gradients were also observed, but with steeper gradients. The synoptic configuration of HWE 1 is thus very similar to what is shown in Figure 6–4, but with enhanced pressure gradient and thermal gradient.

6.6 Coral Harbour

The five most severe HWEs for the period 04/1979 to 04/2007 for the dominant wind regime at Coral Harbour are presented in Section 6.6.1. Then, a surface composite map of these events is calculated and discussed in Section 6.6.2.

6.6.1 The Five Most Severe High Wind Events

The five most severe HWEs from the dominant NNW wind regime at Coral Harbour are presented in Table 6–4. Recall that this dominant wind regime was determined in Section 5.3.2.

Table 6-4: The five most severe NNW HWEs at Coral Harbour.

		Basic values			Weighted values			
HWE rank	Starting date	u_{max}	\bar{u}	au	u_{max}	\bar{u}	au	S
	(mm-dd-yy)	(m/s)	(m/s)	(h)				(out of 100)
1	10-16-82	20.0	16.3	65	17.4	11.1	27.5	56.0
2	11-26-82	20.6	15.8	55	17.9	10.8	23.2	51.9
3	09-15-79	23.6	16.4	44	20.5	11.2	18.6	50.3
4	02-16-91	20.0	13.8	50	17.4	9.4	21.2	48.0
5	02-27-86	21.7	15.1	42	18.8	10.3	17.8	46.9

The two most severe HWEs occurred within 40 days of each other. Note that the third most severe HWE occurred in the warm season, and all the others HWEs in the cold season. HWEs 1 to 5 have relatively low values of S, from 46.9 to 56.0.

For the event occurring in September (HWE 3), the greatest contribution to severity is by u_{max} . The longest duration HWE is the most severe, due to the significant contribution of τ to S.

6.6.2 Average Surface Conditions Leading to High Wind Events

The surface composite map of the five most severe NNW HWEs at their peak intensity at Coral Harbour is shown in Figure 6–5.

As seen in Figure 6–5, a surface low pressure system located over Hudson Strait is counterbalanced by the existence of an anticyclone over northern Central USA. Note that the 10-m winds in the vicinity of Coral Harbour are approximately geostrophic. The closed isobars of the surface cyclone cover the entire eastern Canadian Arctic. Although the waters of Hudson Strait typically freeze by the end of November, some polynyas can form year round and act as a source of moisture [21]. Diabatic effects could therefore contribute to the maintenance of the storm system.

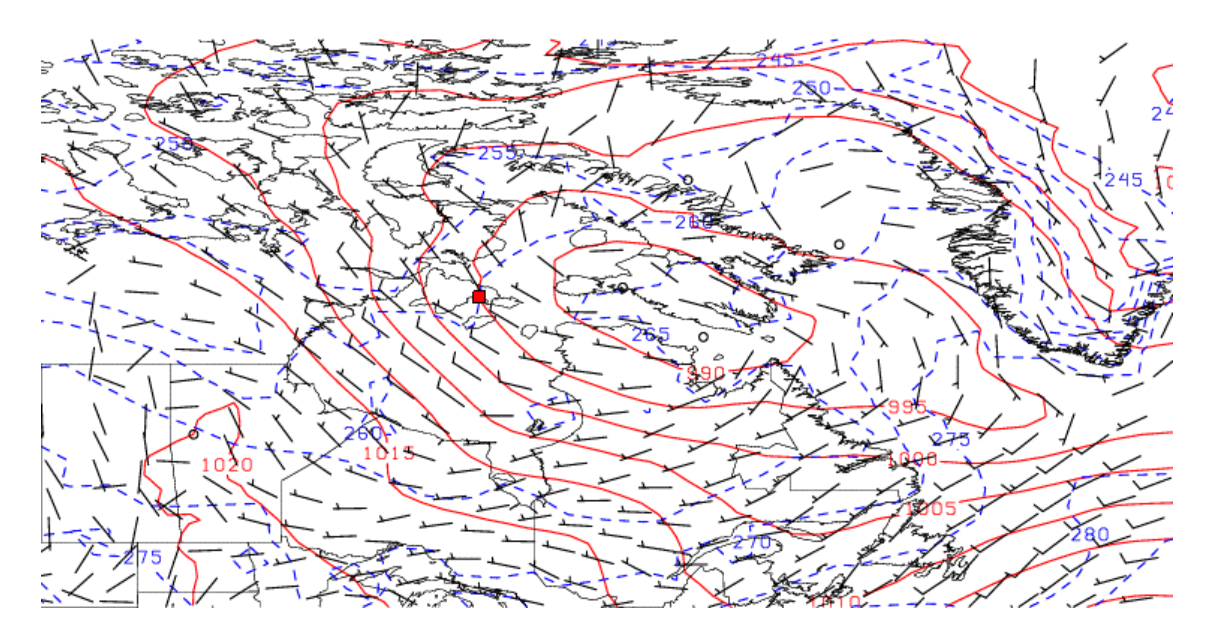


Figure 6–5: Composite surface map of synoptic conditions during the peak intensity (as defined in Section 6.2.2) of the five most severe NNW HWEs at Coral Harbour (indicated by a red square). Isobars of mean sea level pressure (in hPa) are plotted in solid red lines. Isotherms (in K) are shown by the blue dotted lines. The vectors represent the 10-m wind field (in m/s).

Regarding upper-level support, there is a cut-off low pressure system at 500 hPa, and it is situated directly above the surface cyclone (see Figure 8–10 in Appendix C). As seen in Section 6.1.2, this indicates that the surface cyclone is old, occluded and stalled.

The surface map of the most severe HWE was inspected. We observed a weak low pressure center (995 hPa) located over Foxe Basin, thus closer to Coral Harbour than the 990 hPa cyclone shown in Figure 6–5. It is the persistence of this feature that is responsible for the severity of the HWE 1. Moreover, since all HWEs have a similar severity (see Table 6–4), we should not expect individual cases to differ significantly from the composite map shown in Figure 6–5.

6.7 Hall Beach

The five most severe HWEs for the period 04/1979 to 04/2007 for the dominant wind regime at Hall Beach are presented in Section 6.7.1. Then, a surface composite map of these events is calculated and discussed in Section 6.7.2.

6.7.1 The Five Most Severe High Wind Events

The five most severe HWEs from the WNW dominant wind regime at Hall Beach are presented in Table 6–5. Recall that this dominant wind regime was determined in Section 5.3.5.

Table 6–5: The five most severe WNW HWEs at Hall Beach.

		Basic values			Weighted values			
HWE rank	Starting date	u_{max}	\bar{u}	au	u_{max}	\bar{u}	au	S
	(mm-dd-yy)	(m/s)	(m/s)	(h)				(out of 100)
1	10-25-85	20.6	14.9	86	24.5	10.0	50.0	84.5
2	10-08-98	19.2	14.5	68	22.9	9.8	39.4	72.1
3	03-19-07	19.2	13.5	63	22.9	9.1	36.5	68.5
4	11-08-87	20.6	15.9	57	24.5	10.8	33.1	68.4
5	12-11-90	20.6	12.1	56	24.5	8.2	32.5	65.2

All the HWEs presented in Table 6–5 occurred in the cold season. Three of them (HWEs 1, 2 and 4) were in the first half of autumn. Note the presence of a gap between the HWE 1 and the four others HWEs, as the difference in S between HWE 1 and HWE 2 is 12.4.

The most severe WNW HWE at Hall Beach, with S=84.5, has the longest duration recorded at that station ($\tau=86$ h). The contributions of u_{max} and \bar{u} to S are very similar for the five HWEs.

6.7.2 Average Surface Conditions Leading to High Wind Events

The surface composite map of the five most severe WNW HWEs at their peak intensity at Hall Beach is shown in Figure 6–6.

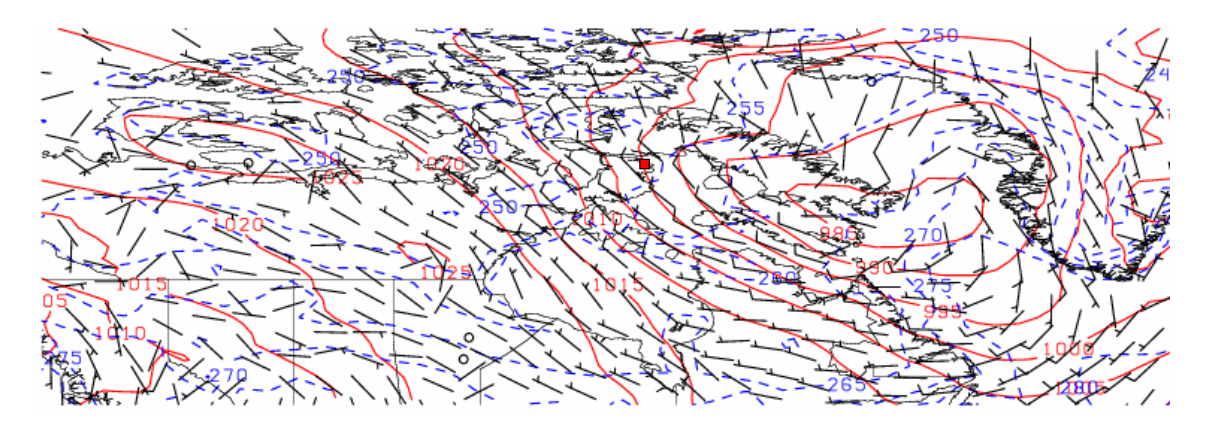


Figure 6–6: Composite surface map of synoptic conditions during the peak intensity (as defined in Section 6.2.2) of the five most severe WNW HWEs at Hall Beach (indicated by a red square). Isobars of mean sea level pressure (in hPa) are plotted in solid red lines. Isotherms (in K) are shown by the blue dotted lines. The vectors represent the 10-m wind field (in m/s).

The station is situated between a cyclone to the east and an anticyclone to the west. This cyclone-anticyclone couplet is consistent with wintertime climatological conditions in the Arctic (as seen in Section 6.1.1): high pressure in the western Arctic and low pressure in the eastern Arctic. Note the presence of cold air in the northern sector of the anticyclone (close to the northern part of the upper 1025-hPa isobar contour).

The surface low pressure system is supported by an important trough at 500 hPa situated over Baffin Island (see Figure 8–11 in Appendix C), so the surface cyclone is still intensifying.

The surface map of synoptic conditions was also investigated. Although a weak low is located in Davis Strait, the main feature is a 1025 hPa anticyclone directly located over Baker Lake. It is thus the persistence of the anticyclone-cyclone couplet that is responsible for the high severity of the HWE 1.

6.8 Iqaluit

The five most severe HWEs for the period 04/1979 to 04/2007 for the dominant wind regime at Iqaluit are presented in Section 6.8.1. Then, a surface composite map of these events is calculated and discussed in Section 6.8.2.

6.8.1 The Five Most Severe High Wind Events

The five most severe HWEs from the NW dominant wind regime at Iqaluit are presented in Table 6–6. Recall that this dominant wind regime was determined in Section 5.3.6.

Table 6–6: The five most severe NW HWEs at Iqaluit.

		Basic values			Weigl	nted		
HWE rank	Starting date	u_{max}	\bar{u}	τ	u_{max}	\bar{u}	au	S
	(mm-dd-yy)	(m/s)	(m/s)	(h)				(out of 100)
1	02-10-79	23.1	15.9	155	22.6	8.2	50.0	80.8
2	12-04-82	30.8	17.5	40	30.1	9.1	12.9	52.1
3	01-27-80	20.6	15.5	71	20.1	8.0	22.9	51.0
4	03-04-07	20.0	12.8	71	19.6	6.6	22.9	49.1
5	12-30-96	23.6	17.5	52	23.1	9.1	16.7	48.9

Note that all events listed in Table 6–6 occurred in the cold season, preferentially in winter. Note that the three most severe HWEs all occurred within four years of each other.

The most severe NW HWE at Iqaluit is the one with the longest duration. As discussed in the Introduction, it started on 10 February 1979 and was characterized by surface winds above 10 m/s for 155 consecutive h (6.5 days). There is an important contrast in duration between HWE 1 and 2 (155 h versus 40 h).

For the second most severe NW HWE at Iqaluit, the contribution of u_{max} to S is more than twice the one of τ (30.1 versus 12.9). There is also a large gap between the severity of HWE 1 versus the severity of HWEs 2 to 5, as S for HWE 1 is 80.8 and it drops down to 52.1 for HWE 2. This is due to significantly smaller values of τ for HWEs 2 to 5.

6.8.2 Average Surface Conditions Leading to High Wind Events

Average Surface Conditions. The surface composite map of the five most severe NW HWEs at their peak intensity at Iqaluit is shown in Figure 6–7.

In the Iqaluit area, the winds at low levels are highly ageostrophic. This is indicative of pressure-driven channeling due to the deep cyclone located in Labrador Sea. The existence of a steep thermal gradient along the Labrador coast and across Davis Strait should also be noted.

In terms of upper-level support, a weak cut-off low pressure system embedded in a strong trough is situated above the easternmost tip of Labrador at the 500-hPa level (see Figure 8–12 in Appendix C). Thus, the westward tilt of the cyclone with height indicated that the system is intensifying.

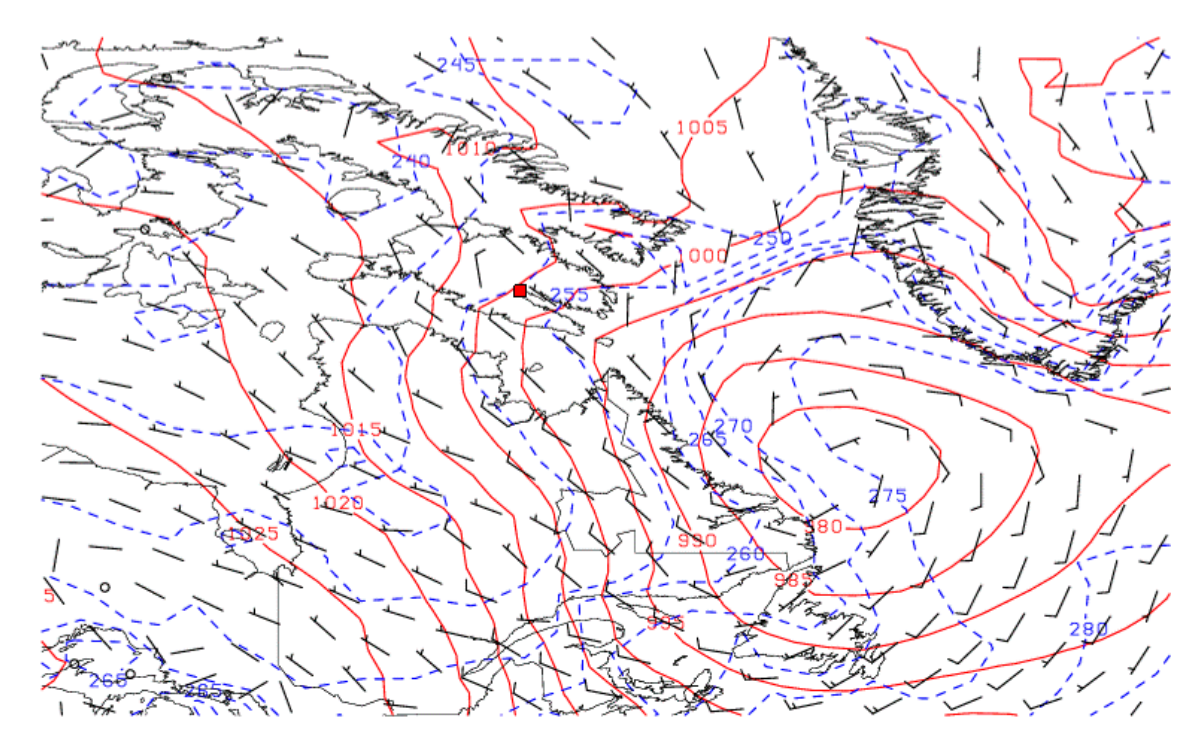


Figure 6–7: Composite surface map of synoptic conditions during the peak intensity (as defined in Section 6.2.2) of the five most severe NW HWEs at Iqaluit (indicated by a red square). Isobars of mean sea level pressure (in hPa) are plotted in solid red lines. Isotherms (in K) are shown by the blue dotted lines. The vectors represent the 10-m wind field (in m/s).

The surface map of the synoptic conditions for the most severe HWE was also inspected. A 975 hPa cyclone (versus 980 hPa for the composite) is located in Labrador Sea, and is associated to two steep thermal gradients, similar to what is observed for Clyde River, in Figure 6–4. As seen in Figure 6–7, there is high pressure located west of Quebec. It is the persistence of the cyclone that is responsible for the high severity of the HWE 1.

Average Sounding. The average sounding for the five most severe NW HWEs at their peak intensity for the period 01/1979 to 03/2007 at Iqaluit is shown at Figure 6–8.

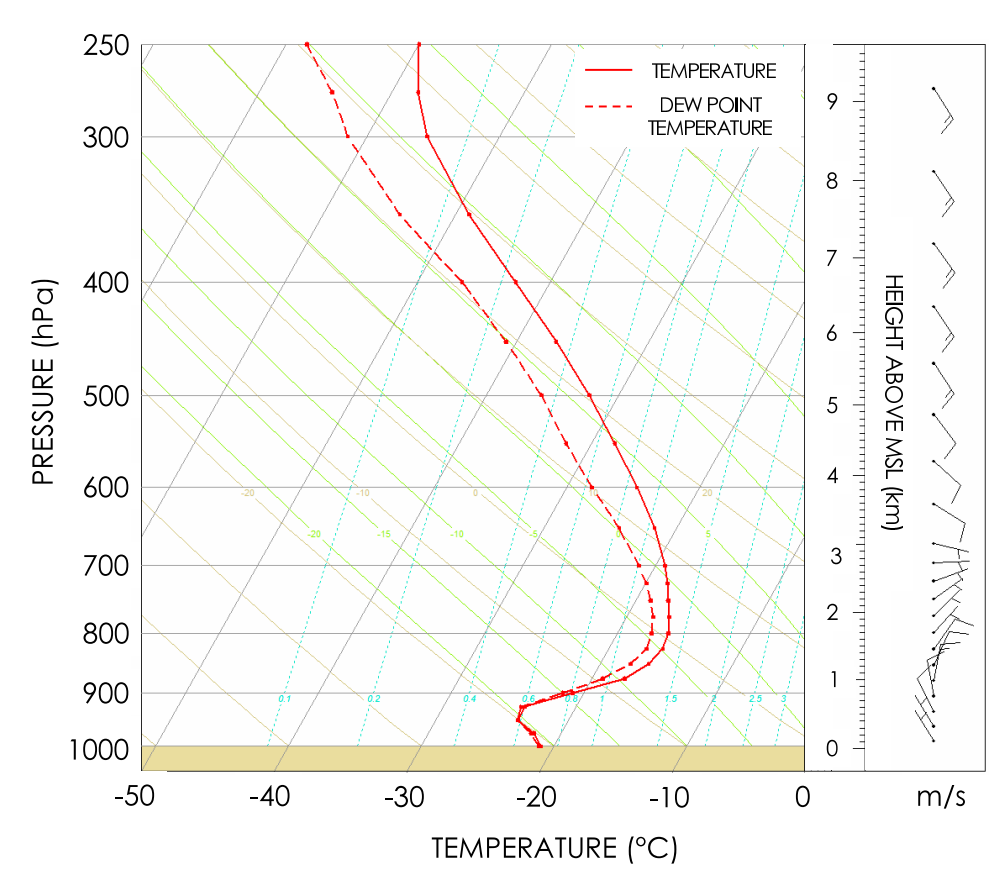


Figure 6–8: Mean atmospheric profile during the peak intensity of the five most severe NW HWEs at Iqaluit.

A strong temperature inversion is observed above ridge-top level. From 925 hPa to 825 hPa, the atmosphere warms up by 8°C. With the ridge-top level at 600m (or approximately at 920 hPa), and the base of the temperature inversion approximately at ridge-top level, we conclude that the downward turbulent flux of momentum is very limited. Indeed, the stable air suppresses the vertical eddies (i.e. vortices with

horizontal axis) [7]. Thus, the main factor explaining the most severe NW strong winds events at Iqaluit is large-scale pressure-driven channeling.

As seen in Figure 6–8, the atmosphere is mainly saturated from the surface up to the 700 hPa level. A maximum in wind speed is observed at 900 hPa. This is above the climatological level of low-level jets [9]. NARR is likely to be unable to resolve that particular feature, although it is capable of revealing low level jets in midlatitudes environments (Gulf of California; Great Plains) [34].

In a mountainous area, the wind shear with height is due to two factors:

- the tendency for the along-valley wind at lower-levels to align to the geostrophic wind above mountain-top level;
- the turning of the geostrophic wind caused by temperature advection [9].

6.9 Conclusions

Although a few cases of severe HWEs occurred at the beginning and ending of the cold season, the vast majority of the most severe HWEs occurred well within the cold season. All cases were also characterized by the presence of a surface cyclone.

We found that the nature of the nearby surface features influences the formation of HWEs. For instance, local topography significantly contributes to the formation of HWEs at Clyde River and Iqaluit. At both stations, the winds are highly ageostrophic as a result of the influence of topography. From the average sounding for NW winds at Iqaluit, it was found that the presence of stably-stratified air above ridge-top level prevents vertical mixing between the overlying winds and valley winds. As a result, the most severe strong surface winds from the NW are caused by pressure-driven channeling.

For stations over flat terrain (Baker Lake, Cambridge Bay, Coral Harbour and Hall Beach), the dominant factor for the occurrence of HWEs is a strong synoptic-scale pressure gradient. At these stations, the winds are approximately geostrophic.

The circumpolar vortex is an important spatial forcing factor for surface cyclones generating HWEs. Additionally, in all the stations except Coral Harbour, the surface cyclone generating strong winds at the peak intensity of HWEs was still intensifying, as seen from its vertical structure. At Coral Harour however, the cyclone was vertically stacked and occluded, thus in its final stage.

CHAPTER 7

Translation of Storm Systems Generating High Wind Events

7.1 Introduction

As seen in Chapter 6, a major factor causing High Wind Events (HWEs) in southern Nunavut is the occurrence and intensity of large-scale storm systems. These systems tend to follow common tracks although, in some cases, their trajectories can significantly differ from the climatological mean. In this chapter, we will study the motion of storm systems generating HWEs. Before our detailed analysis, the common storm tracks affecting the Canadian Arctic will be briefly discussed in Section 7.1.1. In Section 7.2, common storm tracks for different wind regimes during HWEs will then be presented; in particular, cyclogenesis and cyclolysis zones of storms causing HWEs in southern Nunavut. In Section 7.4, we will study the cross-correlation between the occurrence of local maxima of wind speed between different stations, to determine whether or not the same storm system can generate strong wind events at more than one station. Finally, in Section 7.3, the position and motion of cyclones during HWEs will be illustrated using cyclone frequency maps.

7.1.1 Review of Storm Tracks Affecting Southern Nunavut

Figure 7–1 qualitatively illustrates the storm tracks affecting the Canadian Arctic [21]. Only tracks 1 to 5 affect southern Nunavut.

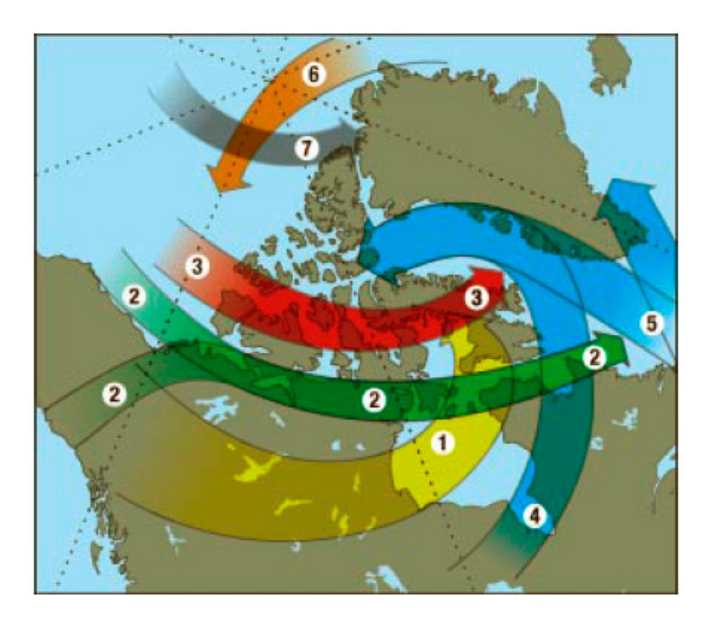


Figure 7–1: Storm tracks affecting the Canadian Arctic. Adapted from [21].

Track 1. The cyclones following track 1 form over the northern Prairies and are typically associated with relatively warm airmasses. This warm air is forced upward when the low meets the waters of Hudson Bay (where it can re-develop at the ice-water margin), then curves northward as it is steered by the climatological upper-level low situated over eastern Nunavut. Depending on the strength of the upper-level vortex, the cyclone can also re-strengthen on the east coast of Baffin Island and dissipate over Baffin Bay [21].

Track 2. Cyclones following track 2 originate either over the Gulf of Alaska or Beaufort Sea. They travel eastward and dissipate over Labrador Sea.

Track 3. Cyclones moving along track 3 follow a similar trajectory as those moving along track 2, but further north. As a result of smaller thermal gradients, they are typically weaker [21].

Track 4. This track is typically followed by storms originating in the Midwest as well as over Quebec and southern Ontario. Storms following this track are typically associated with blizzard conditions at Iqaluit [21].

Track 5. These cyclones form off the East Coast of the United States, travel parallel to the shore until they cross the maritime provinces of Canada and converge over Labrador Sea. Then, their trajectory is very similar to cyclones from track 4, i.e. they cross Davis Strait and dissipate over Baffin Bay [21]. This major storm track is often referred to as the 'North Atlantic storm track' [40].

7.2 Storm Tracks Associated with High Wind Events

7.2.1 Methods

The objective of this section is to track storm systems generating HWEs, for each wind regime at each station. For this purpose, we first divided the HWEs into different wind regimes (see Section 5.2).

Subsequently, for each HWE, the closest cyclone track was identified, with the help of the Key and Chan 1000-hPa cyclone center database [41]. Regarding this database, for the period from 1958 to 1998, at 12-hourly intervals, low pressure systems at the surface were identified and tracked with the help of an automated program. Data from the NCEP/NCAR reanalysis were used, with a latitudinal and longitudinal spacings of 2.5° and 5°, respectively. Surface cyclones were identified with local height minima, with a closed contour at least 30 m or higher [41].

Once each HWE was associated with a storm track, for each wind regime, three cyclone frequency maps were plotted (see Figure 7–2). The first one shows the start

point of each of the cyclones, i.e., the zones of cyclogenesis. The second map shows the trajectory followed by the cyclone between its start and its end point. The third map was the end point for each of the cyclone, i.e. showing zones of cyclolysis. Storm tracks were then manually classified into 'corridors' of high cyclonic activity. The 'corridors' of major (most intense) cyclonic activity were defined as major tracks, whereas 'corridors' of moderate cyclonic activity were defined as minor tracks. To identify in which direction the cyclones were moving, we compared cyclogenesis frequency maps with cyclolysis frequency maps (the cyclones move from the region where they form toward the region where they dissipate).

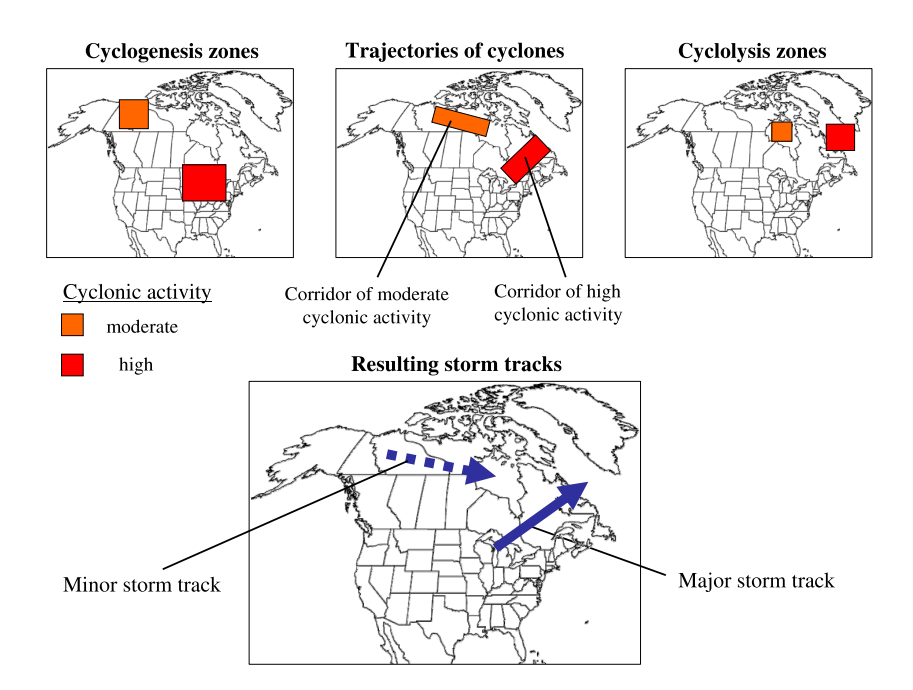


Figure 7–2: Methodology for the identification of storm tracks associated with HWEs for each station.

In this section, for each wind regime (see Table 5–1), we present the major and minor storm tracks and discuss their origins and differences.

7.2.2 Baker Lake

The storm tracks associated with HWEs at Baker Lake are presented in Figure 7–3.

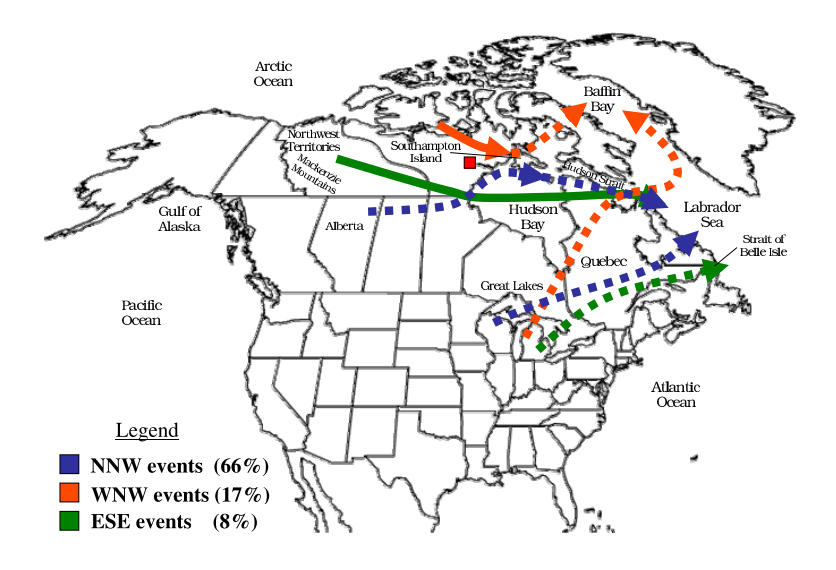


Figure 7–3: Storm tracks for HWEs at Baker Lake (red square). The frequency of occurrence of each wind regime is indicated in the bottom left corner. Major storm tracks are represented by solid lines, minor storm tracks by dotted lines. Tracks go from cyclogenesis to cyclolysis zones.

NNW Events. Cyclogenesis regions are found mostly over the northern Prairies and over the Great Lakes. NNW winds are typically associated with a low pressure system stalled over the central part of Hudson Bay. It should be noted that all major storm tracks are associated with storm systems originating north of the 60th parallel.

Two minor trajectories can be observed. One originates over northern Alberta, traverses the northern Prairies, shifts northeast toward Southampton Island and then ceases in Labrador Sea. These systems seem to be part of track 1 (see Section 7.1). They form over the northern Prairies initially with warm airmasses cooling off when the systems reach Hudson Bay, where they typically re-strengthen. The other minor

track starts over the Great Lakes, traverses southern Quebec and ends in Labrador Sea.

WNW Events. The storm track associated with WNW events starts in the central Canadian Arctic and passes close to the northern shore of Southampton Island. Some systems dissipate in northern Hudson Bay, but most of them move northward, cross Baffin Island and weaken in Baffin Bay. A minor track starts over the Great Lakes, traverses Quebec and then leades around southern Baffin Island to end in Baffin Bay.

ESE Events. The cyclones typically form to the lee of the Mackenzie mountains, in the southern Northwest Territories, then travel along the 60th parallel, cross Hudson Bay and fill in Labrador Sea. A minor storm track connects the Great Lakes to the eastern tip of Quebec, past the Strait of Belle Isle.

General Discussion. There are essentially two main routes for the cyclones causing HWEs at Baker Lake. One starts over the Great Lakes and converges over the Labrador Sea. Another one starts in the western Arctic, crosses the northern half of Hudson Bay and is directed toward Labrador Sea and Hudson Bay. As we see here, large water bodies can have an impact on synoptic activity [15, 42].

7.2.3 Cambridge Bay

The storm tracks associated with HWEs at Cambridge Bay are presented in Figure 7–4.

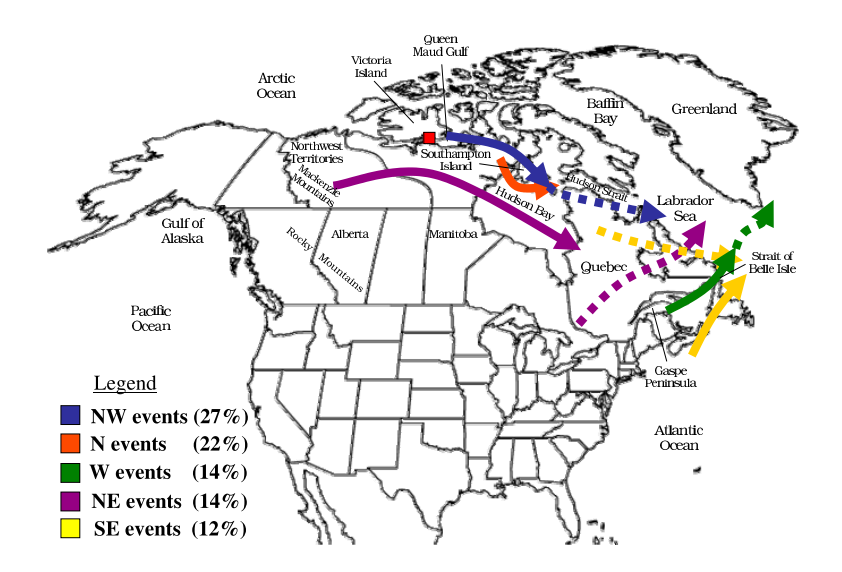


Figure 7–4: Storm tracks for HWEs at Cambridge Bay (red square). The frequency of occurrence of each wind regime is indicated in the bottom left corner. Major storm tracks are represented by solid lines, minor storm tracks by dotted lines. Tracks go from cyclogenesis to cyclolysis zones.

NW Events. The main cyclogenesis zone is located in the Queen Maud Gulf, just east of Victoria Island and Cambridge Bay. Cyclones then follow a path similar to northerly HWEs, with some of them decaying in Hudson Bay. Other storms continue their trajectory until they reach Labrador Sea. As seen in Section 7.1.1, these low pressure systems are typically weaker than the storm systems forming further south. Finally, a minor track connects northern Quebec and Labrador Sea.

N Events. One short, but clear tendency for storm tracks is to start in the continental sector of central Nunavut, to lead around Southampton Island to the south and end up at the mouth of Hudson Strait. The small mean displacement of perturbations over Hudson Bay suggests the existence of stationary systems.

W Events. Low pressure systems form over the Gaspe Peninsula, travel across the Strait of Belle Isle, some of them filling in Labrador Sea and others on the eastern side of the southern tip of Greenland.

Interestingly, the main path for cyclones for westerly HWEs at Cambridge Bay is located extremely far from the station. This is explained by the fact that, in this study, we are interested in large-scale pressure gradients located between a zone of low and high pressure. Typically, close to the centre of a cyclone, the large-scale pressure gradient is strong. Still, in some cases like here, intense and persistent gradients can form even if the cyclone and anticyclone are far from each other.

NE Events. The major storm track starts lee of the Mackenzie mountains, travels across the continental sector of the Canadian Arctic, shifts from an easterly to a southeasterly direction and ceases in western Quebec. A minor track involves storms forming in southwestern Quebec and dying in Labrador Sea.

SE Events. Two trajectories were identified here: the North Atlantic storm track (from north-eastern USA to Labrador Sea) and one crossing northern Quebec and Labrador to end up in Labrador Sea too.

General Discussion. The two main storm tracks are very similar to those found for Baker Lake. Systems either form in the central Arctic and travel toward the east, or form in eastern Canada and travel to the northeast. We suspect that the large distance between Cambridge Bay and some storm tracks over eastern Canada might be explained by another synoptic perturbation causing the severe winds: either an anticyclone or a short-lived low pressure system.

7.2.4 Clyde River

The storm tracks associated with HWEs at Clyde River are shown in Figure 7–5.

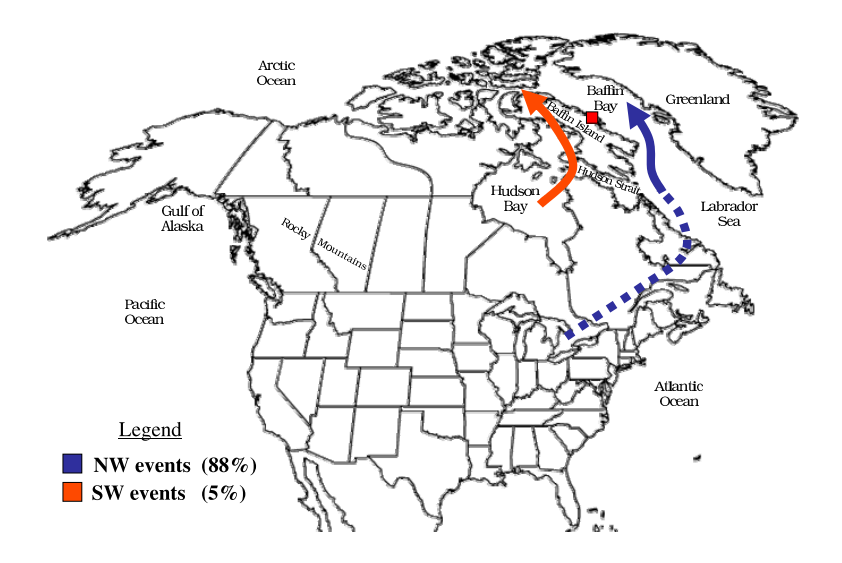


Figure 7–5: Storm tracks for HWEs at Clyde River (red square). The frequency of occurrence of each wind regime is indicated in the bottom left corner. Major storm tracks are represented by solid lines, minor storm tracks by dotted lines. Tracks go from cyclogenesis to cyclolysis zones.

NW Events. The major storm track starts in Labrador Sea and ends in Baffin Bay. However, some cyclones form or converge in the Great Lakes area and connect to the principal storm track in Labrador Sea. This minor storm track is known to generate strong northwesterlies at Clyde River [21] and to be the 'most prominent surface low trajectory affecting the Arctic Islands' [28]. Moreover, it is a 'classical blizzard track' for Iqaluit [21]. The associated main cyclolytic zone is located over Baffin Bay, close to Greenland.

SW Events. Very few SW events were recorded. Nonetheless, the major storm track represents systems with different origins regrouping at the northeastern part of Hudson Bay, running parallel to the west side of Baffin Island and crossing the island at its northern tip.

General Discussion. Baffin Bay is a crucial water body for the generation of strong surface winds at Clyde River. It represents a zone of high cyclonic activity. The waters from the Atlantic Ocean and from higher latitudes mix, thus offering important contrasts in surface temperature and humidity [5] that could provide energy to sustain surface cyclones. Moreover, Baffin Bay is situated between high topography on Baffin Island to the west and on Greenland to the east. This strongly restrains cyclone displacement and development [6].

7.2.5 Coral Harbour

The storm tracks associated with HWEs at Coral Harbour are shown in Figure 7–6.

NNW Events. Cyclogenesis occurs principally over Hudson Bay. The main tendency for storms is to move from Hudson Bay and to Cumberland Sound by crossing Hudson Strait. The end of the trajectory shows a mean position between two cyclolysis zones: southern Baffin Island and the northern part of Labrador Sea. Additionally, there is a minor track that connects southern Quebec to the Labrador Sea.

NE Events. The short displacement vector represents stalled cyclones whose displacement is very limited, basically being restricted between Hudson Bay and Ungava Peninsula.

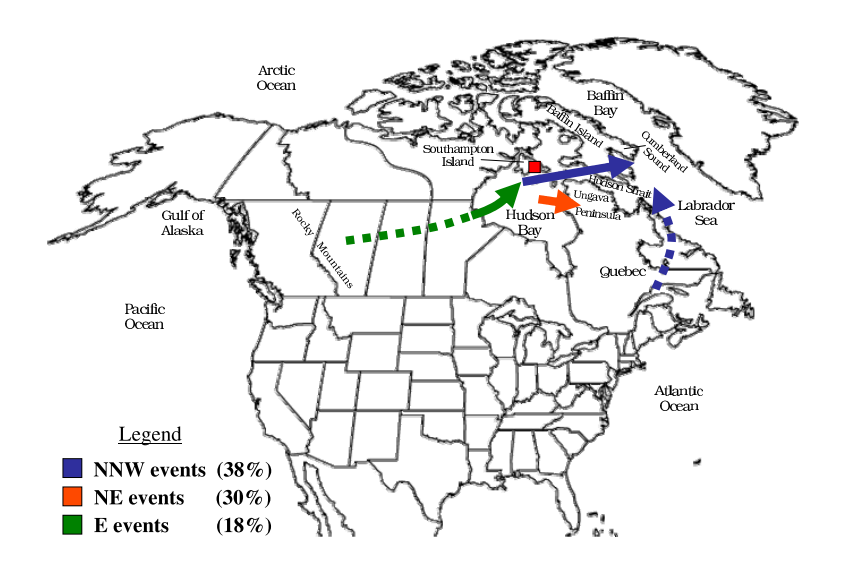


Figure 7–6: Storm tracks for HWEs at Coral Harbour (red square). The frequency of occurrence of each wind regime is indicated in the bottom left corner. Major storm tracks are represented by solid lines, minor storm tracks by dotted lines. Tracks go from cyclogenesis to cyclolysis zones.

E Events. These cyclones typically approach Coral Harbour from the southwest. Most of them form to the lee of the Rocky Mountains, but also along the way to Coral Harbour. The path crosses northern Prairies and reaches the waters of Hudson Bay, where cyclones stall, re-generate and eventually fill. The storms connect to the major path which simply travels from southwest corner of Hudson Bay up to the southernmost tip of Southampton Island.

General Discussion. Severe winds at Coral Harbour are highly influenced by the presence of Hudson Bay. Indeed, Hudson Bay acts as a supply of energy and moisture for storms. Most of the surface of Hudson Bay starts to freeze in Mid-November [21], but some areas are regularly open year-round. As a result, Hudson

Bay represents a zone where cyclones stagnate and can regenerate. Consequently, the distance traveled by storms affecting Coral Harbour is relatively small.

7.2.6 Hall Beach

The storm tracks associated with HWEs at Hall Beach are presented in Figure 7–7.

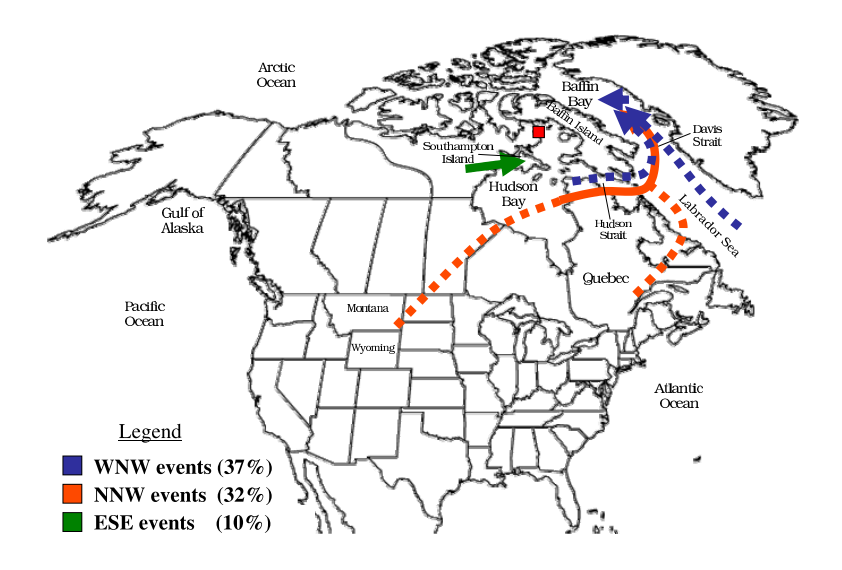


Figure 7–7: Storm tracks for HWEs at Hall Beach (red square). The frequency of occurrence of each wind regime is indicated in the bottom left corner. Major storm tracks are represented by solid lines, minor storm tracks by dotted lines. Tracks go from cyclogenesis to cyclolysis zones.

WNW Events. The main tendency for cyclones is to form and dissipate in Baffin Bay, as shown by the major storm track in Figure 7–7. This region is affected by high cyclonic activity, thus cyclones can remain stationary for an extended period of time. However, there are two minor storm tracks leading to WNW strong wind events at Hall Beach. One crosses Hudson Strait from west to east and reaches Baffin Bay via Davis Strait. The other starts in Labrador Sea and ends in Baffin Bay.

NNW Events. The most important cyclogenesis zones are at the border of Montana and Wyoming (western minor storm track) and off the east American coast (eastern minor storm track). Thus, cyclones with various origins tend to converge in Labrador Sea, cut through Davis Strait and end up in Baffin Bay. Storms that are moving along the eastern shore of Hudson Bay, cross northern Quebec and then go round Baffin Island up to Baffin Bay.

ESE Events. The main cyclogenetic region is located over Baker Lake. Cyclones stall over Hudson Bay, as seen by the short associated displacement vector. Intense cyclolysis is observed over Southampton Island. No minor track is observed.

General Discussion. The most important wind regime at Hall Beach is caused by the intense synoptic activity over Baffin Bay. Thus, the importance of this basin is undeniable, although elevated ice caps and a 1500-m mountain range stand between Hall Beach and it. Additionally, Hall Beach is mostly affected by storms moving northward into the Canadian Arctic [11].

7.2.7 Iqaluit

The storm tracks associated with HWEs at Iqaluit are presented in Figure 7–8.

NW Events. The main origin of NW HWEs is via the North Atlantic storm track, i.e. cyclones that form off the coast of New Jersey, enter the continent via Maine, travel across north-eastern Quebec and stall in the Labrador Sea. Storms located over Labrador Sea tend to cause channeling at Iqaluit, as seen in Section 6.8.2. The North Atlantic storm track cyclogenesis region is a place where air masses with significantly different origins and thus temperatures tend to meet. Cold air anomalies

from the high latitudes are forced to warm as they approach the Atlantic Ocean [43]. Other systems converge at the southern tip of James Bay, where they cross Quebec in a northeastward trajectory.

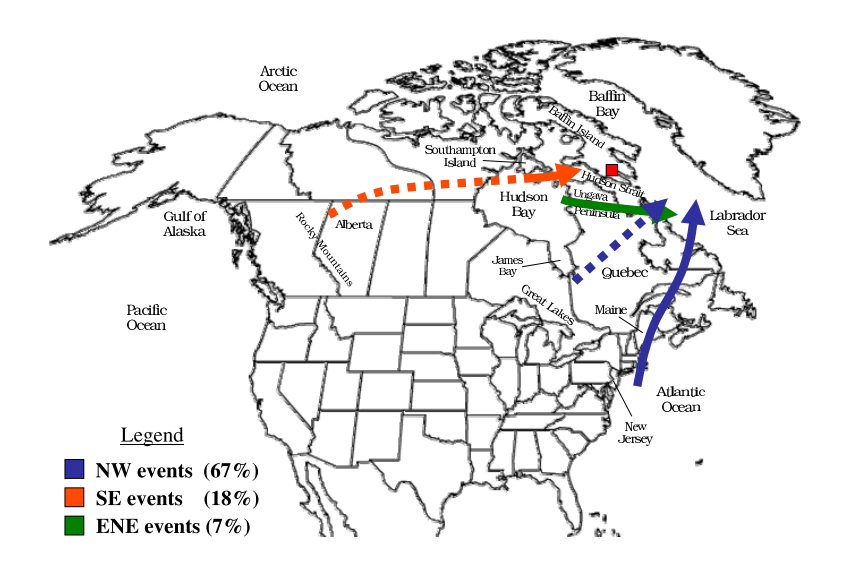


Figure 7–8: Storm tracks for HWEs at Iqaluit (red square). The frequency of occurrence of each wind regime is indicated in the bottom left corner. Major storm tracks are represented by solid lines, minor storm tracks by dotted lines. Tracks go from cyclogenesis to cyclolysis zones.

SE Events. The main cyclogenesis region for SE HWEs is at the southern-most tip of Southampton Island. Storms tend to travel due east until they reach the entrance of Hudson Strait. Other storms, which form to the lee of the Rocky Mountains in northern Alberta, connect with the major storm track over Hudson Bay.

ENE Events. Cyclogenesis occurs on the east side of Hudson Bay. Storms then propagate from the Ungava Peninsula to Labrador Sea, where they dissipate.

General Discussion. The Labrador Sea represents an important cyclogenesis area, as cold continental air and warm maritime air meet [5]. It has been shown that storms from the North Atlantic are the most intense throughout the year [23]. Since cyclones formed at midlatitudes are typically deeper than those formed in the Arctic, Iqaluit's proximity to the North Atlantic major storm track is a crucial factor in the generation of local HWEs.

7.3 Cyclone Frequency Maps during High Wind Events

In this section, maps of cyclonic occurrences during HWEs are presented, with the help of the cyclone center database detailed in Section 7.2.1. Mean cyclone center displacement (magnitude and direction) were calculated on a 24 x 20 grid with a latitudinal and longitudinal spacings of 2.5° and 5° respectively. These results were determined to contrast zones of high versus low cyclonic occurrence and to estimate the impact of surface forcing mechanisms on the position of storm systems generating HWEs.

7.3.1 Overall

The cyclone frequencies for HWEs at all stations are presented on Figure 7–9.

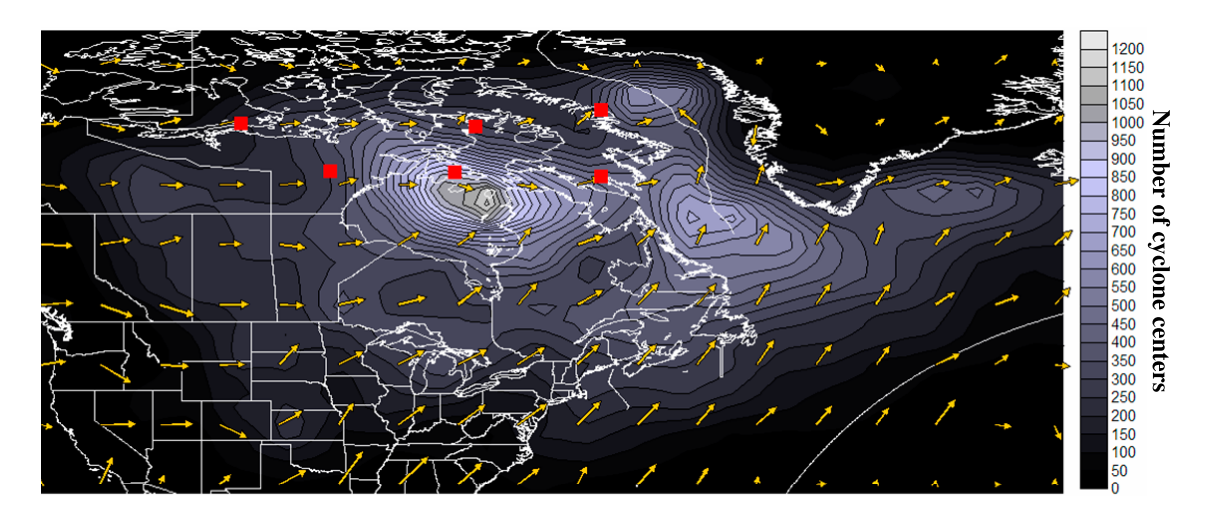


Figure 7–9: Cyclone frequencies for all HWEs and all stations (indicated by red squares). From left to right: Cambridge Bay, Hall Beach, Clyde River, Baker Lake, Coral Harbour and Iqaluit.

To highlight the regional contrasts in mean storm displacements, Figure 7–10 illustrates the average storm speed for all HWEs at all stations.

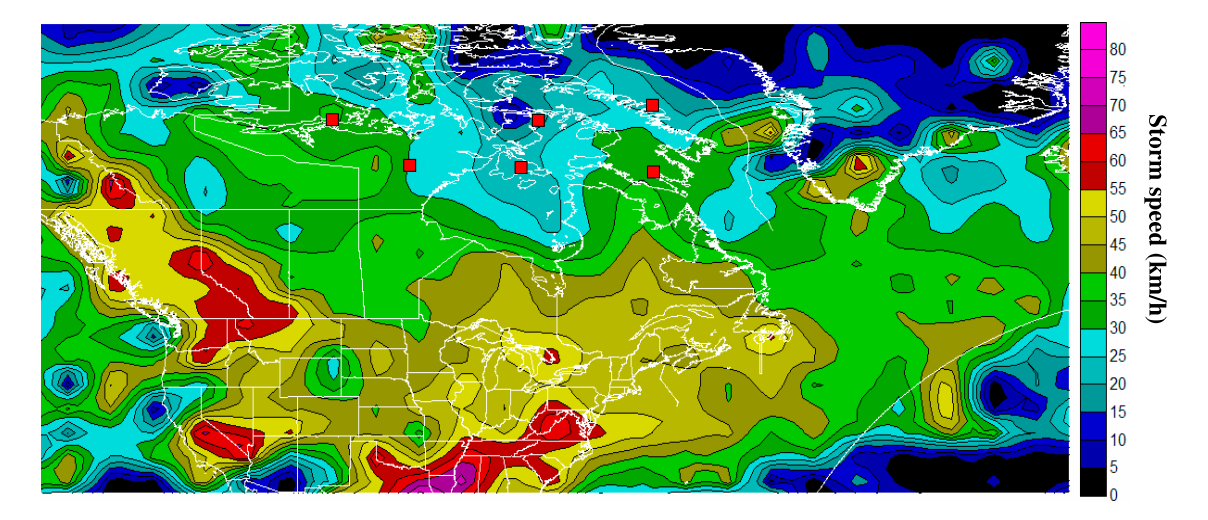


Figure 7–10: Average storm speed for all HWEs and all stations (indicated by red squares). From left to right: Cambridge Bay, Hall Beach, Clyde River, Baker Lake, Coral Harbour and Iqaluit.

As seen in Figure 7–9, there are three main zones of high cyclonic activity during strong wind events: northeastern Hudson Bay, Labrador Sea and Baffin Bay. In northeastern Hudson Bay, the storm speed is approximately 25 km/h; in Labrador Sea, from 20 to 35 km/h (note the local minimum of 20 km/h close to the northeastern tip of Quebec); in Baffin Bay, from 5 to 25 km/h. These storm speeds thus indicate that storm systems tend to stall over this large water body.

On the other hand, large storm speeds (> 60 km/h) are found in three regions: along the BC-Alberta boundary as well as in the southwestern and southeastern USA. The local maximum observed along the BC-Alberta boundary is due to Rocky Mountain lee cyclogenesis and the presence of high northwesterly winds aloft, that strongly steer the surface cyclone once it is formed. This is consistent with the average storm displacement toward the SE observed in Figure 7–9 at the southern

part of the BC-Alberta boundary. The two other local maxima are located too far south to impact on our region of interest.

Regarding the spatial variation of storm speeds, as seen in Figure 7–10, a SW-NE gradient in storm speed is observed in the Arctic. In the south-west sector of the Arctic, the storm speeds are approximately 30-35 km/h, whereas they are approximately 10-15 km/h less over northern Baffin Island and Baffin Bay. Moreover, from 30°N to 80°N, a north-south gradient in storm speed is observed.

Regarding the direction of storm propagation, the general tendency for storms is to move toward the east-northeast, as seen in Figure 7–9. From the west coast to the western shore of Hudson Bay, storm systems generally move east. From Ontario to the Maritimes, the storm systems tend to move toward the northeast. In the Labrador Sea area, the high topography of Greenland blocks systems and forces them to enter Davis Strait. As a result, the northward component of storm propagation west of Greenland is significant and cyclone frequencies over Greenland are extremely low.

7.3.2 Baker Lake

Figure 7–11 illustrates the position of storm systems during HWEs at Baker Lake for the period 1958 to 1998.

The absolute maximum of cyclone occurrence for HWEs at Baker Lake is located over northeastern Hudson Bay. Local maxima of cyclonic frequency are also found in Labrador Sea and Baffin Bay. The fact that these zones of high cyclonic frequency are restricted over water suggests that diabatic effects act as a forcing mechanism for the maintenance of storm systems.

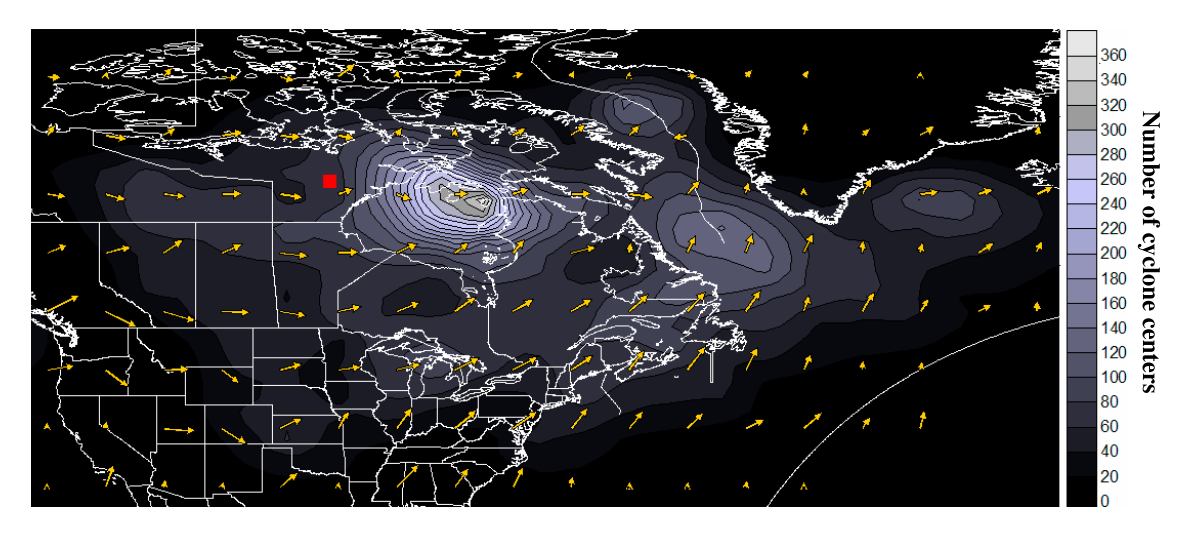


Figure 7–11: Cyclone frequencies during HWEs at Baker Lake (indicated by a red square). The vectors show the average storm displacement at each grid point. The color scale of vectors is proportional to the average storm speed.

A large majority of cyclone occurrences are found east of Baker Lake. This is consistent with the prevailing wind direction originating from the northwestern quadrant, as shown in Figure 5–4.

In terms of storm displacement, smaller storm propagation vectors are observed over Hudson Bay. From western to eastern Canada, the mean storm displacement shifts from east, to northeast, to north-northeast.

7.3.3 Cambridge Bay

A contour map depicting the position of cyclone centers during HWEs at Cambridge Bay is shown in Figure 7–12 for the period 1958 to 1998.

As shown by Figure 7–12, the distribution of cyclone occurrences shows significant spread, with most of the cyclones occurring to the southwest of the station. This is consistent with the variability of prevailing wind directions found in Figure 5–5.

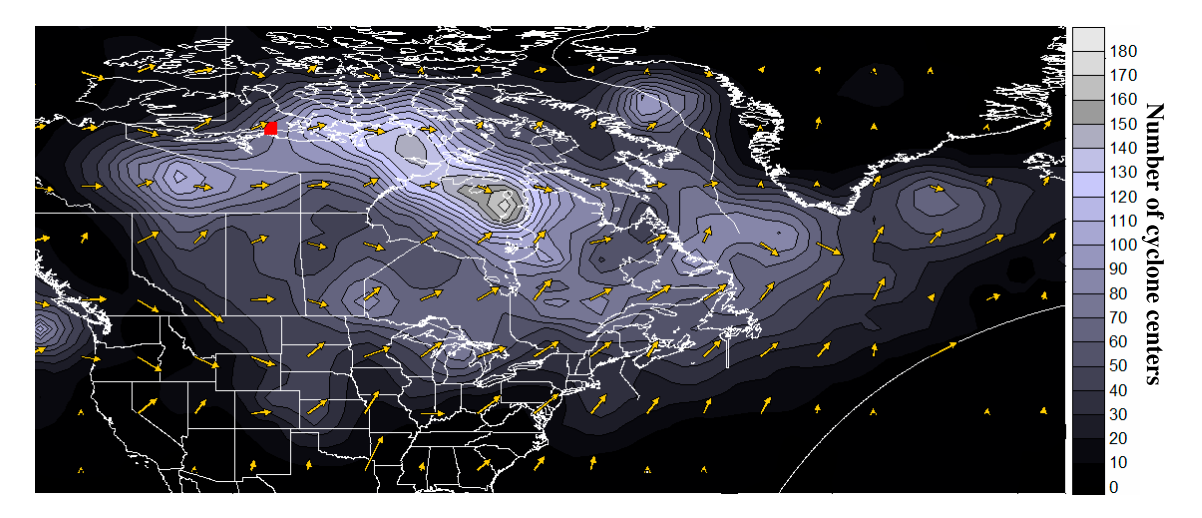


Figure 7–12: Cyclone frequencies during HWEs at Cambridge Bay (indicated by a red square). The vectors show the average storm displacement at each grid point. The color scale of vectors is proportional to the average storm speed.

The zone of highest cyclonic activity is oriented NW-SE, from east of Victoria Island to northeastern Hudson Bay. Additionally, there are two zones of moderate cyclonic activity: from southern Manitoba to Labrador Sea and in the Northwest Territories.

7.3.4 Clyde River

Figure 7–13 illustrates the occurrence of cyclones centers for all HWEs at Clyde River for the period 1958 to 1998.

As shown in Figure 7–13, a peak of cyclonic activity is found in Baffin Bay. This area is known as a region of high cyclonic activity throughout the year as migratory systems enter it in all seasons [5]. The absolute maximum is situated close to the Greenland shore. Thus, the prevailing wind directions during HWEs at Clyde River (see Figure 5–6) are not only due to cold air damming, but also to the presence of

a low pressure system in Baffin Bay. Note the local maxima in cyclone frequency observed over Labrador Sea.

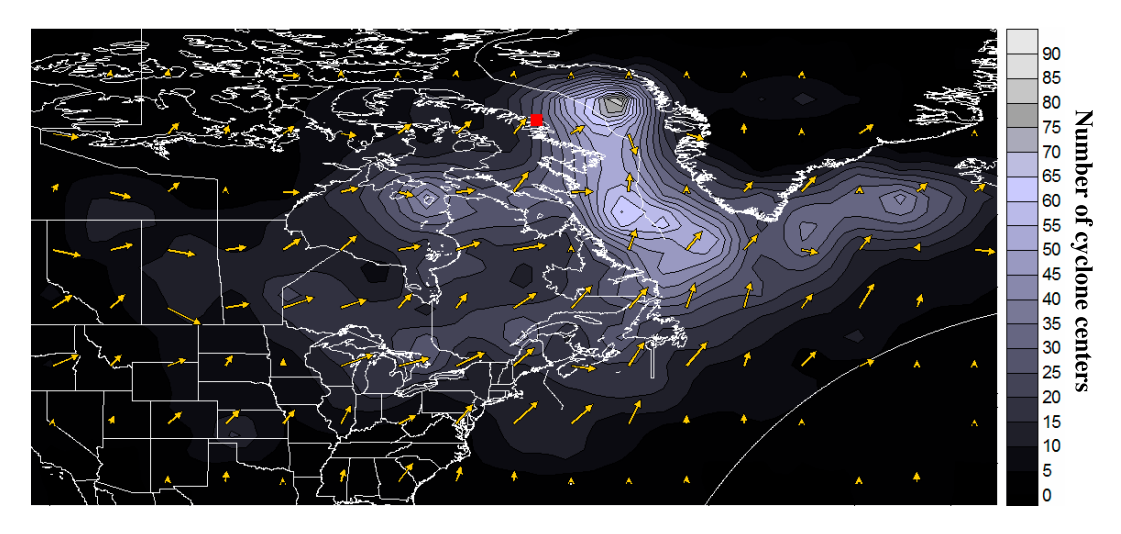


Figure 7–13: Cyclone frequencies during HWEs at Clyde River (indicated by a red square). The vectors show the average storm displacement at each grid point. The color scale of vectors is proportional to the average storm speed.

There are two east-west 'corridors' of moderate cyclonic activity: one from northeastern Hudson Bay to Davis Strait; the other from the Great Lakes to southern Labrador Sea.

Regarding storm displacement, the mean storm displacement in Labrador Sea is toward the north, however, a southward displacement is observed in Davis Strait. This indicates that this is a region where storm systems can stagnate.

7.3.5 Coral Harbour

Figure 7–14 illustrate the position of cyclone centers during HWEs at Coral Harbour for the period 1958-1998.

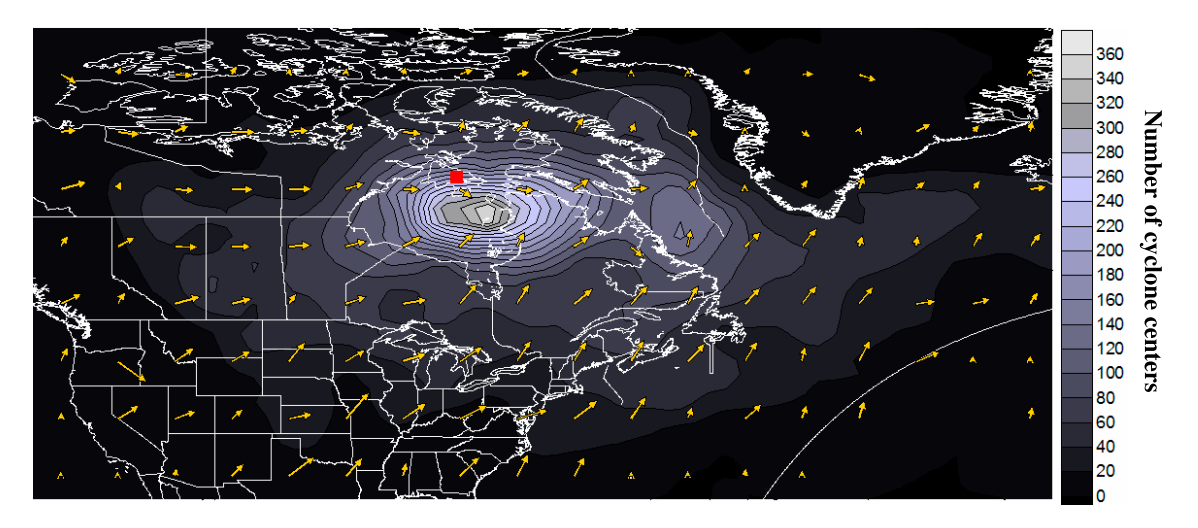


Figure 7–14: Cyclone frequencies during HWEs at Coral Harbour (indicated by a red square). The vectors show the average storm displacement at each grid point. The color scale of vectors is proportional to the average storm speed.

As shown in Figure 7–14, during HWEs, the cyclone centers are almost exclusively located over Hudson Bay, mostly in the northeastern sector. Since this maximum is situated very close to Coral Harbour, small changes in east-west cyclone position will strongly affect the wind direction at the station. This is consistent with the prevailing wind directions found at Figure 5–7.

7.3.6 Hall Beach

For all HWEs occurring at Hall Beach for the period 1958 to 1998, the position of cyclone centers are shown in Figure 7–15.

Figure 7–15 shows that Hall Beach is situated between two regions of high cyclonic frequencies: Southampton Island and Baffin Bay. It is important to note that a major mountain range separates Hall Beach from the peak of cyclonic occurrence found in Baffin Bay.

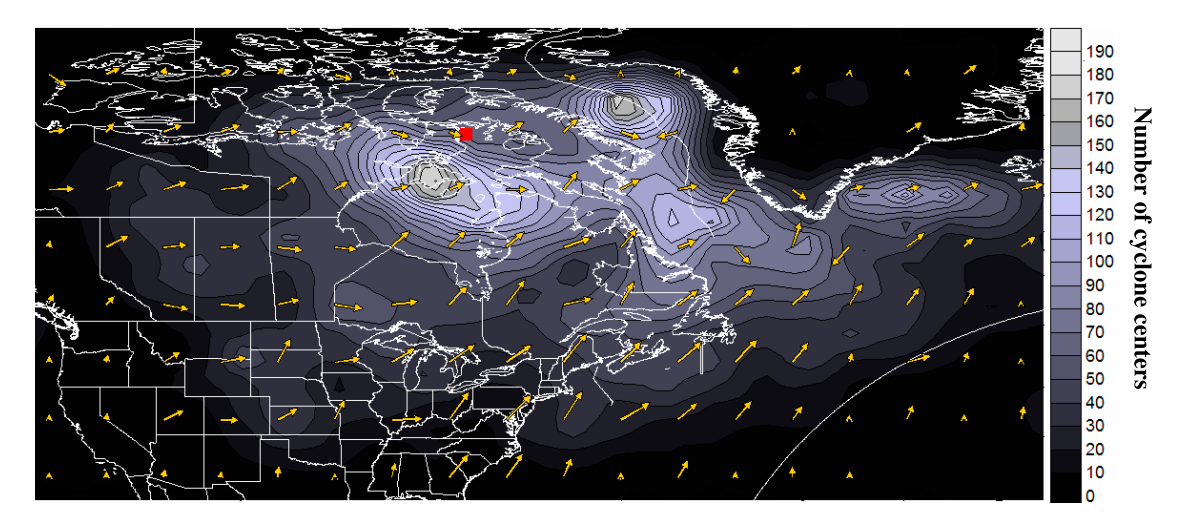


Figure 7–15: Cyclone frequencies during HWEs at Hall Beach (indicated by a red square). The vectors show the average storm displacement at each grid point. The color scale of vectors is proportional to the average storm speed.

7.3.7 Iqaluit

The cyclone frequencies for all HWEs at Iqaluit for the period 1958 to 1998 are shown in Figure 7–16.

The absolute maximum of cyclonic occurrence found in Labrador Sea, as shown in Figure 7–16, is associated with NW channeled winds at Iqaluit. On the other hand, the local maximum found in Hudson Bay is associated with SE channeled winds at Iqaluit. The fact that the NW HWEs are three times more frequent than SE HWEs (see Table 5–1) is confirmed by the more abundant cyclonic activity in Labrador Sea than in Hudson Bay. The moderate occurrence of cyclones along the East Coast of North America illustrates the existence of the North Atlantic storm track.

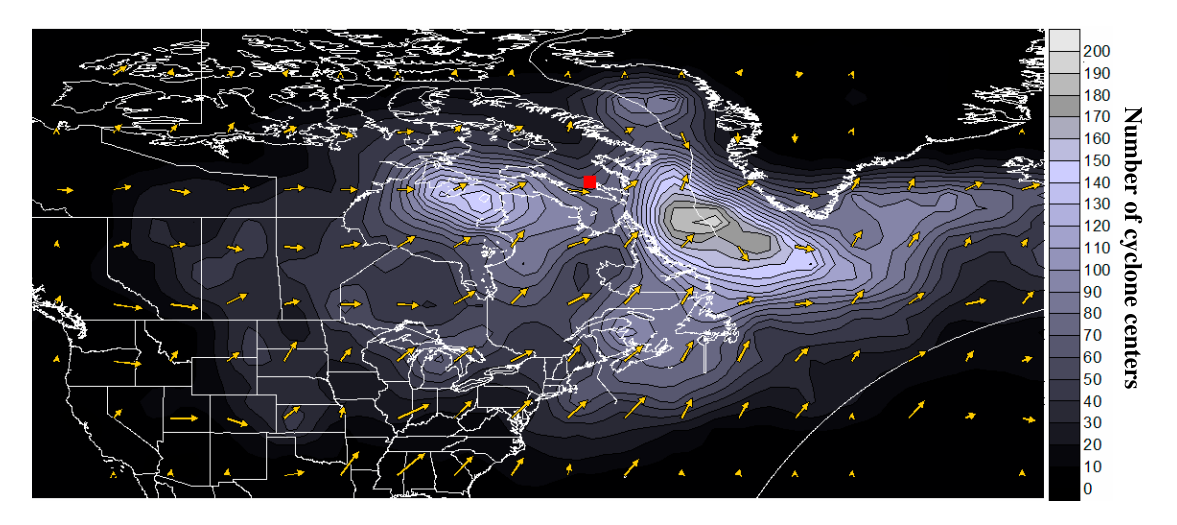


Figure 7–16: Cyclone frequencies during HWEs at Iqaluit (indicated by a red square). The vectors show the average storm displacement at each grid point. The color scale of vectors is proportional to the average storm speed.

7.4 Spatial Connection of High Wind Events

In the last two sections, we have studied the displacement of storm systems associated with the formation of HWEs. Since storm systems can last several days and travel several hundred kilometers, it is important to assess if the same cyclone can produce strong wind events at more than one station.

7.4.1 Methods

For this purpose we study the wind speed time series at different stations and correlate the occurrence of local maxima between two different stations. Figure 7–17 shows a sketch of a typical situation being, in which we observe that the occurrences of local maxima in wind speed are correlated between station 1 and station 2.

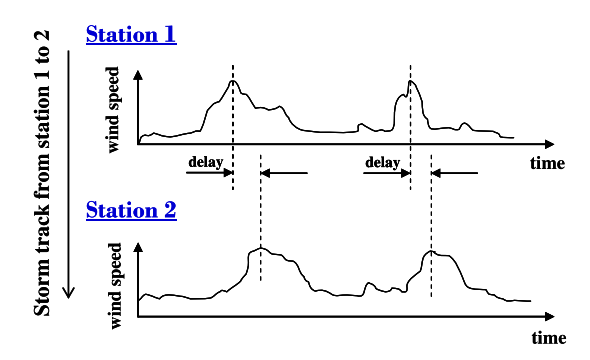


Figure 7–17: Delays between occurrences of local maxima in wind speed time series, for storms moving from station 1 to station 2.

To obtain consistent data, the analysis is restricted to the period during which all stations used in this study were operational, thus from 04/1977 to 04/2007 (see Table 2–1). Missing data are linearly interpolated. To remove diurnal effects, timeseries are smoothed by running means with averaging intervals of 24 h.

At the first station along a given climatological storm track, we divide the times series into 20-day segments centered around the occurrence of local speed maxima of at least 10 m/s. We then perform a cross-correlation analysis between these timeseries x(t) at station 1 and 20-day time series y(t) at station 2, shifted relative to x(t) by different delays d. The cross-correlation coefficient r for values of d is then given by Equation 7.1.

$$r(d) = \frac{\overline{(x(t) - \overline{x(t)})(y(t \pm d) - \overline{y(t \pm d)})}}{\sqrt{\overline{(y(t \pm d) - \overline{y(t \pm d)})^2}}}$$
(7.1)

At each location, cross-correlation spectra obtained for all 20-day segments are averaged. The delay d_{max} at which each cross-correlation spectrum attains its maximum is then compared with the typical translation speed of cyclones in the given region.

7.4.2 Results

The average cross-correlation spectra for combinations of stations showing a maximum values $r(d_{max})$ greater than 0.25 are presented below.

Cambridge Bay - Baker Lake. Figure 7–18 illustrates the spatial connection between the wind speed time series at Cambridge Bay and Baker Lake.

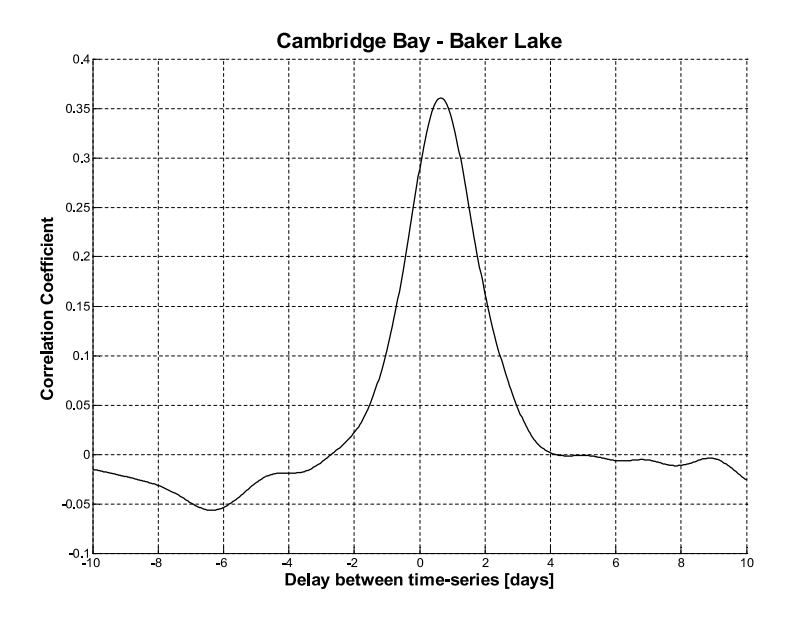


Figure 7–18: Average cross-correlation spectrum for wind speed time series at Cambridge Bay and Baker Lake.

The maximum average correlation coefficient found (d_{max}) is 0.36 and is associated with a delay of 16 h. This correlation is likely to be caused by eastward moving

storms. There are three storm tracks in the east-west direction at Cambridge Bay (see Figure 7–4: NW HWES, N HWES, NE HWEs) and Baker Lake (see Figure 7–3: WNW HWEs, ESE HWEs, NNW HWEs). The overlapping of these storm tracks suggests that storm systems can generate strong wind events at both stations.

For instance, a composite plot of surface conditions for the five most severe N HWEs at Cambridge Bay (see Figure 8–13 in Appendix C) illustrates a cyclone situated directly above Baker Lake. The northwestern part of the cyclone is generating strong surface winds at Cambridge Bay, whereas winds are calm at Baker Lake, as a result of weak pressure gradients. As the surface cyclone moves toward the northeast, the surface wind speed at Baker Lake progressively increases and eventually reaches a peak. The storm system eventually stalls in the northwestern sector of Hudson Bay (see Figure 7–3). NNW winds are then generated at Baker Lake via the strong pressure gradients found in the southwestern part of the surface cyclone.

According to Figure 7–10, storm systems propagate at an average speed of 25 km/h in the western sector of Hudson Bay. Thus, in 16 h, the storm system would travel 400 km, from Baker Lake to the southern tip of Coral Harbour. This distance is consistent with our discussion above, i.e. a storm system causing a N HWEs at Cambridge Bay can also cause a NNW HWE at Baker Lake.

Baker Lake - Coral Harbour. Figure 7–19 illustrates the spatial connection between the wind speed time series at Baker Lake and Coral Harbour.

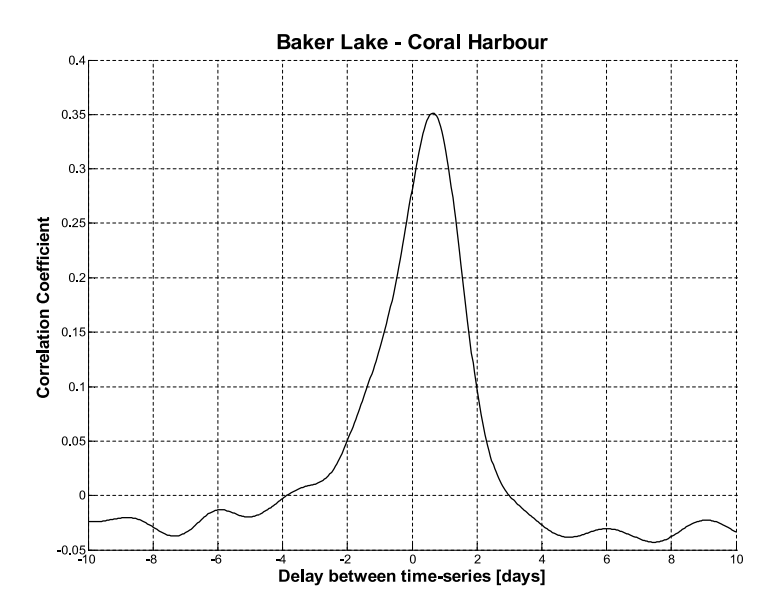


Figure 7–19: Average cross-correlation spectrum for wind speed time series at Baker Lake and Coral Harbour.

The maximum average correlation coefficient found is 0.35 and is associated with a delay of 15 h. There are similarities between the two major NNW storm tracks at Baker Lake (see Figure 7–3) and Coral Harbour (see Figure 7–6). When storms originating over the Prairies enter northern Hudson Bay, Coral Harbour is located in a center of low pressure and the associated wind speeds are thus low. Meanwhile, strong winds affect Baker Lake as it is situated in the western sector of the cyclone, in a zone of strong pressure gradient. This can be seen from the surface composite map for the five most severe NNW HWEs at Baker Lake at their peak intensity (see Figure 6–2). This figure illustrates a surface cyclone located in the southern part of Foxe Channel, halfway between Southampton Island and Ungava Peninsula. When the surface cyclone moves east, the synoptic pressure gradient decreases at Baker Lake and the local wind speed decreases. Meanwhile, wind speed increases at Coral

Harbour, as it is progressively affected by the western sector of the storm system. The surface composite map for the five most severe NNW HWEs at Coral Harbour at peak intensity (see Figure 6–5) shows a cyclone situated on the southern shore of Baffin Island, at the center of Hudson Strait.

The two cyclone center positions depicted by Figs. 6–2 and 6–5 are 475 km away from each other. According to Figure 7–10, storm systems propagate at an average speed of 30 km/h in the Hudson Strait area. Therefore, in 15 h the storm system would travel 450 km. This suggests that the same storm can cause a NNW HWE at Baker Lake and a NNW HWE at Coral Harbour.

Coral Harbour - Hall Beach. Figure 7–19 illustrates the spatial connection between the wind speed time series at Coral Harbour and Hall Beach.

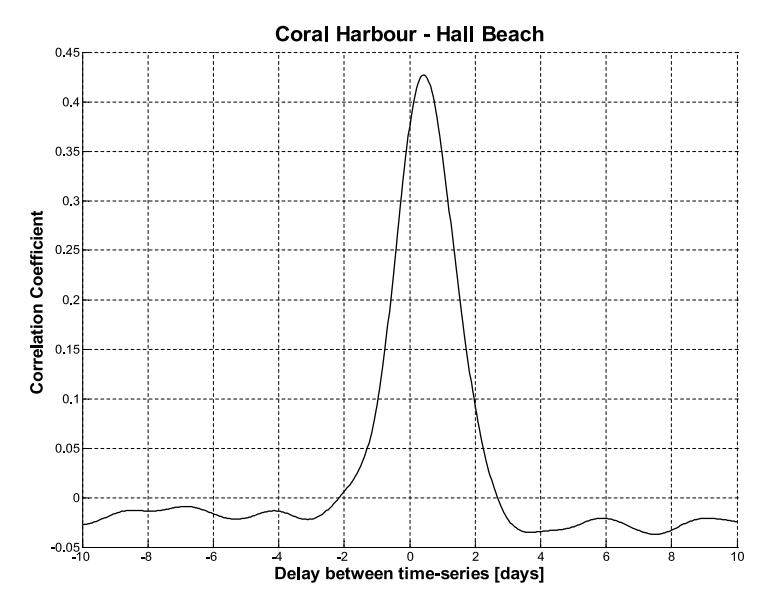


Figure 7–20: Average cross-correlation spectrum for wind speed time series at Coral Harbour and Hall Beach.

The maximum correlation coefficient found is 0.43 and is associated with a delay of 10 h. We hypothesize that a significant portion of storms systems causing NNW HWEs Coral Harbour can also cause WNW HWEs at Hall Beach, since a significant portion of the westernmost minor WNW storm track at Hall Beach (see Figure 7–7) overlaps the major NNW storm track at Coral Harbour (see Figure 7–6).

Note that storm tracks shown in Section 7.2 only indicate the typical propagation of cyclones. Deviations from these storm tracks are regularly observed. For instance, storm systems causing a NNW HWE at Coral Harbour can sometimes propagate in Davis Strait and dissipate in Baffin Bay.

As seen on the surface composite map for the five most severe NNW HWEs at Coral Harbour at their peak intensity (see Figure 6–5), the community is located in the western sector of a cyclone. The cyclone center is situated on the southern shore of Baffin Island, halfway between the two extremities of Hudson Strait. The surface composite map for the five most severe WNW HWEs at Hall Beach at peak intensity (see Figure 6–6) shows a surface cyclone center situated in Davis Strait, close to the Cumberland Peninsula. The distance between the two cyclone centers is approximately 500 km. According to Figure 7–10, in southeastern Baffin Island, storm systems propagate at an average speed of 30 km/h. Thus, in 10 h, the storm system would travel 300 km.

However, it should be noted that it is not the same part of the storm that affects Coral Harbour and Hall Beach. As seen in Figure 6–6, Hall Beach is affected by the northwestern sector of the surface cyclone. As a result, the same storm system can cause a NNW HWE at Coral Harbour followed by a WNW HWE at Hall Beach.

Hall Beach - Clyde River. Figure 7–21 illustrates the spatial connection between the wind speed time series at Hall Beach and Clyde River.

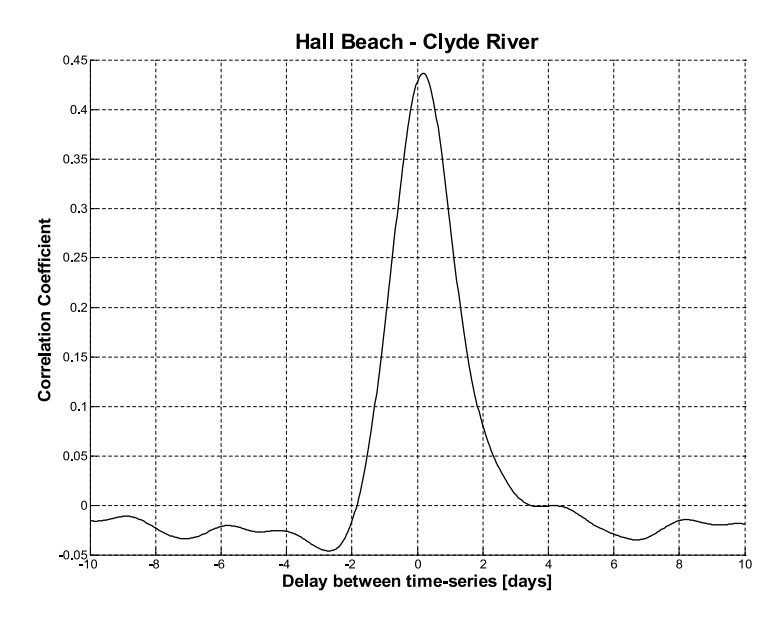


Figure 7–21: Average cross-correlation spectrum for wind speed time series at Hall Beach and Clyde River.

The maximum correlation coefficient found is 0.44 and is associated with a delay of 4 h. This is the highest value of $r(d_{max})$ found in this study. The NW major storm track at Clyde River (see Figure 7–5) is very similar to the NNW major storm track and the two minor WNW storm tracks at Hall Beach (see Figure 7–7). This suggests that the same storm system can cause a NNW or WNW HWE at Hall Beach followed by NW HWE at Clyde River.

As seen on the surface composite map for the five most severe NNW HWEs at Hall Beach at their peak intensity (Figure 6–6, the cyclone center is situated just offshore of Cumberland Peninsula. According to Figure 7–10, storm systems in southeastern Baffin Island propagate at an average speed of 30 km/h. In 4 h, this

storm system would then move 120 km, toward central Davis Strait, where it could start generating strong winds at Clyde River.

Iqaluit - Clyde River. Figure 7–22 illustrates the spatial connection between the wind speed time series at Iqaluit and Clyde River.

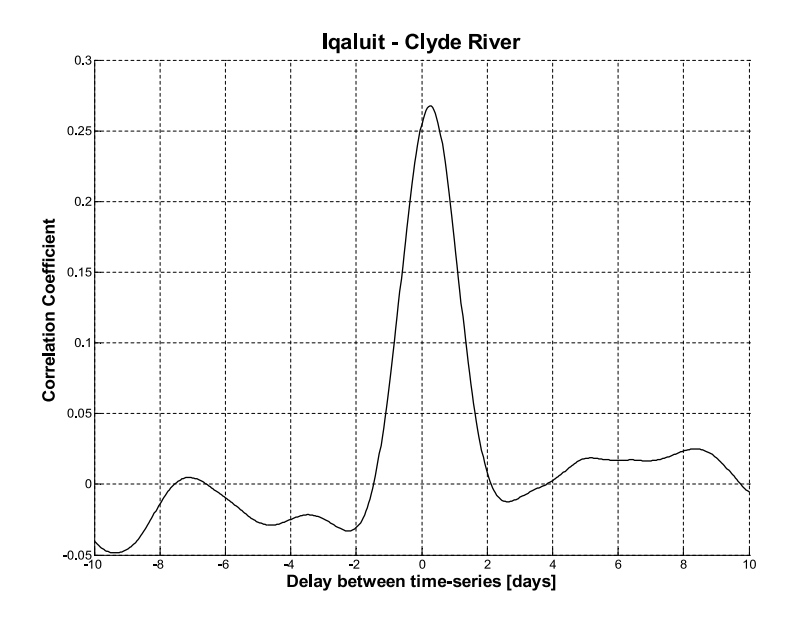


Figure 7–22: Average cross-correlation spectrum for wind speed time series at Iqaluit and Clyde River.

The maximum correlation coefficient found is 0.27 and is associated with a delay of 6 h. This is consistent with the storm tracks causing NW winds at Iqaluit (see Figure 7–8) and Clyde River (7–5). According to Figure 7–10, in Labrador Sea, storm systems propagate at an average speed of 25 km/h. In 6 h, a cyclone could then travel 150 km. This suggests the existence of a threshold in the generation of strong surface winds at Clyde River. This threshold would depend on the location of the surface cyclone in Labrador Sea. A comparison of the composite surface maps for the five most severe NW HWEs at Clyde River 6–4 and Iqaluit 6–7 shows

that the position of the two cyclone centers is separated by the NW-SE distance of approximately 200 km. When the northern sector of the storm system enters Davis Strait, easterly winds are formed in the vicinity of Clyde River and eventually barrier winds. Therefore, the same storm system can cause a NW HWE at Iqaluit followed by a NW HWE at Clyde River.

In summary, the presence of well-defined peaks in the cross-correlation spectra for delays from 4 to 15 h showed that the same storm system can affect more than one station.

7.5 Overall Discussion

This chapter focused on the propagation of storm systems leading to HWEs in southern Nunavut.

It was found that storm systems forming in the Arctic were propagating toward the east, whereas systems forming over eastern Canada traveled toward the NE. The northward component of storm displacement in the Labrador Sea/Davis Strait area is likely to be a result of the interaction of storm systems with the high topography of Greenland and the upper-level forcing.

Three zones of intense cyclonic activity associated with the generation of HWEs were identified: Hudson Bay, Labrador Sea and Baffin Bay. These zones are all associated with low storm propagation speeds, indicating a tendency for cyclones to stall there. These three areas are all large water bodies, and they can act as a source of moisture and energy for cyclones. For instance, Hudson Bay is a zone where cyclones can regenerate [21]. Based on the storm tracks shown in Section 7.2, it was found that Labrador Sea is the most important cyclolysis zone for cyclones

causing HWEs in southern Nunavut. Regarding cyclone formation, the most common cyclogenesis areas are Hudson Bay, the northern Arctic, the Great Lakes and the northeastern USA.

The eastern Canadian Arctic is a zone where cyclones fill [43]. This was shown in part by the presence of a north-south gradient in the storm propagation speed (see Figure 7–10). As latitude increases, the storm propagation speed decreases, suggesting that cyclones stall and slowly fill in the Arctic.

Storm systems can travel large distances and last for several several days. Since all the stations of interest are located within 2000 km of each other, we hypothesized that the same surface cyclone could generate HWEs at more than one station. This was first suggested by the overlapping of storm tracks in Section 7.2. We then showed that there are well-defined maxima in the cross-correlation spectra of wind speed time series for a selected combination of stations. This confirmed that the same storm system can cause HWEs at more than one station, although strong surface winds are not always caused by the same part of the storm system.

CHAPTER 8 Concluding Remarks

An analysis has been conducted on the climatology of strong sustained wind events and on the role of atmospheric circulation and topographic conditions in forcing these events in southern Nunavut.

High Wind Events (HWEs) here are defined as hourly surface wind speed over 10 m/s for a minimum of 3 h. A severity index was defined to rank the HWEs according their duration (accounts for 50% of the total severity), maximum hourly wind speed (accounts for 35% of the total severity), and mean wind speed (accounts for 15% of the total severity).

HWEs were identified using several decades of surface observations at six meteorological stations. Four of these are located on flat terrain (Baker Lake, Cambridge Bay, Coral Harbour and Hall Beach) and two in mountainous terrain (Clyde River and Iqaluit).

8.1 Thesis Summary

This study of HWEs has led to several observations and conclusions. First, a climatology of HWEs in southern Nunavut was developed. Baker Lake is the station with the largest annual number of HWEs (79) whereas the largest mean severity for HWEs is observed at Clyde River (42.8). Overall, long HWEs are always found among the most severe HWEs, as a result of the high importance given to

the duration parameter in our definition of severity. An initial assess of trends in HWEs was also carried out, in which we found no significant trends in the number and severity of HWEs.

The seasonal distribution of HWEs at each of the stations was also investigated. It was found that only 60% of the total number of HWEs occurred in the cold season, from October to April. However, some severe HWEs were also observed in the warm season, from May to September. For instance, the third most severe HWE at Coral Harbour as well as the fourth most severe HWE at Hall Beach occurred in September. HWEs can therefore form anytime of the year.

Prevailing wind directions during HWEs showed that stations located on flat terrain had more spread in the wind direction distribution. At the stations with mountainous terrain, winds were aligned with the local topography in a majority of the cases. As a tool, we used *wind regimes*, defined as 50° sectors centered around the occurrence of local maxima in the wind direction distribution. At all stations, the dominant wind regime originated from the NW quadrant.

Second, the roles of synoptic forcing mechanisms in the generation of HWEs in southern Nunavut were studied. HWEs usually occur when the station is in a zone of intense synoptic pressure gradient and that is the dominant factor over flat terrain. This situation was more likely to occur in winter, as a result of greater synoptic pressure gradients typically observed at that period.

Cyclones generating HWEs of the same wind regime are likely to follow similar storm tracks. As suggested by the overlapping of storm tracks causing HWEs at different stations (for instance, the eastward moving storms affecting Cambridge Bay and Baker Lake), it was found that the same storm system can generate HWEs at more than one station.

Although several zones of cyclonic activity associated with HWEs are found over land, most of the cyclonic activity tracks over water. Indeed, the zones of highest cyclonic frequency during HWEs are all located over large water bodies: Hudson Bay, Labrador Sea and Baffin Bay. This is in part due to the position of the mean polar vortex at 500 hPa, but potentially also to diabatic effects. Open water areas act as a source of moisture and energy and could contribute to an increased intensity of cyclonic activity.

Tracks over these three major water bodies are also all associated with low storm propagation speeds. We found that HWEs are mainly associated with stalled storms. Consequently, we conclude that these large water bodies offered a favoured site for cyclones to stall and cause sustained high winds for several days.

Third, the role of surface topographic forcing was investigated. We found that topography influences the formation of strong surface winds at Clyde River and Iqaluit. Terrain-induced flows were observed at Clyde River based on the wind direction distribution of HWEs, as 88% of the HWEs had winds aligned with the local topography. The surface composite map of the five most severe NW HWEs at their peak intensity clearly showed barrier jets at Clyde River, as a result of the cold stably stratified air accumulating against the mountain range in the vicinity of the station. At Iqaluit, the most severe HWEs were caused by channeling, as indicated by the surface composite maps of the five most severe NW HWEs. Due

to a limited interaction between the flow above and below ridge-top level, pressuredriven channeling is the dominant mechanism for the most severe NW HWEs at Iqaluit. Thus, for these events, downward turbulent flux of momentum is not a contributing factor.

Other aspects of this important issue of strong winds in the eastern Canadian Arctic should be investigated in the future. For instance, it would be useful to study the sensitivity of results to changes in the coefficients defining severity and to study in more detail the occurrence and severity of HWEs. Additionally, more effort needs to be devoted to the issue of trends in the occurrence and severity of HWEs. In particular, we need to determine the impact of the predicted northward shift in Arctic storm tracks [44] on strong surface winds. Since terrain-induced flow like channeling is sensitive to the position of storm systems relative to the local topography orientation, it would be useful to perform sensitivity studies measuring the impacts of variations in the position of the storm system relative to the stations in mountainous terrain. Climate change studies also predict a reduced sea-ice cover and increased temperatures in the Arctic [45]. These could also affect the behavior of strong winds in the eastern Canadian Arctic because they may lead to greater intensification and slowing down of storm systems.

In summary, this thesis has investigated strong sustained wind conditions in southern Nunavut. We found that the occurrence of these conditions was largely due to large-scale synoptic systems, but regional characteristics, including the presence of topographic features, large water bodies and proximity to storm tracks were also crucial contributing factors.

Appendix A: Frequency Distribution of Surface Wind Directions during High Wind Events

Table 8–1: Frequency distribution of hourly surface winds during HWEs at Baker Lake.

Direction	10.0 - 12.5 m/s	12.5 - 15.0 m/s	15.0 - 17.5 m/s	17.5 m/s	Total
	(%)	(%)	(%)	(%)	(%)
N	12	6.5	2.7	1.3	23
NNE	0.84	0.31	0.090	0	1.2
NE	0.56	0.17	0.050	0.0050	0.78
ENE	0.64	0.19	0.040	0.013	0.89
E	2.0	0.87	0.29	0.060	3.2
ESE	2.6	0.87	0.17	0.023	3.7
SE	1.9	0.53	0.12	0.020	2.5
SSE	0.65	0.21	0.033	0.015	0.91
S	0.16	0.050	0.013	0.0025	0.23
SSW	0.035	0.035	0.0025	0	0.073
SW	0.070	0.018	0	0.0025	0.090
WSW	0.12	0.048	0.0075	0.0025	0.18
W	0.84	0.36	0.085	0.033	1.3
WNW	3.3	1.7	0.48	0.17	5.6
NW	12	7.2	2.6	0.77	23
NNW	17	11	4.6	2.0	34
Subtotal	55	30	11	4.4	100

Table 8–2: Frequency distribution of hourly surface winds during HWEs at Cambridge Bay.

Direction	10.0 - 12.5 m/s	12.5 - 15.0 m/s	15.0 - 17.5 m/s	17.5 m/s	Total
	(%)	(%)	(%)	(%)	(%)
N	6.8	3.8	1.6	0.62	13
NNE	5.0	2.6	0.95	0.33	8.8
NE	5.4	2.7	1.0	0.46	9.6
ENE	3.6	1.3	0.50	0.10	5.3
E	3.1	1.0	0.30	0.076	4.5
ESE	2.4	1.2	0.33	0.061	4.0
SE	3.7	1.6	0.52	0.12	5.9
SSE	2.0	0.98	0.29	0.084	3.4
S	0.74	0.30	0.089	0.010	1.1
SSW	0.15	0.031	0.010	0	0.19
sw	0.24	0.094	0.037	0.26	0.39
WSW	0.85	0.26	0.076	0.023	1.2
W	4.6	1.8	0.60	0.16	7.1
WNW	4.1	1.9	0.61	0.18	6.8
NW	8.7	4.8	1.8	0.61	16
NNW	6.9	3.6	1.6	0.77	13
Subtotal	58	28	10.4	3.7	100

Table 8–3: Frequency distribution of hourly surface winds during HWEs at Clyde River.

Direction	10.0 - 12.5 m/s	12.5 - 15.0 m/s	15.0 - 17.5 m/s	17.5 m/s	Total
	(%)	(%)	(%)	(%)	(%)
N	0.61	0.17	0.029	0	0.80
NNE	0.065	0	0	0	0.065
NE	0.22	0.029	0	0	0.050
ENE	0.050	0	0	0	0.050
E	0.19	0.079	0.014	0	0.28
ESE	0.19	0.093	0.029	0	0.32
SE	0.41	0.24	0.014	0	0.66
SSE	0.29	0.21	0.014	0	0.51
S	0.23	0.15	0.029	0.0072	0.42
SSW	0.36	0.24	0.14	0.022	0.76
SW	0.64	0.40	0.23	0.14	1.4
WSW	0.42	0.31	0.086	0.036	0.85
W	0.18	0.093	0.036	0	0.31
WNW	4.9	2.5	1.0	0.50	8.9
NW	36	23	11	4.4	74
NNW	6.3	2.9	1.1	0.34	11
Subtotal	51	30	14	5.4	100

Table 8–4: Frequency distribution of hourly surface winds during HWEs at Coral Harbour.

Direction	10.0 - 12.5 m/s	12.5 - 15.0 m/s	15.0 - 17.5 m/s	17.5 m/s	Total
	(%)	(%)	(%)	(%)	(%)
N	9.0	5.3	3.0	1.5	19
NNE	6.0	3.8	2.5	2.2	15
NE	5.8	3.6	2.4	1.6	14
ENE	5.4	2.9	1.2	0.53	10
E	5.4	2.4	1.1	0.39	9.3
ESE	1.3	0.57	0.22	0.057	2.2
SE	0.95	0.39	0.14	0.054	1.5
SSE	0.55	0.17	0.070	0.0032	0.80
S	0.64	0.24	0.10	0.032	1.0
SSW	0.35	0.093	0.045	0.0032	0.49
SW	0.22	0.11	0.042	0	0.37
WSW	0.43	0.19	0.064	0	0.69
W	1.1	0.48	0.20	0.077	1.9
WNW	1.3	0.79	0.32	0.077	2.5
NW	3.8	1.8	0.86	0.43	6.9
NNW	8.0	4.3	2.3	1.1	16
Subtotal	50	27	15	8.0	100

Table 8–5: Frequency distribution of hourly surface winds during HWEs at Hall Beach.

Direction	10.0 - 12.5 m/s	12.5 - 15.0 m/s	15.0 - 17.5 m/s	17.5 m/s	Total
	(%)	(%)	(%)	(%)	(%)
N	4.7	1.7	0.47	0.062	7.0
NNE	1.4	0.48	0.16	0.025	2.1
NE	1.9	0.57	0.13	0.080	2.7
ENE	2.0	0.76	0.27	0.055	3.1
E	3.6	1.7	0.67	0.24	6.2
ESE	2.3	0.87	0.34	0.18	3.7
SE	1.8	0.77	0.29	0.058	2.9
SSE	2.1	0.85	0.26	0.065	3.3
S	1.9	0.72	0.14	0.034	2.8
SSW	0.25	0.065	0.0092	0	0.33
SW	0.21	0.068	0.015	0.0092	0.30
WSW	0.20	0.055	0.022	0.0062	0.28
W	1.7	0.55	0.19	0.12	2.6
WNW	13	5.7	2.1	1.1	22
NW	17	7.7	3.1	0.96	28
NNW	8.3	3.1	1.0	0.29	13
Subtotal	62	26	9.2	3.3	100

Table 8–6: Frequency distribution of hourly surface winds during HWEs at Iqaluit.

Direction	10.0 - 12.5 m/s	12.5 - 15.0 m/s	15.0-17.5 m/s	17.5 m/s	Total
	(%)	(%)	(%)	(%)	(%)
N	1.7	0.78	0.23	0.084	2.7
NNE	0.18	0.050	0.034	0.10	0.27
NE	0.71	0.46	0.31	0.26	1.7
ENE	0.93	0.73	0.50	0.67	2.8
E	1.3	0.76	0.43	0.26	2.8
ESE	2.0	0.79	0.19	0.094	3.0
SE	6.9	3.2	1.2	0.50	12
SSE	1.9	0.77	0.33	0.047	3.0
S	0.28	0.14	0.034	0.0034	0.45
SSW	0.040	0.010	0.010	0	0.060
SW	0.064	0.020	0.010	0	0.094
WSW	0.024	0.027	0.010	0	0.060
W	0.23	0.14	0.047	0.013	0.43
WNW	1.6	0.73	0.30	0.14	2.8
NW	23	12	5.2	2.8	43
NNW	13	7.4	2.9	1.8	25
Subtotal	54	28	12	6.7	100

Appendix B: Individual Components of Composite Maps

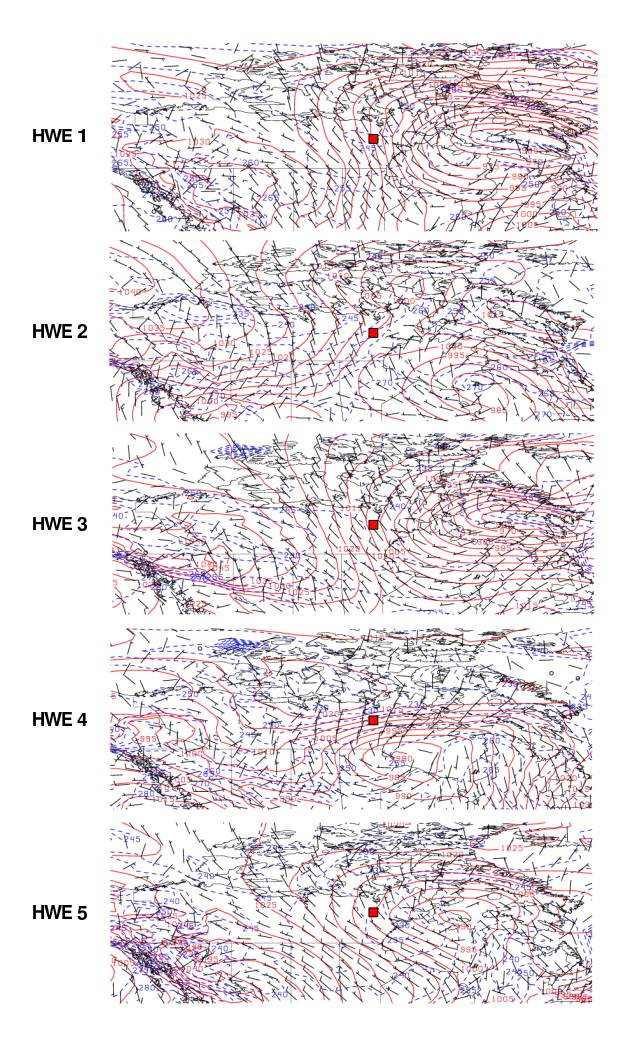


Figure 8–1: Individual surface maps of synoptic conditions during the peak intensity of the five most severe NNW HWEs at Baker Lake (indicated by a red square). Isobars of mean sea level pressure (in hPa) are plotted in solid red lines. Isotherms (in K) are shown by the blue dotted lines. The vectors represent the 10-m wind field (in m/s).

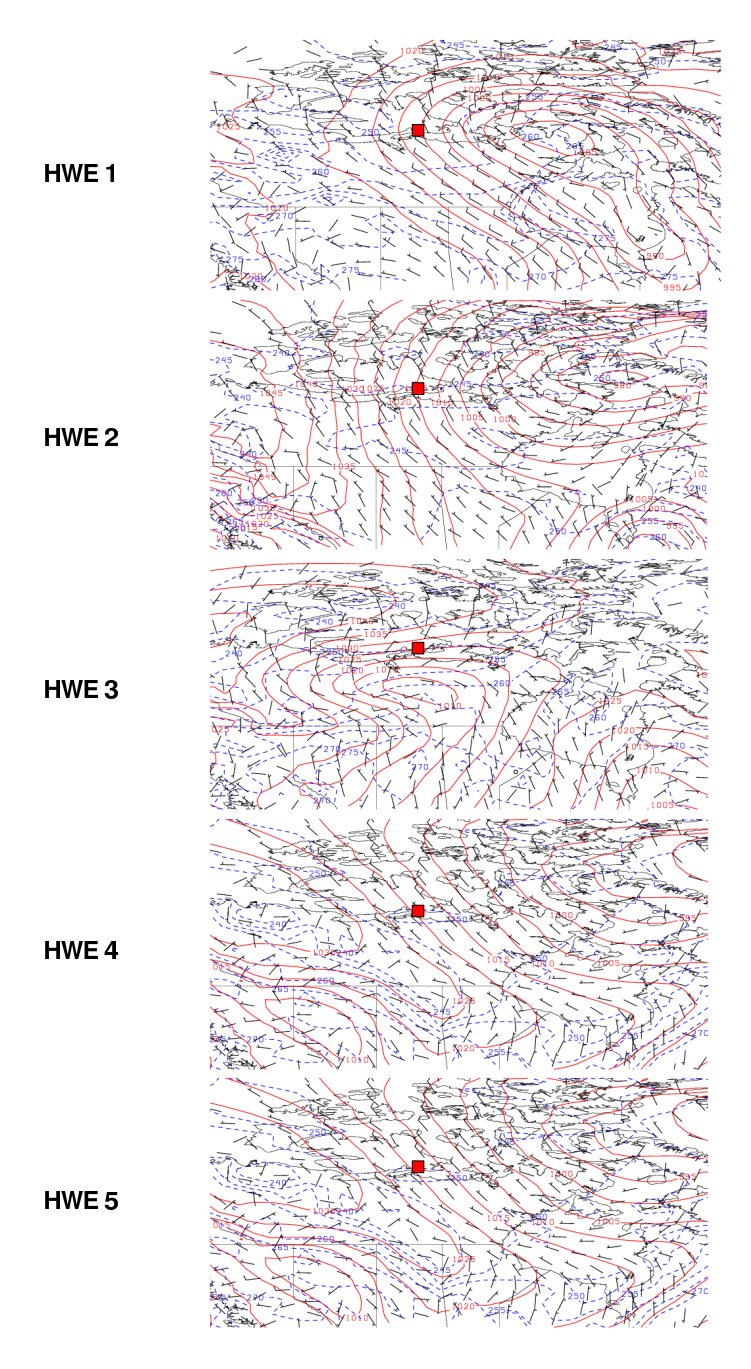


Figure 8–2: Individual surface maps of synoptic conditions during the peak intensity of the five most severe NW HWEs at Cambridge Bay (indicated by a red square). Isobars of mean sea level pressure (in hPa) are plotted in solid red lines. Isotherms (in K) are shown by the blue dotted lines. The vectors represent the 10-m wind field (in m/s).

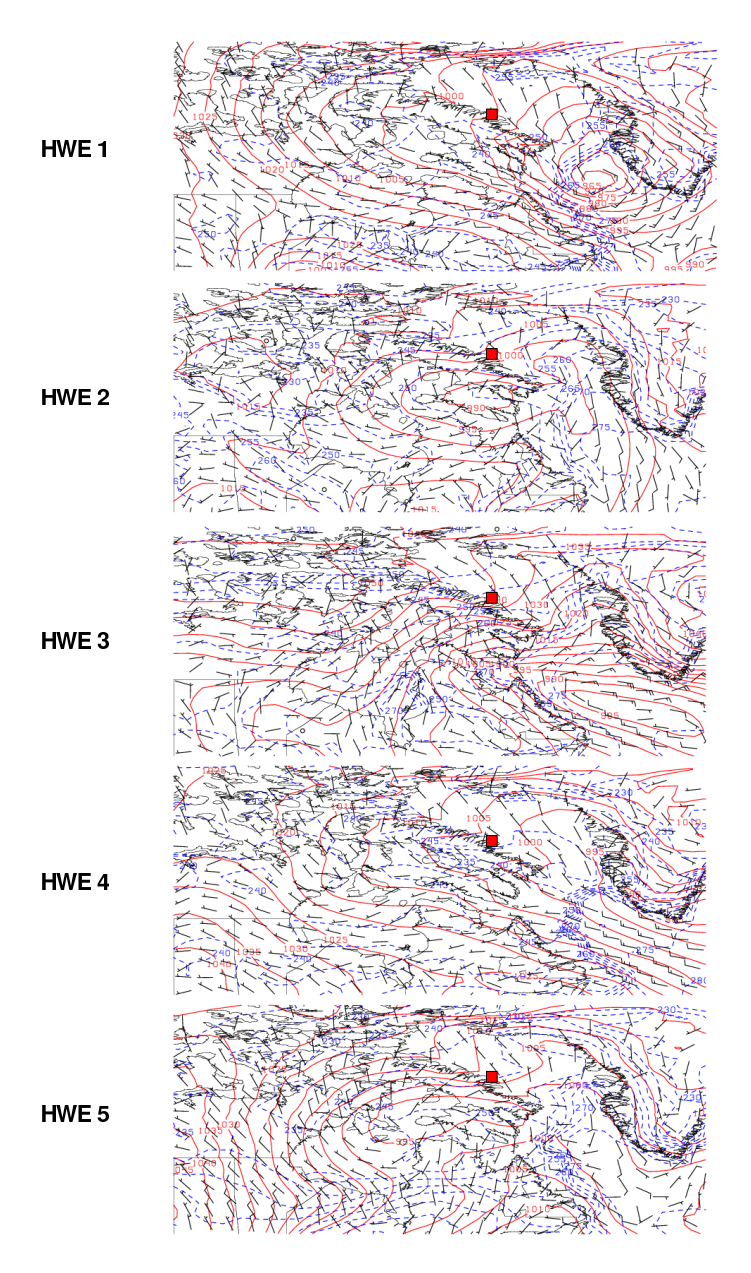


Figure 8–3: Individual surface maps of synoptic conditions during the peak intensity of the five most severe NW HWEs at Clyde River (indicated by a red square). Isobars of mean sea level pressure (in hPa) are plotted in solid red lines. Isotherms (in K) are shown by the blue dotted lines. The vectors represent the 10-m wind field (in m/s).

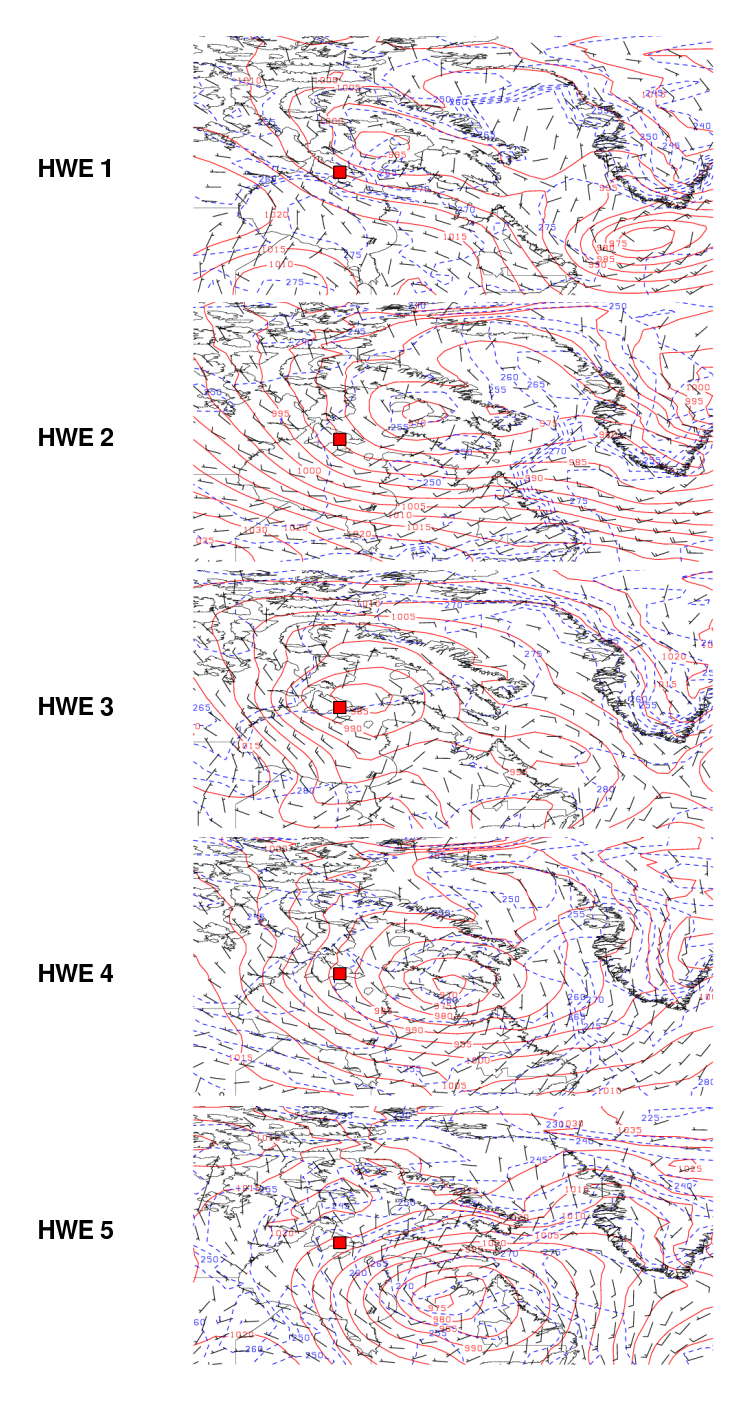


Figure 8–4: Individual surface maps of synoptic conditions during the peak intensity of the five most severe NNW HWEs at Coral Harbour (indicated by a red square). Isobars of mean sea level pressure (in hPa) are plotted in solid red lines. Isotherms (in K) are shown by the blue dotted lines. The vectors represent the 10-m wind field (in m/s).

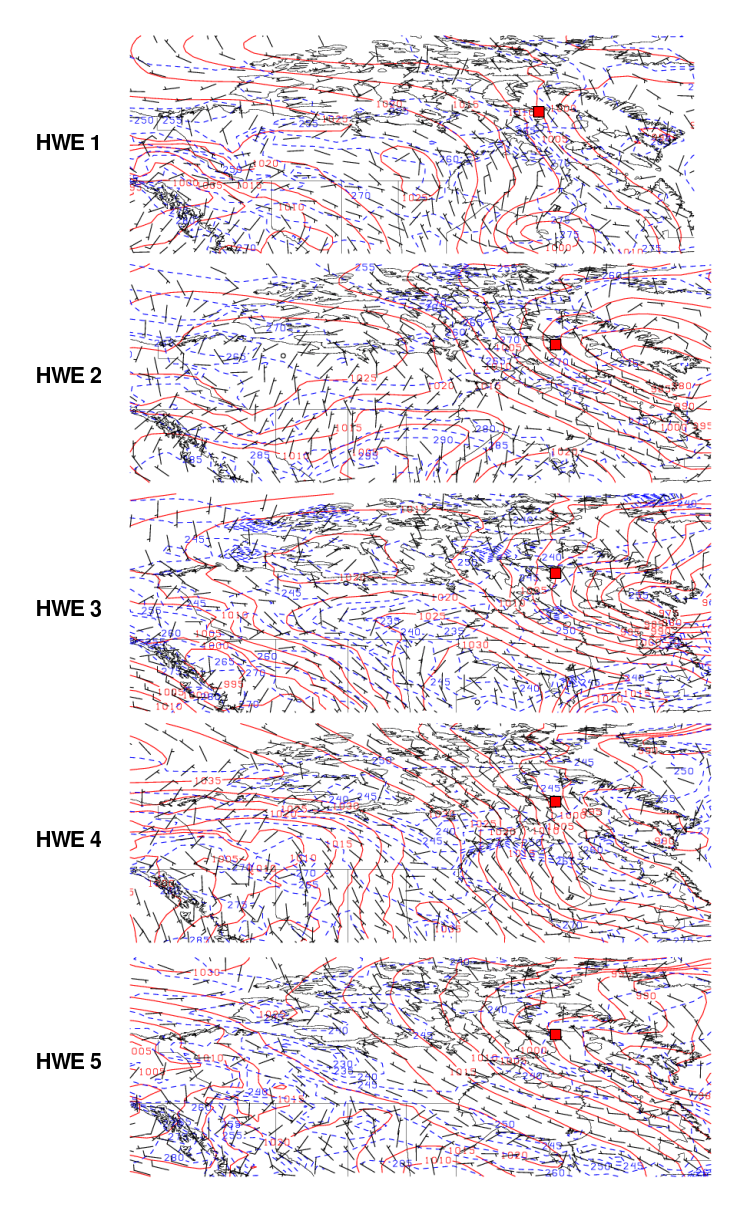


Figure 8–5: Individual surface maps of synoptic conditions during the peak intensity of the five most severe WNW HWEs at Hall Beach (indicated by a red square). Isobars of mean sea level pressure (in hPa) are plotted in solid red lines. Isotherms (in K) are shown by the blue dotted lines. The vectors represent the 10-m wind field (in m/s).

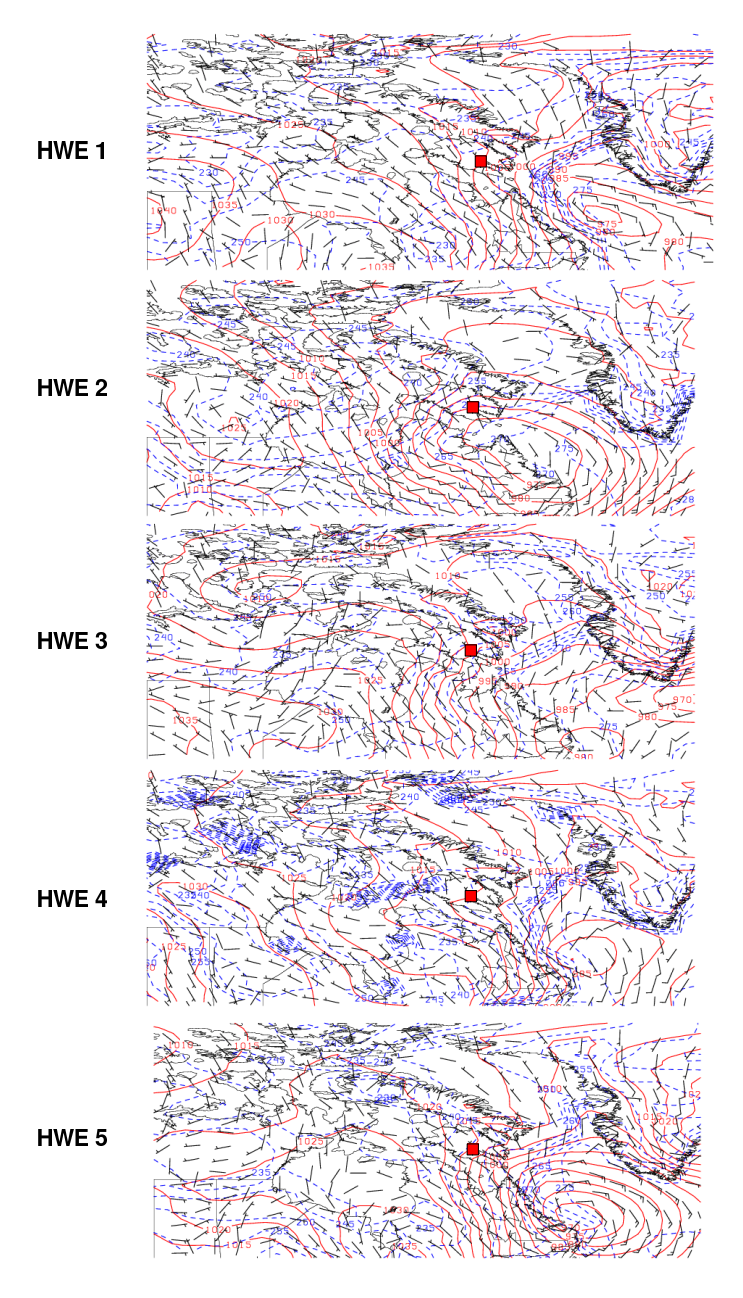


Figure 8–6: Individual surface maps of synoptic conditions during the peak intensity of the five most severe NW HWEs at Iqaluit (indicated by a red square). Isobars of mean sea level pressure (in hPa) are plotted in solid red lines. Isotherms (in K) are shown by the blue dotted lines. The vectors represent the 10-m wind field (in m/s).

Appendix C: Extra Composite Maps

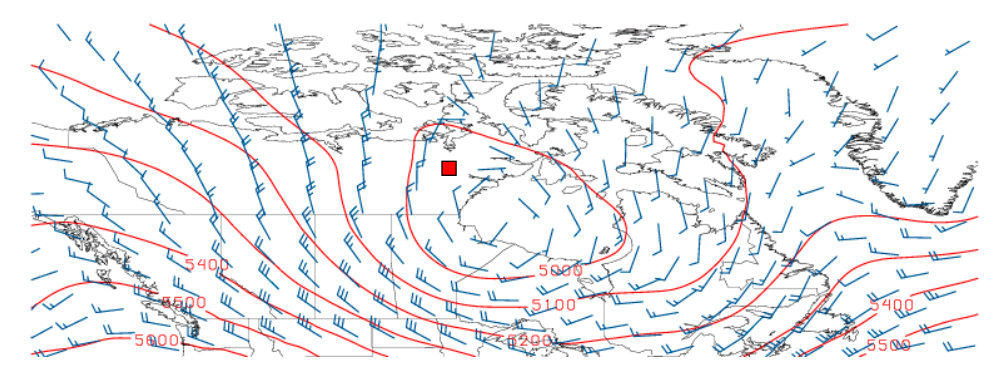


Figure 8–7: Fields of mean 500 hPa geopotential height for the five most severe NNW HWEs at Baker Lake. The vectors represent the geostrophic wind field (in m/s).

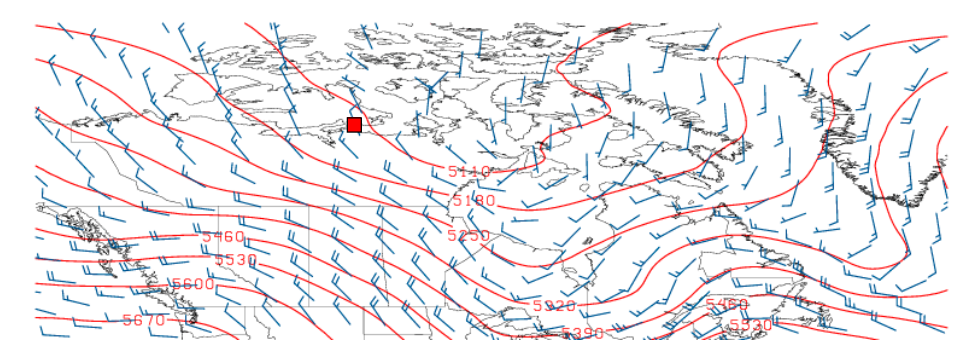


Figure 8–8: Fields of mean 500 hPa geopotential height for the five most severe NW HWEs at Cambridge Bay. The vectors represent the geostrophic wind field (in m/s).

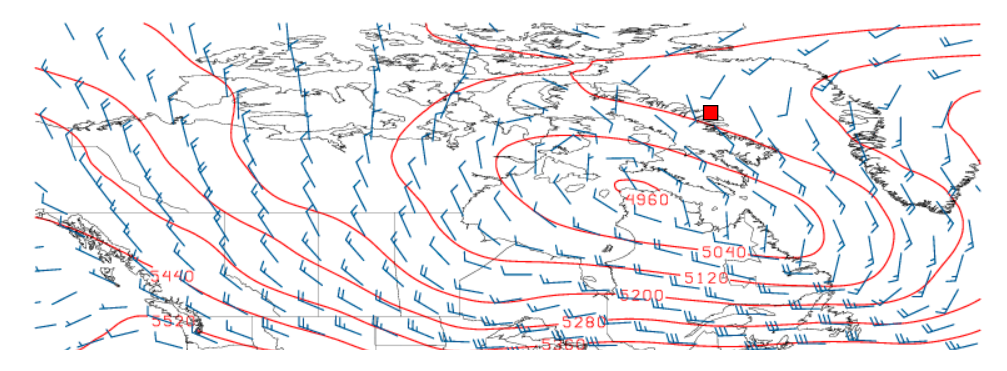


Figure 8–9: Fields of mean 500 hPa geopotential height for the five most severe NW HWEs at Clyde River. The vectors represent the geostrophic wind field (in m/s).

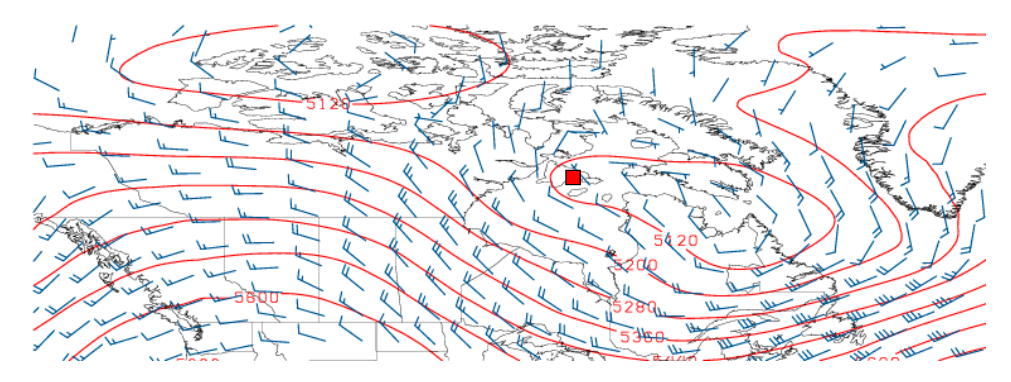


Figure 8–10: Fields of mean 500 hPa geopotential height for the five most severe NNW HWEs at Coral Harbour. The vectors represent the geostrophic wind field (in m/s).

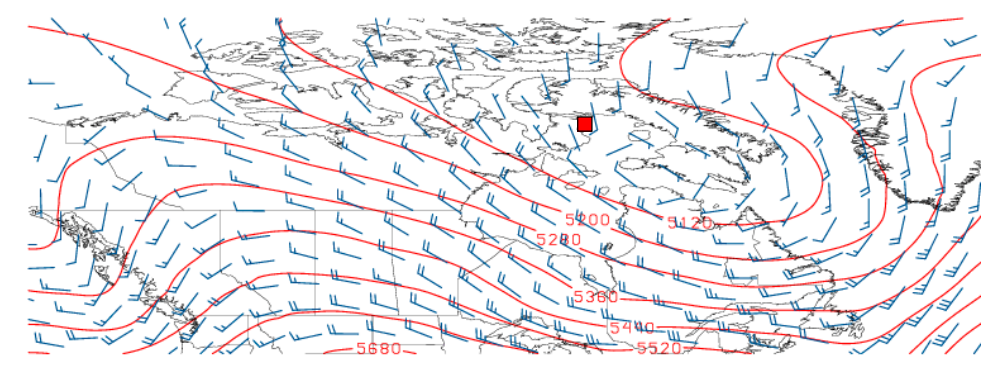


Figure 8–11: Fields of mean 500 hPa geopotential height for the five most severe WNW HWEs at Hall Beach. The vectors represent the geostrophic wind field (in m/s).

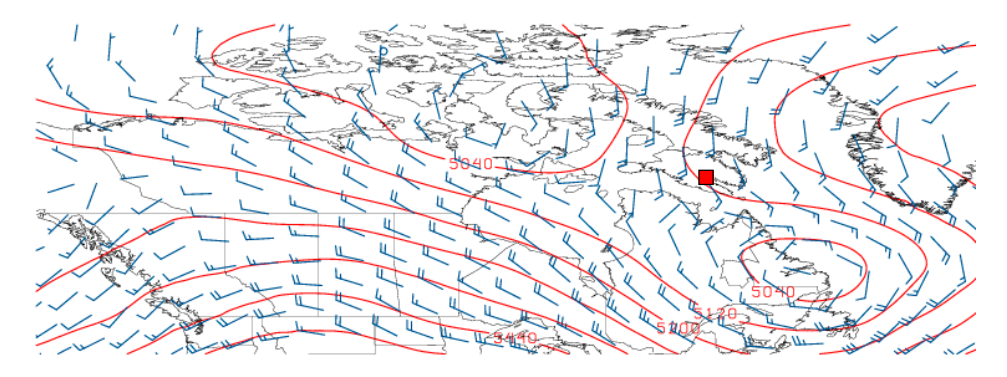


Figure 8–12: Fields of mean 500 hPa geopotential height for the five most severe NW HWEs at Iqaluit. The vectors represent the geostrophic wind field (in m/s).

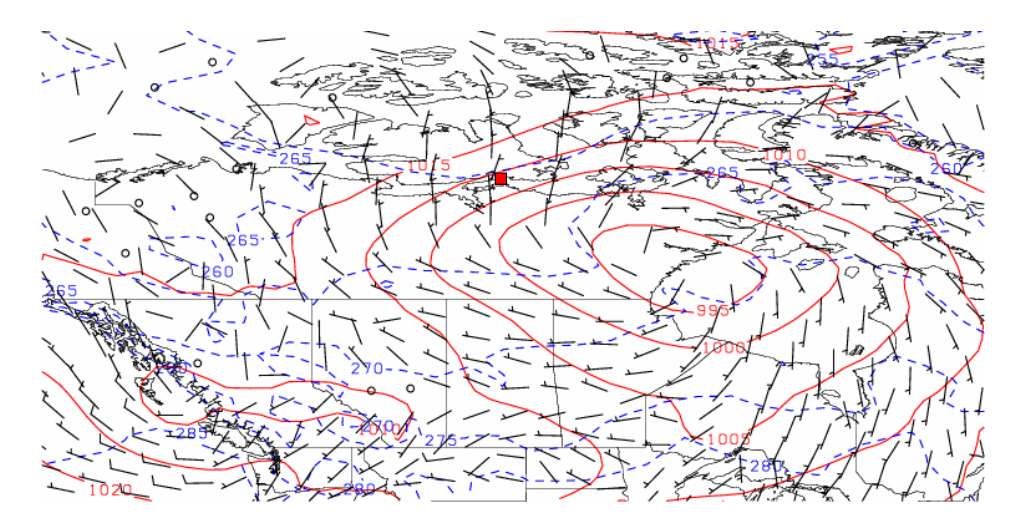


Figure 8–13: Composite surface map of synoptic conditions during the peak intensity of the five most severe N HWEs at Cambridge Bay (indicated by a red square). The pressure field (in hPa) at the mean sea level is plotted in solid red lines. Isotherms (in K) are plotted in blue dotted lines. The vectors represent the 10-m wind field (in m/s).

References

- [1] Government of Nunavut. Our Land. Page consulted on June 28th, 2007. www.gov.nu.ca/Nunavut/English/about/ourland.pdf.
- [2] Natural Resources Canada. The Atlas of Canada. Page consulted on October 29th, 2006. www.atlas.gc.ca.
- [3] Environment Canada. Top Weather Events of the 20th Century. Page consulted on April 10th, 2007. www.msc.ec.gc.ca/media/top10/.
- [4] Phillips D W, Francis D, Gullett D W, and Truhlar E J. *The Climates of Canada*. Environment Canada, Ottawa, Canada, 1990.
- [5] Sechrist F S, Fett R W, and Perryman D C. Forecasters Handbook for the Arctic. Naval Environmental Prediction Research Facility, Monterey, USA, 1989.
- [6] Przybylak R. *The Climate of the Arctic*. Kluwer Academic Publishers, Boston, USA, 2003.
- [7] Whiteman C D. Mountain Meteorology: fundamentals and applications. Oxford University Press, New York, USA, 2000.
- [8] Serreze M C and Barry R G. *The Arctic Climate System*. Cambridge University Press, New York, USA, 2005.
- [9] Nawri N and Stewart R E. Climatological Features of Orographic Low-Level Jets over Frobisher Bay. *Atmosphere-Ocean*, 44:397–413, 2006.
- [10] Hanesiak J M and Wang L X. Adverse-Weather Trends in the Canadian Arctic. Journal of Climate, 18:3140–3156, 2005.
- [11] Intihar M R and Stewart R E. Extratropical Cyclones and Precipitation within the Canadian Archipelago during the Cold Season. *Arctic*, 58:162–174, 2005.
- [12] Roberts E, Nawri N, and Stewart R E. On the Storms Passing over Southern Baffin Island during Autumn 2005. Submitted to *Arctic*, 2007.

- [13] Essery R, Li L, and Pomeroy J. A Distributed Model of Blowing Snow over Complex Terrain. *Hydrological Processes*, 13:2423–2438, 1999.
- [14] Essery R. Spatial Statistics of Windflow and Blowing-Snow Fluxes over Complex Topography. *Boundary-Layer Meteorology*, 100:131–147, 2001.
- [15] Lynch A H, Cassano E N, Cassano J J, and Lestak L R. Case Studies of High Wind Events in Barrow, Alaska. *Monthly Weather Review*, 131:719–732, 2003.
- [16] Gearhead S, Pocernich M, Stewart R E, Sanguya J, and Huntington H. Linking Inuit Knowledge and Meteorological Station Observations to Understand Chaging Wind Patterns at Clyde River, Nunavut. Submitted to Climatic Change, 2007.
- [17] Bluestein H B. Synoptic-Dynamic Meteorology in Midlatitudes Volume I. Oxford University Press, New York, USA, 1992.
- [18] Nawri N and Stewart R E. Channelling of High-Latitude Boundary-Layer Flow. Submitted to *Boundary-Layer Meteorology*, 2007.
- [19] Nadeau D. Interview with J. Shirley and M.E. Thomas, 2006. Nunavut Research Institute.
- [20] Holmes R E, Stearns C R, Weidner G A, and Keller L M. Utilization of Automatic Weather Station Data for Forecasting High Wind Speeds at Pegasus Runway, Antarctica. *Weather and Forecasting*, 15:137–151, 2000.
- [21] Hudson E, Aihoshi D, Gaines T, Simard G, and Mullock J. The Weather of Nunavut and the Arctic. Nav Canada, Canada, 2001.
- [22] Klock R, Hudson E, Aihoshi D, and Mullock J. The Weather of the Yukon, Northwest Territories and Western Nunavut. Nav Canada, Canada, 2001.
- [23] Zhang X, Walsh J E, Zhang J, Bhatt U S, and Ikeda M. Climatology and Variability of the Arctic Cyclone Activity: 1948-2002. *Journal of Climate*, 17:2300–2317, 2004.
- [24] Moore G W K and Renfrew I A. Tip Jets and Barrier Winds: A QuikSCAT Climatology of High Wind Speed Events around Greenland. *Journal of Climate*, 18:3713–3725, 2005.

- [25] Nawri N, Stewart R E, and Roberts E. Climatology and forcing of strong boundary-layer winds at coastal communities of nunavut. 2006 Coastal Zone Canada Conference and Youth Forum, Tuktoyaktuk, Northwest Territories, Canada, 11-18 August 2006.
- [26] Bell G D and Bosart L F. Appalachian Cold-Air Damming. *Monthly Weather Review*, 116:137–161, 1988.
- [27] Whiteman C D and Doran J C. The Relationship between Overlying Synoptic-Scale Flows and Winds within a Valley. *Journal of Applied Meteorology*, 32:1669– 1682, 1993.
- [28] Maxwell J B. The Climate of the Canadian Arctic Islands and Adjacent Waters vol.2. Environment Canada, Atmospheric Environment Service, Downsview, Canada, 1982.
- [29] Stewart R E, Bachand D, Dunkley R R, Giles A C, Lawson B, Legal L, Miller S T, Murphy B P, Parker M N, Paruk B J, and Yau M K. Winter Storms over Canada. Atmosphere-Ocean, 33:223–247, 1995.
- [30] Bromwich D H and Wang S-H. Evaluation of the NCEP-NCAR and ECMWF 15- and 40-Yr Reanalyses Using Rawindonde Data from Two Independent Arctic Field Experiments. *Monthly Weather Review*, 133:3562–3578, 2005.
- [31] Serreze M C, Box J E, Barry R G, and Walsh J E. Characteristics of Arctic Synoptic Activity, 1952-1989. *Meteorology and Atmospheric Physics*, 51:147–164, 1993.
- [32] Maxwell J B. The Climate of the Canadian Arctic Islands and Adjacent Waters vol. 1. Environment Canada, Atmospheric Environment Service, Downsview, Canada, 1980.
- [33] American Meteorology Society. Glossary of Meteorology. Page consulted on September 17th, 2007. amsglossary.allenpress.com.
- [34] Mesinger F. North American Regional Reanalysis. Bulletin of the American Meteorological Society, 87:343–360, 2006.
- [35] Kim D and Stockwell W R. An Online Coupled Meteorological and Air Quality Modeling Study of the Effect of Complex Terrain on the Regional Transport and Transformation of Air Pollutants over the Western United States. *Atmospheric Environment*, 41:2319–2334, 2007.

- [36] Weaver S J and Nigam S. Interannual Variations of the Great Plains Low-Level Jet: Large Scale Circulation Context and Hydroclimate Impacts. 2006 AGU Joint Assembly, Baltimore, Maryland (USA), 23-26 May 2006. American Geophysical Union, USA, 2006.
- [37] Khlopenkov K V and Trishchenko A P. SPARC: New Cloud, Snow, and Cloud Shadow Detection Scheme for Historical 1-km AVHHR Data over Canada. *Journal of Atmospheric and Oceanic Technology*, 24:322–343, 2007.
- [38] Woo M-K and Thorne R. Snowmelt Contribution to Discharge from a Large Mountainous Catchment in Subarctic Canada. *Hydrological Processes*, 20:2129–2139, 2006.
- [39] Unidata. GEMPAK/N-AWIPS. Page consulted on August 15th, 2006. www.unidata.ucar.edu/software/gempak/.
- [40] Moore G W K. Gale Force Winds over the Irminger Sea to the east of Cape Farewell, Greenland. *Geophysical Research Letters*, 30:1894–1897, 2003.
- [41] Key J R and Chan A C K. Multidecadal Global and Regional Trends in 1000 mb and 500 mb Cyclone Frequencies. Geophysical Research Letters, 23:2053–2056, 1999.
- [42] Ledrew E F. The Role of Local Heat Sources in Synoptic Activity Within the Polar Basin. *Atmosphere-Ocean*, 3:309–327, 1984.
- [43] Hoskins B J and Hodges K I. New Perspectives on the Nortern Hemisphere Winter Storm Tracks. *Journal of Atmospheric Sciences*, 59:1041–1061, 2002.
- [44] McCabe G J, Clark M P, and Serreze M C. Trends in Northern Hemisphere Surface Cyclone Frequency and Intensity. *Journal of Climate*, 14:2763–2768, 2001.
- [45] Nickels S, Furgal C, Buell M, and Moquin H. Unikkaaqatigiit Putting the Human Face on Climate Change: Perspectives from Inuit in Canada. Joint publication of Inuit Tapiriit Kanatami, Nasivik Centre for Inuit Health and Changing Environments at Université Laval and the Ajunnginiq Centre at the National Aboriginal Health Organization, Ottawa, Canada, 2006.